UNIVERSITA' DEGLI STUDI DI ROMA

TorVergata

Università

MALDI-TOF MASS SPECTROMETRY APPLICATION TO THE STUDY OF VIRUS-HOST INTERACTIONS

Federica Fratini

Dottorato di Ricerca in Biologia
Cellulare e Molecolare
XVII ciclo

Ai miei genitori
per tutte le possibilità che mi hanno offerto,
per essere stati delle guide
e aver sempre incoraggiato
la mia ricerca...
GRAZIE!

RINGRAZIAMENTI

Desidero ringraziare il Professor Mauro Piacentini per avermi dato la possibilità di svolgere il dottorato nei laboratori dell'Istituto Nazionale per le Malattie Infettive "L. Spallanzani" e la possibilità di introdurmi nell'affascinante mondo della Proteomica.

Desidero ringraziare il Dr. Fimia per l'importante e fondamentale collaborazione durante questi anni e tutti gli amici del laboratorio, in particolare Marta, Marco, Carmine, Valentina, Alessandra Rom, Fabiola, Cesca e Tony per il supporto scientifico e umano che mi hanno sempre dimostrato.

Desidero ringraziare gli amici della TUM e del Max Planck Institut di Monaco, in particolare Irena, per aver sempre condiviso e stimolato la mia passione per la ricerca scientifica e per avermi fatto sentire a casa ogni volta che sono tornata.

Desidero ringraziare Marco Inglessis, tutti i miei pari, e tutta la mia struttura, in paricolare Mara, Alessandra, Francesca, Stefano, Rossana, Sintu e Viviana, per il progetto e la crescita comune che stiamo condividendo e per l'inesauribile fonte di Energia e Forza che rappresentano.

Un grazie a Claudio e Francesca M. per avermi sopportato e supportato durante il periodo di scrittura della tesi.

Da cuore a cuore grazie a tutti voi e a tutti coloro che sicuramente ho dimenticato di menzionare!

1. INTRODUCTION

1.1 Definitions of Proteome and Proteomics

The words “proteome” and “proteomics,” related to genome and genomics, were coined in 1995 by a group in Australia (Wasinger VC *et al.*,1995). "Proteome" derives from the words "PROTein" and "genOME": as the set of genes of an organism is its genome, the set of proteins expressed in a cell is its proteome. Proteomics, then, is the science concerned with the study of proteomes.

Genome and Proteome mirror the functional difference between DNA and proteins in the cell: while DNA is the central memory of the cell, coding for the whole repertoire of proteins and RNAs, proteins are the molecular machines of the cell and provide most of the functions the cell needs to live its life.

In this respect, the major difference between genomes and proteomes is immediately apparent. While the genome can be well-defined for an organism: is relatively static and remains unchanged in time (unless you spend, nowadays, too much time in the sun!) between the cell types of an organism and throughout its life span; the proteome is a highly dynamic entity, tissue and cell specific, which varies between cell types and within a cell type depending on the conditions the cell is facing. For example, our liver cells and our lung cells have the same genome, but they perform very different functions as a result of their different proteomes. A cell's proteome expression continually changes in response to environmental and intracellular stimuli.

The human genome contains the complete set of genes required to build up a functional human being. However, the genome is only a source of information. In order to function, it must be expressed (Fig.1.1). The transcription of genes is the first stage of gene expression and is followed by the translation of messenger RNA to produce proteins. The proteome is the complete set of proteins produced by the genome at any one time, much more complex than genome due to different patterns of gene expression and different patterns of post-translational protein modifications. Proteins show a tremendous chemical heterogeneity in virtually all parameters that can be measured (weight, solubility, hydrophilicity, Isoelectric point) and are present in extremely divergent concentrations in cells.

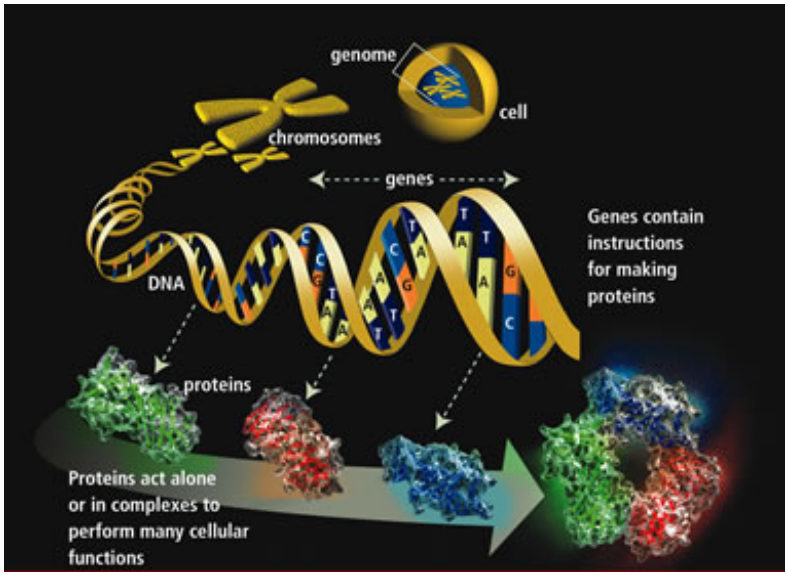

Fig.1.1 From genes to proteins.

Taking in mind the complexity and dynamicity of the proteome of an organism; all scientists attending the symposium entitled "Defining the Mandate of Proteomics in the Post-Genomics Era" (National Academy of Sciences, February 25, 2002; *Molecular & Cellular Proteomics 1:763–780, 2002*) agreed that the most useful definition of proteomics is likely to be the broadest: "***Proteomics represents the effort to establish the identities, quantities, structures, and biochemical and cellular functions of all proteins in an organism, organ, or organelle, and how these properties vary in space, time, and physiological state.***" Protein analysis is more complicated than figuring out the linear sequence of DNA genes, proteomics includes not only the identifying and quantifying of proteins, but also determining their localization, modifications, interactions, activities, and, ultimately, defining their function. Proteomics is thus a huge, long-term task, much more involved than sequencing the genome: a proteome being estimated an order of magnitude more complex than the genome (Fields, 2001)

1.2 Mass Spectrometry in Biological Research

The biological applications of MS currently encompass such diverse areas that a recent search on PubMed for the phrase “mass spectrometry” resulted in over 67183 total hits, with over 10660 of these articles published just in the last two years. The current importance of MS to biological research has been highlighted by the 2002 Nobel Prize in Chemistry, which was awarded to John Fenn and Koichi Tanaka “for their development of soft desorption ionization methods for mass spectrometric analysis of biological macromolecules”.

Ionization of larger molecules such as proteins was not possible until 1981 (see Tab.1 for brief history of MS), when the fast atom bombardment ionization method was introduced (Barber *et al*, 1981). The ability to ionize larger molecules was further improved with the advent of Electrospray Ionization (ESI) by Fenn and co-workers in 1988 (Fenn, 1989). The electrospray ion source was easily connected to on-line liquid chromatography (LC), which made possible the analysis of complex mixtures.

Time-of-flight (TOF) mass analysis had been developed and commercialized by 1956, but relatively poor mass resolution was a problem until improvements were made in the early 1970s (Thogersen *et al.*, 1974). An ionization technique for biological molecules that could be used with TOF analysis was introduced in 1991. This ion source, Matrix-Assisted Laser Desorption/Ionization (MALDI), was the result of work in Germany by Hillenkamp, Karas, and coworkers (Karas *et al*, 1988) and in Japan by Tanaka and coworkers (Tanaka *et al*. 1988). Like ESI, the MALDI ion source was capable of ionizing and vaporizing large molecules, up to m/z 100,000, such as proteins.

This methods solved the problem of generating ions from large, non-volatile analytes, such as proteins or peptides, without significant analyte fragmentation. The ability to do that conferred to these two methods the attribute of "soft" ionization methods. Michael Gross, director of the Washington University Center for Biomedical and Bioorganic Mass Spectrometry, observes that the development of MALDI and ESI was "evolutionary. But their impact, he says, "is perhaps revolutionary". He notes, for example, that before there was MALDI, mass spectrometrists had fast atom bombardment ionization, a matrix-based technique that uses atomic collisions to ionize the sample, instead of a laser. Similarly, the concept of laser desorption has been known for over 20 years. The union of

these two techniques in MALDI, however, vastly enhanced the ability of researchers to analyze biological samples. (Perkel, 2001).

Tab. 1 A Brief History of the Development of Mass Spectrometry

A Brief History of the Development of Mass Spectrometry
1897 – J.J. Thompson discovers the electron and determines its m/z ratio (Nobel Prize in 1906)
1912 – J.J. Thompson constructs first mass spectrometer and obtains mass spectra for O_2, N_2, CO, CO_2, and $COCl_2$
1918 – A.J. Dempster develops electron ionization source and magnetic sector with directional focusing
1948 – A.E. Cameron and D.F. Eggers publish design and mass spectra for a linear Time-of-Flight (TOF) mass spectrometer
1949 – H. Sommer, H.A. Thomas and J.A. Hipple describe the first application in mass spectrometry of Ion Cyclotron Resonance (ICR)
1953 – W. Paul and H.S. Steinwedel describe the quadrupole analyzer and ion trap in a patent (Paul received Nobel Prize in 1989)
1956 – First coupling of gas chromatography with mass spectrometers by F.W. McLafferty and R.S. Gohlke
1966 – M.S.B Munson and F.H. Field discover chemical ionization
1974 – First coupling of liquid chromatography with mass spectrometry by A.J. Arpino, M.A.Baldwin and F.W. McLafferty
1974 – M.D. Comisarov and A.G. Marshall develop Fourier Transform ICR (FTICR)
1978 – R.A. Yost and C.G. Enke build first triple quadrupole masS spectrometer, one of the most common tandem mass spectrometers today
1987 – M. Karas, D. Bachmann, U. Bahr and F. Hillenkamp discover Matrix Assisted Laser Desorption Ionization (MALDI)
1988 – J. Fenn develops electrospray for Electrospray Ionization (ESI); First spectra for proteins larger than 20,000 Daltons (Nobel Prize in 2003)

1.3 Virus-Infection Biology

Viruses are obligatory intracellular parasite and use cellular biosynthetic machinery for replication. To replicate and cause disease, viruses must overcome cellular and humoral immune responses, defeat innate cellular defence systems, arrogate cellular factors, and reprogram the normal biology of the cell. During the course of evolution, viruses devised various strategies to exploit host cell transcription machinery; to regulate cellular signal transduction pathways; to take over the cellular RNA processing and transport machinery; to redirect translational machinery for optimization of viral protein synthesis and to circumvent host defences. They often utilise the most sophisticated methods in gene regulations in order to cope with and/or to modulate their host gene-expression systems.

Some of the cytopathic effects of virus infection on a host cell are caused by specific alterations in host-cell metabolism or structure that allow viral replication events. The effects on the host cell may be mediated by different mechanisms, such as the addition or substitution of a virus-specific macromolecule into a cellular complex or structure; a covalent or non-covalent modification of a host-cell molecule; a disassembly or rearrangement of a host-cell complex or structure, the assembly of a new specific complex or structure in the infected cell (for review see Gale *et al.*, 2000). These effects are usually not simply cytopathic and/or toxic effects of virus infection. Interactions of viruses with host cells may involve subtle changes in the host cell, and an understanding of the nature of the interactions between viral gene products and the host-cell molecules often provides insight into the metabolic processes and critical regulatory events of the host cell.

The innate immune system is the first response to all types of pathogens prior to the appearance of the adaptive or specific response. It involves natural killer (NK) cells, the complement, cytokines and apoptosis. The NK cells are cytolytic cells that use an antigen-independent mechanism. They are activated by low level of autologous major histocompatibility complex class I (MHC-I) molecules on the surface of infected cells.

The complement is a component of the innate system as well as the specific immune system. It is composed of soluble molecules (C1q, C3b, etc.) that can interact directly with viruses, or with virus-antibody complexes, or with receptors on cells of the immune system. The complement-binding activates a cascade of proteases that leads to lysis or the activation of cells of immune response.

INFS and other cytokines are a large family of multifunctional secreted proteins involved in antiviral defensive responses and many other physiological process including cell proliferation and apoptosis. They play an important role in both innate and specific immune response. IFNs were originally discovered as antiviral proteins that inhibit viral replication. Upon virus infection, IFNs are induced in the host cell and thus mediate cellular defensive responses. The IFNs has been classified into two types. Type I IFNs are produced in most cell types and are typically induced by double-stranded RNA, which is either synthesized in the course of many viral infections, or by other cytokines and growth factor, such as interleukins 1 and 2 (IL-1 and IL-2) and tumour necrosis factor (TNF). Type I IFNs consist of the products of IFN-α multigene family, which are predominantly synthesized by leukocyte, and the product of IFN-β gene, which synthesized by most cell types but particularly by fibroblasts. Type II IFN (IFN-g) is synthesized mainly by T lymphocytes and is involved in the antigen- specific immune response. Type II IFNs consist of the product of the IFN-γ and is synthesized in response to the recognition of infected celles by activated T lymphocytes and natural killer cells (Vilcek & Sen, 1996). Both types of IFNs stimulate an antiviral state in target cells, whereby the virus replication is blocked or impaired due to the synthesis of a number of enzymes that interfere with cellular and viral process. The IFN signaling pathway has been extensively studied (for reviews see Samuel, 2001; Sen, 2001; Goodbourn *et al.*, 2000). Upon binding of IFNs to their cognate receptors, the JAK-STAT signal transduction pathway is triggered, culminating in the transcription of IFN-stimulated genes (ISGs) that mediate IFN function. The proteins encoded by ISGs include many antiviral effectors such as the double-stranded RNA-activated protein kinase PKR (which inhibits viral protein synthesis by phosphorylation of the translational initiation factor eIF2α); the 2'-5' oligoadenylate synthetase (2'-5' OAS, which activates RNase L to degrade viral RNA); and the Mx GTPases (which block viral transport inside the cell).

The apoptotic process also appears to be a host innate defence mechanism against viral infections and tumourigenesis, as well as a component of the specific immune response, involving the cytotoxic activity. Programmed cell death is required to destroy cells that represent a threat to the integrity of the organism. In cells infected with viruses apoptotic cell death can be induced through the function of cytotoxic T lymphocytes (CTLs) and natural killer cells. The apoptotic process has been considered to be a frequent pathway of

interruption of viral replication and elimination of virus-infected cells by the host (Hasnain, 2003).

Besides the cellular effectors, the specific immune response makes use of humoral effectors comprised of antibodies secreted by activated B lymphocytes. CTL response is responsable for the elimination of infected cells and antibodies can bind free virus and mediate lysis of infected cells as well. Helper T cell (Th) secretes cytokines that are important for optimal responses of B cells and antibody production or CTL. Two types of Th are distinguished according to the type of cytokines they secrete. Th1, important for CTL activation, secretes IFN-γ, TNF-β and IL-2. Th2, important for B cell activation and secretion of antibodies, secretes IL-4, IL-5, IL-6 and IL-13. Several viruses impair the function of helper T lymphocytes by causing a shift from a Th1 to a Th2 cytokine profile. This induce an inappropriate and less-effective immune response which can results in virus escape and chronic infection (Goodbourn *et al.*, 2000).

In most instances, host derived innate and acquired antiviral and immune responses are effective in suppressing virus replication and dissemination. On the contrary, many virus genomes encode proteins, which repress the apoptotic process so as to escape from the host immune attack. Viruses have devised fascinating tricks to inhibit host apoptosis and many such mechanisms are vital for viruses to establish their propagation and persistent infetion. These 'anti-death' mechanisms include the inhibition of IFNs pathway (Katze *et al.*, 2002); the modulation of the anti-apoptotic members of the Bcl-2 family, resulting in inhibition of formation of ‘apoptosome’; the inactivation of the tumour suppressor p53, and caspase inhibition (Hay & Kannourakis, 2002).

In the case of persistent virus infections the host response is either inadequate and/or the virus employs strategies to thwart or avoid host responses. Continued disruption of host cell responses is also mechanistically involved in the various pathologies arising from chronic infection.

Hepatitis C virus (HCV) is a prime example of a virus which frequently (>75% of the time) progresses to chronicity because the virus modulates the host antiviral and immune responses. It is unclear which viral strategies contribute to virus persistence, pathogenesis and clinical manifestations (cryoglobulinemia, fibrosis, cirrhosis, hepatocarcinoma, etc.).

HCV has developed several strategies to counteract the immune system of the host. Combination of these different strategies probably allows HCV to establish persistence at a high frequency. The fact that HCV exists as an

evolving quasispecies (see pp. 30-31) plays an important role in the selection of escape mutants that are not recognized by the immune system. Furthermore, viral proteins can interact with effectors of various signalling pathways involved in cell proliferation, apoptosis or transformation. Intracellular interactions have been demonstrated between the viral NS5A, E2 or Core proteins with PKR (Gale *et al.*, 1997; Pavio *et al.*, 2000; Delhem *et al.*, 2001); between Core and several members of the TNFR family (Zhu *et al.*, 1998; 2001) and between NS3 and PKC (Borowski *et al.*, 1999). These interactions may result in the modulation of apoptosis pathways or interference with the IFN-α pathway (Kountouras *et al.*, 2003; Fimia *et al.*, 2004). Modulation of cellular functions can also involve interaction of circulating virus particles with cell surface receptors, such as interaction between E2 and CD81 on NK cells (Tseng & Klimpel, 2002) or T cells (Wack *et al.*, 2001) and sensitize these cells to apoptotic stimuli. These strategies impair both innate and specific immune responses. In addition HCV does not only infect hepatocytes but infect B and T cells as well and affect their normal functions.

However, depending on the experimental model used, a large but often contradictory literature exist concerning the impact of expression of HCV proteins on cellular processes.

Owing to its antiviral and immune-response properties, IFNs have been successfully applied as therapeutics against several types of cancers and infectious diseases including multiple sclerosis, hepatitis and genital warts (Sen, 2001). One of the most prominent clinical applications of IFNs is treatment of patients infected by hepatitis C virus (HCV). In the absence of a protective vaccine, the only useful therapeutic regimen is the interferon-alpha (IFN-α) together with ribavirin, a broad spectrum antiviral nucleoside. However, more than 50% of HCV-infected patients showed low rates of response to this therapy, in particular patients infected by genotype-1 HCV which is a more infectious sub-genotype among Americans and Europeans.

Much of the search for the molecular basis of HCV resistance to IFN has centred on the viral non-structural 5A (NS5A) protein. This focus began with evidence that the amino acid sequence of a region of NS5A, termed the IFN sensitivity determining region (ISDR), correlates with therapeutic outcome (Enomoto *et al.*, 1996). Subsequent in vitro studies demonstrated that NS5A from an IFN-resistant isolate inhibits the IFN-induced protein kinase PKR (Gale *et al.*,1997; 1999), suggesting a mechanism for IFN resistance. However, the link between NS5A and resistance to IFN still remain ambiguous because of the high divergence of results (Tan & Katze,

2001). A number of factors, including the level of NS5A expression, cells specific factors, or the presence of other HCV proteins may contribute to these disparate results (Geiss *et al.*, 2003).

Precise knowledge of the pathogenic mechanisms by which viruses replicate in specific tissues, spread, cause persistent infection and disease must come, at least in part, from studies of the intracellular replication of the virus. A better understanding of the immunopathogenesis of viral infection may, in fact, facilitate the development of immunotherapeutic strategies and, much more, definition of antiviral strategies requires knowledge of the replicative mechanisms of viruses and the identification of replicative steps that involve virus-specific processes and not host-cell processes. Each virus may have a few specific steps of replication that may be used as targets for highly selective, carefully aimed chemotherapeutic agents. Therefore, proper use of such drugs requires a thorough knowledge of the suitable targets, based on a precise understanding of the replicative mechanisms of the offending virus.

Until recently, investigation of HCV replication mechanisms and the cellular consequences of HCV infection have been hampered significantly by the absence of a robust in vitro infection-replication system, as well as the lack of a suitable small animal model. However, recent progress has led to the establishment of autonomously replicating subgenomic HCV RNAs, expressing only NS proteins (Lohmann *et al.*, 1999; Blight *et al.*, 2000), termed 'replicons'. These RNAs replicate efficiently and stably under selective pressure in Huh7 cells, a human hepatoma-derived cell line.

The work I will present in this thesis had the aim to investigate the mechanisms of HCV replication and the impact of infection into the host cell in such a way to get the most representative system of in vivo infection. We used this 'replicon system' and a proteomic approach looking for differences in the proteome expressed by Huh7 cells in the presence or absence of HCV replicon.

Looking to virus-host interaction, namely the host immune reaction to the presence of a virus, I have also apply the proteomic analysis to investigate Mixed Crioglobulinemia, the most common extracellular manifestation of HCV infection. Moreover, to better test this kind of technical approach in the investigation of virus-host interaction, I applied the same analysis to another RNA virus recently discovered that has determined a world-wide outbreak in 2003, the causative agent of the Severe Acute Respiratory Syndrome (SARS) coronavirus (CoV). The molecular basis of SARS-CoV induced pathology is still largely unknown. Anyway, SARS infection course has a completely different characteristics in respect to HCV, included the ability to

infect and replicate in different tissues (included liver) and cell lines, a latent period of only 5 hours post infection (h.p.i.) and, mainly, a fast growth (faster than other known human coronaviruses) that induce dramatic cytopathic effects within the first 24 h.p.i. and apoptosis within 48 h.p.i. (Ng *et al.*, 2003) SARS induced hepatitis has also been reported (Chau *et al.*, 2004).

2. MASS SPECTROMETRY PRINCIPLES and INSTRUMENTATIONS

Mass spectrometric measurement are carried out in the gas phase on ionized samples. Mass spectrometers generally couple three devices (Fig.2.1):

- an ion source
- a mass analyzer which measure the mass-to-charge ratio (*m/z*) of the ionized analytes
- a detector that registers the number of ions at each *m/z* value.

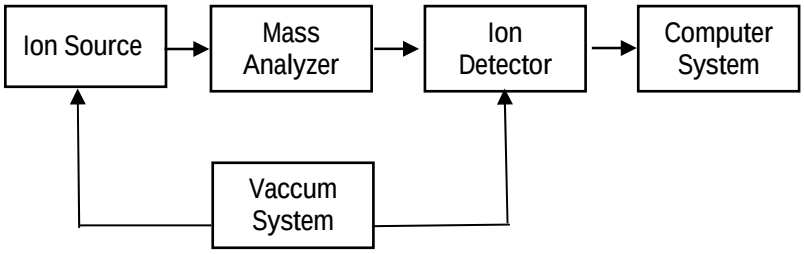

Fig.2.1 Basic components of a mass spectrometer.
All mass spectrometers contain at least three major components: ion source, mass analyzer and a ion collection/detection system. The instrument must also be connected to a computer system to process and record data and a vacuum pump to control the pressure into the instrument : all internal components are maintained at very low pressure (10^{-6}-10^{-8} torr) to limit the number of ions collisions.

2.1 Ion Sources

The most common ionization techniques used in biology to volatilize and ionize proteins and peptides are MALDI and ESI. ESI ionizes the analytes out of a solution and it is therefore readily coupled to a liquid-based separation tools, as liquid chromatography (Niessen & Tinke, 1995) or capillary electrophoresis (Krylov & Dovichi, 2000), which may be used to concentrate and purify individual peptides prior to mass analysis. In an **ESI source** (Fenn *et al*. 1989 e 1990, Fig.2.2) the sample is ionized when large charged droplets are produced forcing the analyte solution through a needle, at the end of which is applied a potential sufficiently high to disperse the

emerging solution into a very fine spray of charged droplets all at the same polarity (Fig.2.3). The solvent evaporates away, shrinking the droplet size and increasing the charge concentration at the droplet's surface. When Coulombic repulsion overcomes the droplet's surface tension, the droplet explodes. This 'Coulombic explosion' forms a series of smaller, lower charged droplets. The process of shrinking followed by explosion is repeated until individually charged 'naked' analyte ions are formed and realised as gas-phase ions (Mann, 1990). The completely desolvated ions are formed at atmospheric pressure and then guided into the high-vacuum region of the mass spectrometer through a capillary or by a series of differentially pumped skimmers. Electrospray results in a continuous production of gas-phase ions, the charges are statistically distributed amongst the analyte's available charge sites, leading to the formation of multiply charged ions. In the case of proteins and peptides, on average, one positive charge per kDa (Mann, 1995), at the basically charged sites – the amino terminus, arginyl, histidyl and lysyl residues. Multiple charged ions [(M + nH)n+] are mathematically transformed into a simple mass spectrum that reveals the molecular weights of the fragments (Mann 1989; Reinhold 1992).

Increasing the rate of solvent evaporation, by introducing a drying gas flow counter current to the sprayed ions or a heated capillary (Fig.2.2), increases the extent of multiple-charging. Decreasing the capillary diameter and lowering the analyte solution flow rate i.e. in nanospray ionization, will create ions with higher *m/z* ratios (i.e. it is a softer ionization technique) which are of much more use in the field of bioanalysis (Wilm & Mann, 1996).

Before a MALDI-MS can be acquired, a sample containing peptides/proteins has to undergo a sample preparation (Kussmann *et al.*,1997). Firstly, the sample has to be purified from any contaminants (buffers, salts, detergents or denaturants), secondly it has to be crystallize with the opportune matrix. **MALDI ionization** involves a protein suspended or dissolved in a crystalline structure (the matrix) of small, organic, UV-absorbing molecules. The matrix is normally an organic aromatic weak acid, which strongly absorb energy at the wavelength of the laser, most commonly N_2-lasers (337 nm) and Nd-YAG (355 nm) have been successfully applied. The analyte is mixed with matrix material in solution and the mixture is allowed to dry as a crystalline coating on a metal target plate. (Fig.2.4).

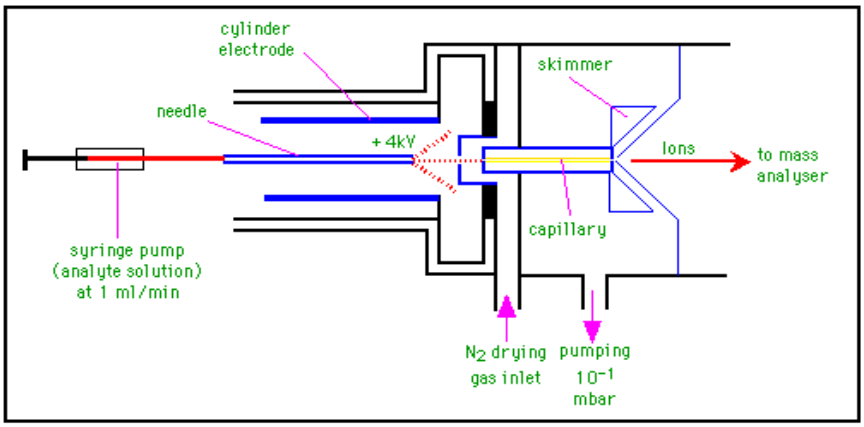

Fig. 2.2. Schematic diagram of an electrospray source.

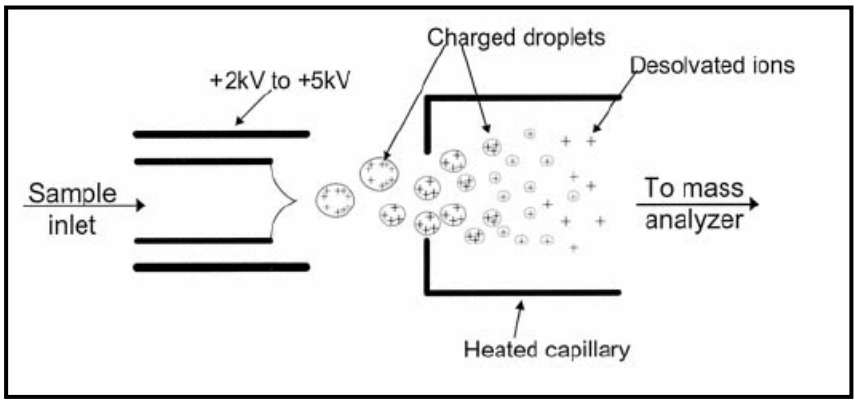

Fig.2.3 Electronspray ion source. The liquid sample exits a capillary on which a voltage is applied. This process ionizes the sample and causes the exiting liquid to form a spray of small droplets.

The MALDI-matrix plays an important role in several ways: (i) it absorbs energy and protects the analyte from excessive energy i.e. analyte decomposition, (ii) it enhances the ion formation of the analyte by photoexcitation or photoionization of matrix molecules followed by proton transfer to the analyte molecule, (iii) the sample dilution into the matrix prevents association of analyte molecules .

The resulting crystals are irradiated with laser pulses at the wavelength at which the matrix has high spectral absorption. This process desorbs the mixture and photoexcites the matrix. The excited matrix then ionizes the analyte thought proton transfer causing the subsequent passage of matrix and analyte ions into the gas phase (Fig.6).

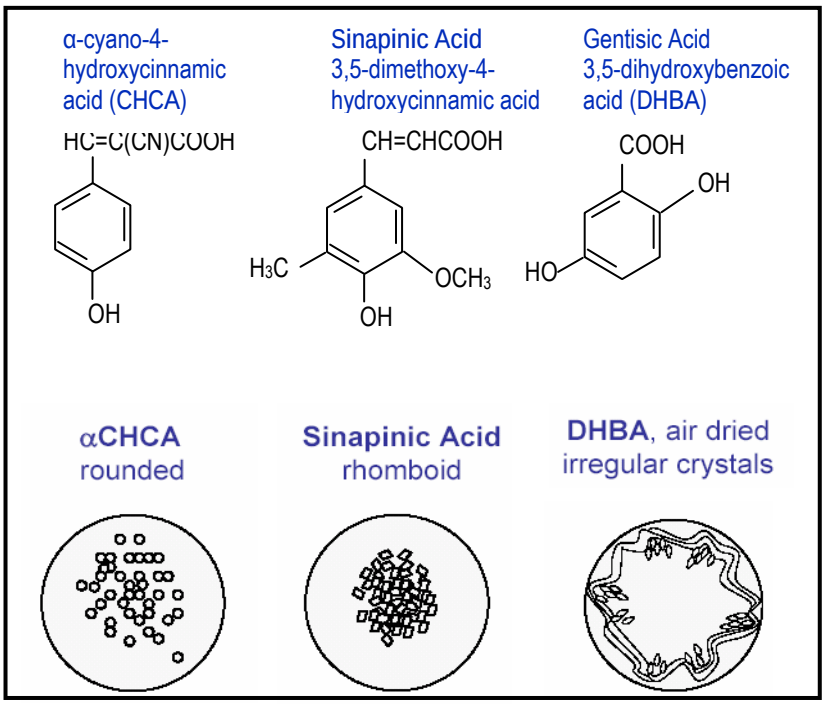

Fig.2.4 Commonly used matrix for MALDI-MS of peptides and proteins.

The principal ion detected using threshold laser intensity for MALDI is (M + H+), although signals for multiply charged ions and oligomeric forms of the analyte may be seen, especially for large proteins. At the time that the laser is pulsed a voltage is applied to the target plate, the ionized sample is then accelerated by the electrostatic field and expelled into a flight tube (Fig.2.6).

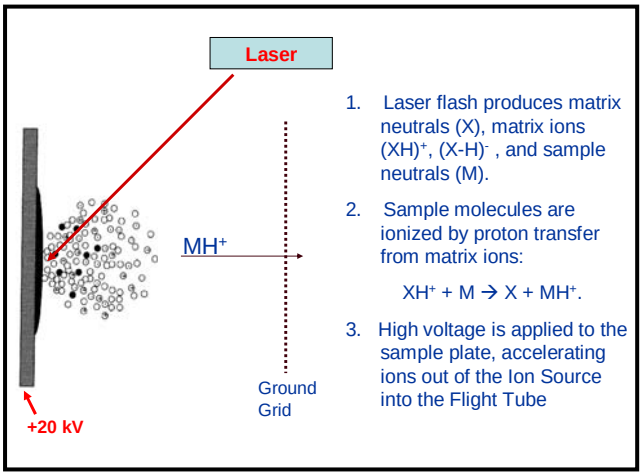

Fig.2.5 Matrix Assisted Laser Desorption Ionization (MALDI).

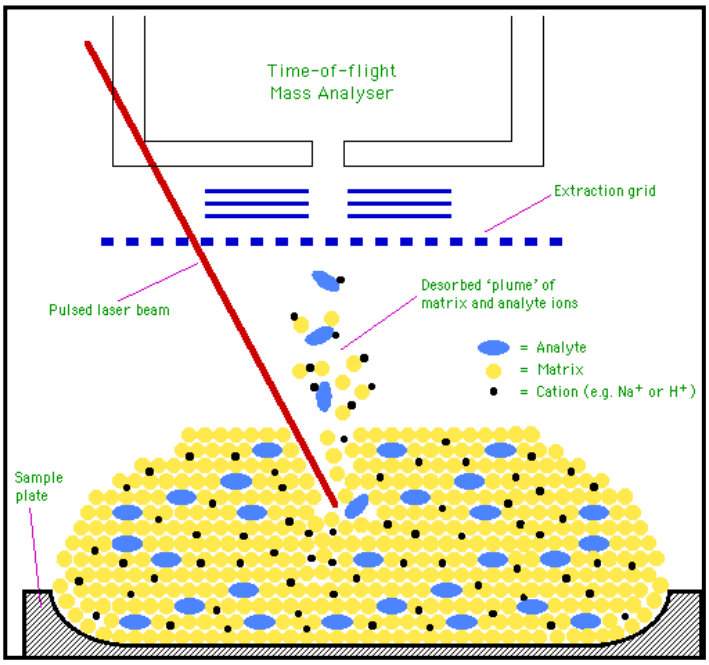

Fig.2.6 Acceleration of ionized sample through the extraction grid into the flight tube.

2.2 Mass Analyzers

Once a sample has been ionized, it must be mass analyzed. The beam of ions is then focused and directed into a mass analyzer which separates the ions in respect to their *m/z* value. In the context of proteomics, the key parameters of a mass analyzer are sensitivity, resolution and mass accuracy (Russel DH & Edmondson RD, 1997). There are four most commonly used mass analyzers for protein biochemistry applications: time-of-flight (TOF), quadrupole, ion trap and Fourier transform ion cynclotron (FT-MS). They are very different in design and performance, each with its own strength and weakness; often they are used in tandem to take advantage of differences (Deutzmann R., 2004).

Quadrupole mass analyzers consists of four parallel rods or electrodes arranged in pairs in an angles of 180° thereby able to form a "tube" of electric fields. (Fig.2.7). As the ions travel through the quadrupole they are filtered according to their *m/z* value so that only a single *m/z* value ion can strike the detector. The *m/z* value transmitted by the quadrupole is determined by the Radio Frequency (RF) and Direct Current (DC) voltages applied to the electrodes. If the pairs of rods have opposite DC voltages and an RF field phase shift of 180°, the quadrupole will produce an oscillating electric field that functions as a filter.

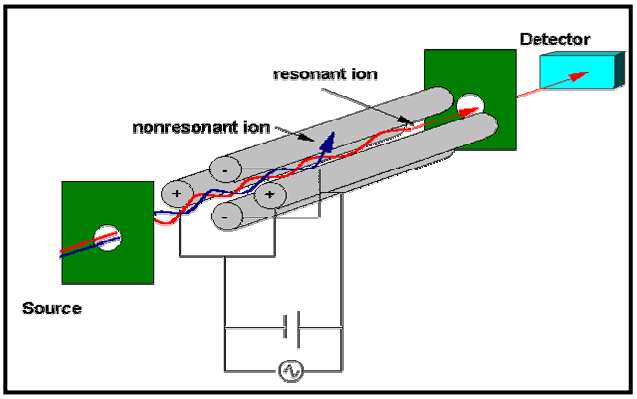

Fig.2.7 Quadrupole mass analyzer scheme.

As the electric field is imposed, the gas-phase ions entering the quadrupole will oscillate according to their *m/z* value and, depending on the RF voltage, only ions of particular *m/z* value will have the correct oscillation path that enables it to pass the filter and reach the detector. The RF and DC fields are scanned (either by potential or frequency) to collect a complete mass spectrum.

One common setup of the quadrupole mass analyzer is used in the **triple-quadrupole** mass spectrometer (Yang L, 2002; Fig.2.8), in which three quadrupoles are aligned with an ESI source. Ions of a specific *m/z* value are selected in the first quadrupole (Q1) and fragmented in the second, which is filled with a collision gas (es. Argon) and works as a collision chamber (MS/MS or CID experiments, Hunt DF. *et al.*, 1986). The fragments are then analysed in the third quadrupole.

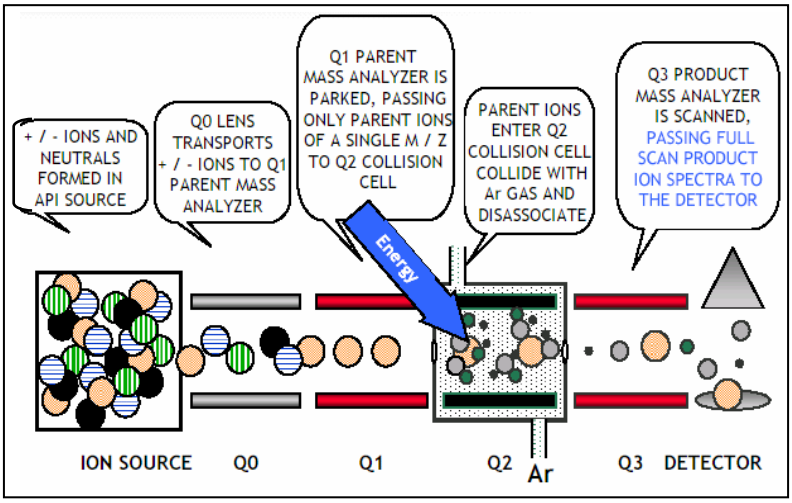

Fig.2.8 Triple-quadrupole mass analyzer

Ion trap analyzer can be aligned with both ESI and MALDI source (Schwartz JC *et al.*, 1996).It composed of a ring electrode and two end-cap electrodes (Fig.2.9). The pulses of an electrostatic ion gate inject ions into the ion trap. A combination of RF and DC voltages is applied to the electrodes to create a quadrupole electric field similar to the electric field for the quadrupole mass analyzer. Initially, the field within the trap is such that all ions that enter the analyzer begin a stable oscillation and are "trapped" in a potential energy well at the centre of the analyzer. Trapped ions are focused into the centre of the trap through the use of an oscillating potential

called the fundamental rf, applied to the ring electrode. An ion will be stably trapped depending upon its *m/z* value. The time during which ions are allowed into the trap, the "ionization period", is set to maximize signal while minimizing space-charge effects. Space-charge results from too many ions in the trap that cause a distortion of the electrical fields leading to an overall reduction in performance. The ion trap is typically filled with helium to a pressure of about 1 mtorr. Collisions with helium dampens the kinetic energy of the ions and serve to quickly contract trajectories toward the center of the ion trap, enabling trapping of injected ions. The mass spectrum is acquired by scanning the RF and DC fields to destabilize low mass to charge ions. These destabilized ions are ejected through a hole in one endcap electrode and strike a detector. The mass spectrum is generated by scanning the fields so that ions of increasing *m/z* value are ejected from the cell and detected.

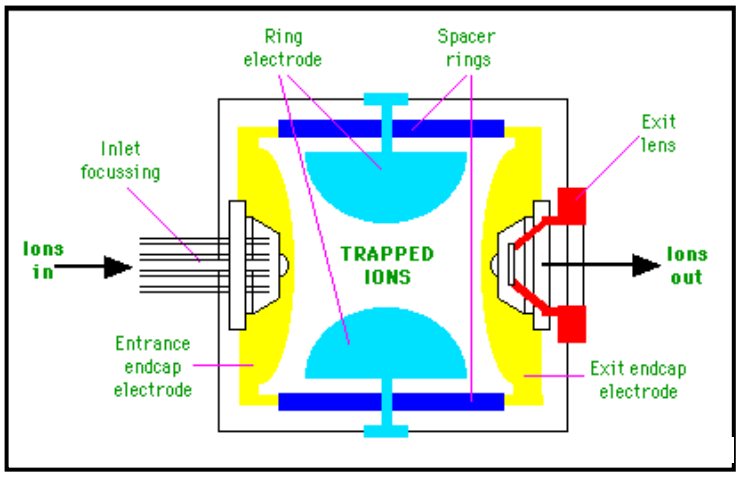

Fig.2.9 Basic components of a typical ion trap mass analyzer.

Ion traps are especially suited to perform MS/MS^n experiments It is possible to selectively isolate a particular *m/z* in the trap by ejecting all the other ions from the trap. Fragmentation of this isolated precursor ion can then be induced by CID experiments. The isolation and fragmentation steps can be repeated a number or times and is only limited by the trapping efficiency of the instrument.

The **linear ion trap** is based on the ion path of a triple quadrupole mass spectrometer in which Q3 is a linear ion trap with axial ion ejection (Fig.2.10). This arrangement allows de-coupling of precursor ion isolation and fragmentation from the ion trap itself. The result is a high sensitivity tandem mass spectrometer with triple quadrupole fragmentation patterns and no low mass cut-off, multiple-reaction monitoring (MRM), as well as precursor and constant neutral loss scanning (Hager JW *et al*., 2003; Hopfgartner G. *et al*., 2004).

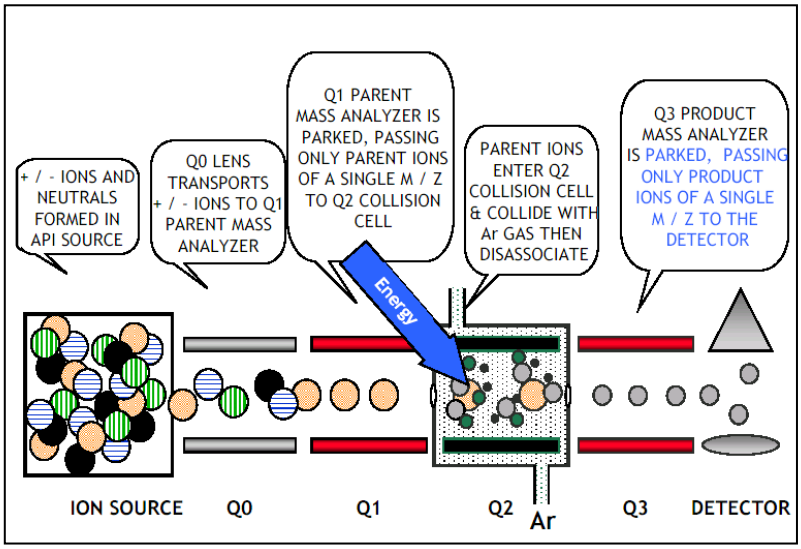

Fig.2.10 Linear Ion Trap mass analyzer

Fourier-transform ion cyclotron resonance mass spectrometry **(FT-ICR-MS** or just **FT-MS)** is probably the most complex method, has the highest mass resolution (> 10^7) and is also useful for tandem mass spectrometry experiments, of course it also very expensive (Zhang LK. *et al*., 2004).
The standard arrangement for the analyser region, of the FT-ICR instrument, is an ion-trap located within a spatially uniform static magnetic field of strength B, that causes ions travel in a circular path (Fig.2.11). The *cyclotron frequency* (ω_c) of the ion's circular motion is determined by the magnetic field strength (B) and the *m/z* value of the ion ($\omega_c = Bz/2\pi m$), this means that by measuring the cyclotron frequency, it is possible to determine an ion's

mass. When the ions enter the ion trap pressure is in the range of 10^{-10} to 10^{-11} mBar with temperature close to absolute zero to minimize ion-molecule reactions and ion-neutral collisions that damp the coherent ion motion. The signal is measured by placing electrodes on each side of the ions circular orbit.

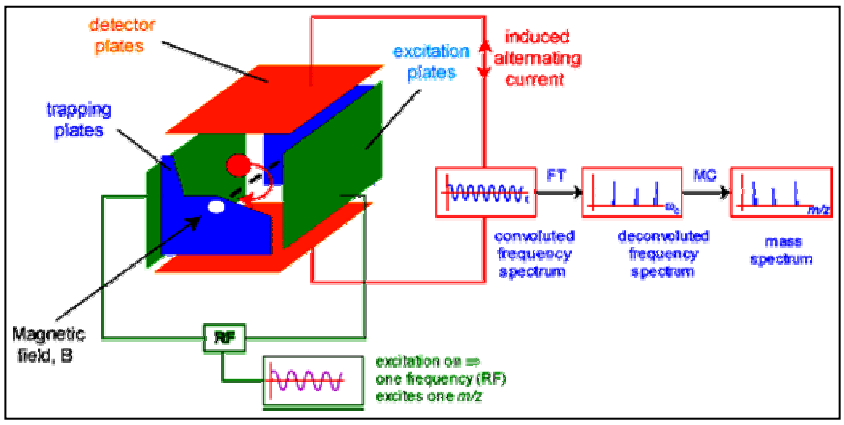

Fig.2.11 FT-ICR-MS scheme.

A fast RF pulse is applied to the transmitter electrodes. Each individual excitation frequency will couple with the natural motion of resonant ions and excite them to a higher orbit where they induce an alternating current between the detector plates. The frequency of this current is the same as the cyclotron frequency of each m/z ion present and the intensity is proportional to the number of ions. The various frequencies and their relative abundances can be extracted mathematically by using a *Fourier transform* which converts a time signal (the image currents) to a frequency spectrum which is then converted to the mass spectrum ($m/z = B/2\pi\omega_c$).
In tandem MS experiments, precursor ions are selected by applying an RF waveform to eject all other ions from the ion trap, so that only the precursors remain. These are accelerated to a higher kinetic energy by applying another RF pulse that increases the precursor ion's radius (kinetic energy). The accelerated ions are trapped for a period of several milliseconds or longer to allow them to collide with the inert gas. The collision gas is either introduced continuously or added with a pulsed valve. The product ions are

then excited into coherent motion with another RF pulse and the ion image currents are detected and transformed.

Time of Fligh (TOF) analyzer is conceptually the simplest spectrometer. Applying a fixed voltage (V) at the source (ca. 20kV) the ionised gas-phase sample is accelerated to a fixed kinetic energy (E_k) and then guided into a high-vacuum field-free flight tube, through which they reach the detector (*Linear mode*, Fig.13). The separation of ion species in the TOF occurs in agreement with the fundamental physical low of kinetic energy:

$E_k = mv^2/2 = zV$

$\downarrow$

$m/z = 2Vt^2/L^2$

E_k= kinetic energy
m = ion mass
v = ion velocity
z = number of charges
V = source potential
L = length of TOF
t = time of flight

Because the flight tube is a field-free region, all the E_k of the ions results from their initial acceleration, therefore a group of ions accelerated with the same constant voltage, at a fixed point and initial time, and allowed to drift in a field-free region, will traverse this region and separate in a time which depends upon their m/z ratios. Measuring that time-of-flight at the detector it is possible to determine the *m/z* value.
Earlier MALDI-TOF spectra were characterised by poor mass resolution due to the distribution of kinetic energy among ions that vary in initial desorption velocity (Beavis & Chait, 1991; Zhou et **al.,**1992) and in energy deficits from collisions within the plume of desorbed matrix during ion acceleration.
In continuous ion extraction linear mode, there was no compensation for ions with the same *m/z* value but different initial velocity. To overcome this problem two improvements have been implemented in present TOF instruments configurations. Firstly, the events of desorption/ionization and acceleration has been separated by applying the acceleration field with a slight delay, up to hundreds of nanoseconds, relative to the laser pulse enabling the ions to be focused (Brown & Lennon, 1995; Vestal *et al*., 1995).
In the DE-mode, in fact, a variable voltage grid in front of the source (Fig.13) allows MALDI-generated ion cloud to expand in a transient field-

free region (grid has the same voltage of source). Then a fast high-voltage pulse (grid has slightly lower voltage than source) creates a potential gradient in the ionization region that accelerates slow ions more then fast ones. This pulse voltage and time delay corrects the initial velocity differences in such a way that identical *m/z* ions arrive simultaneously at the plane of the detector, enhancing resolution of the mass spectrum.
The second improvement was the introduction of a *Reflectron* (Mamyrin *et al*.,1973) at the axial-end of the field-free drift region. Even applying DE-mode, after ions are accelerated and velocity-focused (ions of the same mass align in time), they can defocus flying down the tube causing broadening of signal detector. The reflectron is an electrical mirror, with a voltage potential applied across the sides, which creates a retarding field at a voltage slightly higher than the accelerating one. The ions are sequentially slowed down through the reflector until they stop, turn around and re-accelerate back in a second drift region to a second detector (Reflector Detector, Fig.2.12). Ions species with a kinetic energy lower than the accelerating voltage will penetrate less in the reflector and will turn back sooner (as ions species with higher kinetic energy will penetrate deeper and turn back later) allowing ions of the same *m/z* value and slightly difference in flight times to be packed and focused in space and time to the detector.

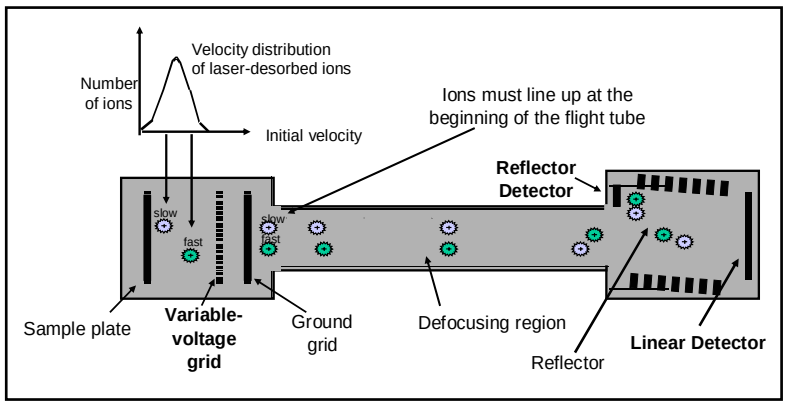

Fig.2.12 Velocity focusing in reflectron mode.

Gas-phase ions generated in MALDI source may decompose before reaching the detector by prompt or metastable defragmentation (Spengler *et al.*, 1991;

Karas *et al*., 2000). Prompt ion fragmentation occurs at the time of the desorption event within the source region and it is generally absent for MALDI generated peptide/protein ions. Metastable ion decay, instead, can be studied with modern MALDI-TOF instruments either using DE technique and linear TOF-MS (In-Source Decay) or, more widely, using the reflector device as an energy analyzer to performed a Post-Source Decay (PSD). "Post source decay" has been chosen as a rather *instrumental* term for any fragmentation phenomena relevant for MALDI-TOF instruments in the field free region, regardless of the location (metastable ion decay, low/high - energy collision induced dissociation) (Spengler B, 1997). Increasing gas pressure is a favourable method for enhancing high-energy Collision Induced Decay (CID). In typical PSD instruments, a complete product spectrum has to be acquired in several steps (> 10). This because the reflector is able to analyze energies (i.e. PSD ion masses) only within certain range with sufficient resolution. This requires the reflectron potential to be stepped down in order to focus lower m/z ions (PSD ions has basically the same velocity but lower energy owing to their lower mass). Finally, all sections of the PSD spectrum have to concatenated by the computer and mass calibrated.

To allow the fragmentation of MALDI-generated precursor ions, MALDI sources have been recently coupled to quadrupole ion-trap mass spectrometers (Krutchinsky, 2001) and two types of TOF instruments: the quadrupole TOF hybrid instrument(QqTOF[1]; Loboda, 2001; Fig.2.13) and the MALDI-TOF-TOF (Medzihradszky *et al*., 2000). A collision cell is inserted between the two analyzer. Ions of a particular *m/z* value are selected in the quadrupole mass filter or in the first TOF, fragmented in the collision cell and the fragments ions masses are read out by a TOF analyzer(Fig.2.14). These instruments have very high sensitivity, resolution, mass accuracy and high speed data acquisition.

During MS/MS analysis, MALDI-TOF-TOF instrument offers the possibility to finely control fragmentation conditions and simultaneously provides both low-energy and high-energy collision induced spectra.

The degree of fragmentation and structural information obtained are related to adjustment in laser intensity, collision gas pressure and collision energy. A collision energy of 1-2 keV in the CID-cell results in the production of low mass internal fragments, ions from amino acid side chain fragmentations, ions specific of particular amino acids increasing the

[1] QqTOF can be used interchangeably with an ESI source.

confidence in the peptide sequence interpretation and identification of multiple proteins from complex mixtures.

In recent years, MS has become one of the most important analytical techniques for the identification of proteins and for the analysis of post-translational modifications (PTM). As a result of its semplicity, excellent mass accuracy, high resolution and sensitivity, MALDI-TOF MS is much commonly used to identify proteins.

Proteolytic digestion of proteins into peptides and mass analysis of peptide mixture provides what is known as *peptide mass fingerprint*. Proteins are then identified by matching the list of experimental peptide masses with the theoretical fingerprints of all sequences in a comprehensive protein database. This method, also referred as peptide mapping, requires an essentially purified target protein and this is the reason why it is commonly used in conjunction with prior protein fractionation using high resolution two-dimensional Polyacrylamide Gel Electrophoresis (2D-PAGE).

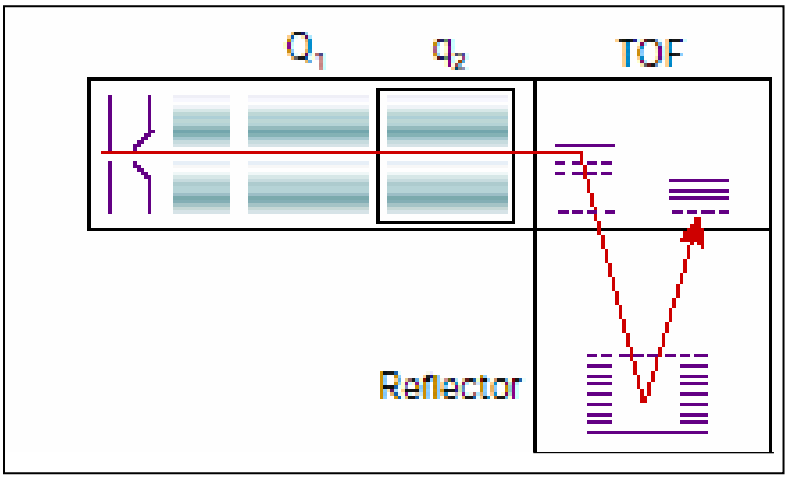

Fig. 2.13. Quadrupole-TOF

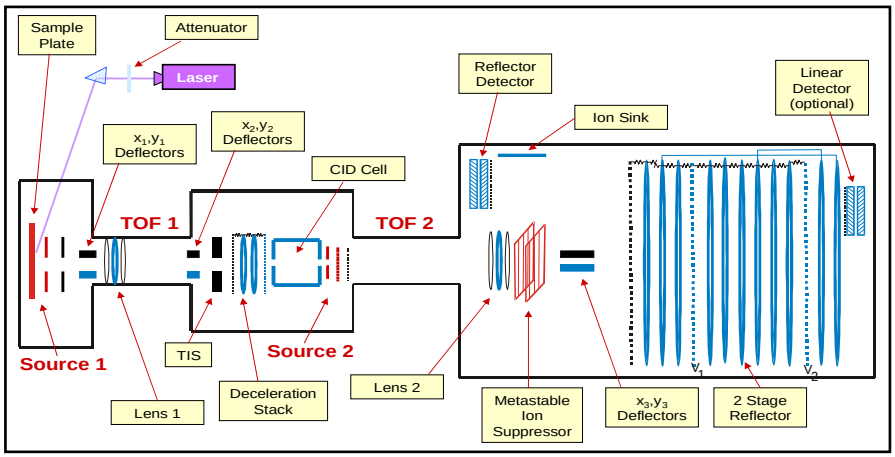

Fig.2.14 MALDI TOF-TOF AB 4700 TOF/TOF™ Ion Optics

3. TWO- DIMENSIONAL ELECTROPHORESIS

Two-dimensional gel electrophoresis (2-DE) (O'Farrell 1975) so far is the only technique able to efficiently separate hundreds or even thousands of proteins or post-translational modified proteins.
The high resolving power of 2-DE enables the separation of high number of protein species like present in a cell proteome.
Proteins are separated according to charge (isoelectric point, pI) by isoelectric focusing (IEF) in the first dimension and according to size (Mr) by SDS-PAGE in the second dimension.
Due to the zwitterionic character of proteins, the electrophoretic mobility of each protein is a characteristic value (pI).
Commercially available immobilized pH gradient gel strips (IPGs) for IEF have solved long time problems of pH gradient instability and irreproducibility (Bjellqvist *et al.*, 1982). IPGs allow the generation of pH gradients of any desired range (broad, narrow or ultra-narrow) between pH 3 and 12 and since sample loading capacity of IPG-IEF is also high, 2-DE with IPGs is a method of choice for micro-preparative separation and spot identification. Anyway, the tremendous heterogeneity and significant differences in abundance of all proteins expressed in eukaryotic cells and tissue makes the analysis of complex cellular proteomes by 2-DE still a big challenge.
What is termed the "classic approach" in proteomics (Dreger, 2003) is characterized by a one-step sample preparation from a crude homogenate followed by 2-DE in order to display the whole map of expressed proteins within the studied system under given physiological conditions. This approach theoretically provides a complete overview of all proteins in the sample based on protein spot patterns. These patterns may be compared between two samples such as a control and an investigated system under specific conditions. These expectations were based on the assumptions of a 2-DE system capable of representing all proteins of the sample and not only for visualizing but also for identification (including their post-translational modifications). Despite the exceptional analytical power of this approach, systematic limitations at the present state of the technology became apparent.

A fundamental question about proteomics is what percentage of a cellular proteome our technology can display.

The number of different proteins in a given time under defined biological conditions is likely to be in the range of several thousand for simple prokaryotic organisms and up to at least 10.000 in eukaryotic cell extracts. Current proteomic studies reveal that the majority of identified proteins are abundant housekeeping proteins that are present in numbers of 104- 106 copies per cell, whereas proteins in much lower concentrations, such as 100 copies per cell, are usually not detected. Consequently, improving methods for enrichment of low-abundance proteins, such as prefractionation procedures, as well as more sensitive detection and quantitation methods, are currently an area of intense investigation. (for reviews Gorg *et al.*, 2004; Molloy 2003; Stasyk, 2004; Lilley *et al.*, 2002). Several prefractionation strategies (subcellular fractionation, affinity purification, fractionation of proteins and peptides according to their physicochemical properties) has been successfully applied to the study of well defined groups of proteins, like proteins of purified organelles, membrane proteins, or proteins isolated through characteristic PTMs (Wu & Yates, 2003; Mann & Yensen 2003; Dreger, 2003). Fractionation and sample enrichment can be fundamental first steps to increase analysis resolution , however none of the currently available proteomics techniques allows the analysis of an entire proteome. Technological developments of last years in proteomics field has resulted in the definition of several "-omics", like phosphoproteomics, membranomics, degradomics, immunoproteomics, complexomics, glycoproteomics, secretomics, etc. Together these fields cover the various aspects biological and pathological processes whose data and knowledge have to be fully integrate to a complete overview of a biological system.

4. HEPATITIS C VIRUS (HCV)

4.1 Epidemiology and history

The estimated worldwide prevalence of HCV infection is 2.2%, or approximately 130 million HCV-positive persons (Centers for Disease Control and Prevention [CDC], unpublished data, 2003). Region- or country-specific overall prevalence does not necessarily reflect the risk for spread of HCV because this risk is not homogenous either between or within most countries. Age-specific HCV prevalence rates are more variable, and their patterns provide clues to geographic and temporal differences in the risk for acquiring HCV infection Throughout the world, blood transfusion from infectious donors, unsafe therapeutic injection practices, and injection drug use have been the predominant modes of spread for hepatitis C virus (HCV) infection. In most developed countries, blood donor testing has virtually eliminated transfusion-related transmission of HCV. In these countries, injection drug use has been the major risk factor for HCV infection during the past 10 years, and the highest prevalence of infection is found in young to middle-aged adults. In many developing countries, unsafe therapeutic injection practices appear to be responsible for the geographic clustering of high rates of infection because of inadequate or nonexistent supplies of sterile syringes, administration of injections by non-professionals outside the medical setting (Higuchi, 2002).

Hepatitis C was first recognized as a separate disease entity in 1975 when the majority of cases of transfusion-associated hepatitis were found not to be caused by the only two hepatitis viruses recognized at the time, hepatitis A virus and hepatitis B virus. The disease was called "non-A non-B hepatitis," and it was demonstrated to be transmissible to chimpanzees (Alter H.J. *et al.,* 1978; Tabor E. *et al.,* 1978). It was not until 1989, however, that the cloning and sequencing of the viral genome of the non-A non-B hepatitis virus was first reported (Choo *et al.,* 1989) and the virus was renamed "hepatitis C virus" (HCV).

HCV shares genomic organization and slight sequence identity with flaviviruses and pestiviruses and it has been classified in a separate genus (*Hepacivirus*) within the Flaviviridae family (Francki *et al*., 1991).

HCV exhibits significant genetic heterogeneity as a result of the accumulation of mutation during viral replication. This high mutation rate, which is characteristic of RNA viruses, can be attributed to an error-prone

RNA-dependent RNA-polimerase that lacks proofreading activity. HCV circulates in an infected individual as a population of closely related, yet heterogeneous, sequences, defined as "quasispecies" (Forns *et al*., 1999).
This genetic diversity is not evenly distributed in the viral genome. The non-coding regions are relatively conserved, while the envelope regions, especially Hypervariable region 1 (HVR1) located at the N-terminus of the envolope protein E2 (see later description of HCV genome), have the highest mutation rate. This genetic diversity resulted in the classification of HCV into at least 6 major genotypes (1 to 6) and many subtypes, based on the analysis of the NS5 region (Simmonds P, 1993). Different genotypes may differ by 30 to 35% of their viral genomes, while subtypes may differ by 15-20% of their nucleotide sequences.

4.2 Natural Course of Disease

Being infected with HCV does not necessarily mean that liver disease will occur and anyway it can take several years – decades, in many cases – for HCV to cause life-threatening liver disease.
Soon after HCV enters the body, it infects hepatocytes cells. Only a small number of people (approximately 25%) actually experience symptoms of infection, such as fatigue, decreased appetite, nausea, or jaundice (yellowing of the skin and eyes). However, almost all people infected with HCV experience an increase in their liver enzymes – such as serum alanine aminotransferase (ALT) – which can be detected by a simple blood test. An increase in ALT means that some liver cells are becoming damaged by the HCV infection.
Approximately 15% of people who are infected with HCV are able to clear the virus from their bodies, usually within six months after becoming infected. However, the majority of people (85%) who are infected with HCV have "chronic" hepatitis C – an infection that will stay with them for life. Of the 85% people with chronic hepatitis C, approximately 20% of them will remain healthy – their liver enzymes will stay normal, even though HCV can be detected in their livers and in their blood, and they will not go on to develop liver disease or experience symptoms of the infection. The remaining 60-65% people with chronic hepatitis C will go on to experience some signs and symptoms of liver disease, such as fatigue, nausea, muscle aches, and abdominal pain – usually after 13 to 15 years of being infected with HCV. Approximately 20-25% of these people, usually after 20 years of

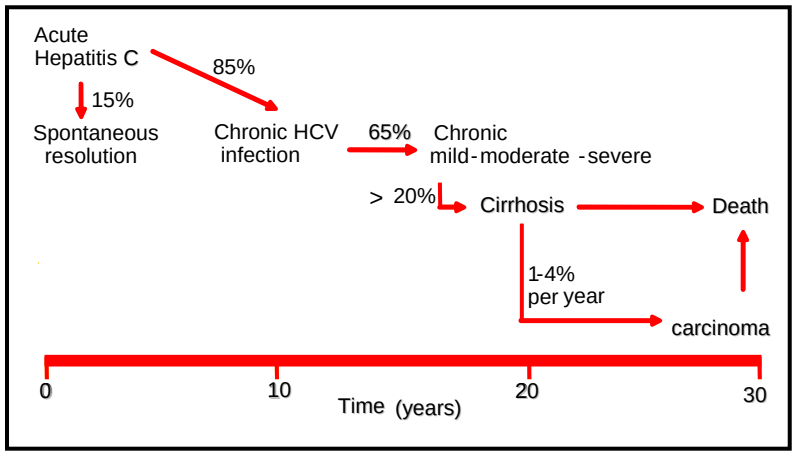

Fig. 4.1 Natural courses of HCV infection.

HCV infection, will develop cirrhosis – a scarring of the liver that results from widespread fibrosis (an extreme overgrowth of the liver's connective tissue). Although cirrhosis is not life threatening, it can affect the way the liver works and increases the risk of liver cancer. Of the 20-25% people with HCV who develop cirrhosis, 5-10% of them will develop liver cancer and possibly liver failure after another five years (Fig. 4.1).

4.3 HCV Genome and Polyprotein Processing

HCV is an enveloped virus with a 9.6-kb single-stranded RNA genome of positive polarity comprising a 5' untranslated region (UTR), a large open reading frame (ORF) encoding a large polyprotein of about 3000 amino acids, and a 3' UTR.
Translation of the viral RNA occurs through a cap-independent mechanism via an internal ribosomal entry site (IRES) located in the 5' UTR (fig. 4.2).
A combination of cellular and virally encoded protease activities leads to processing of the polyprotein into individual structural and non-structural proteins (Lohmann *et al.*, 1996). At the amino terminal of the polyprotein three ***structural proteins*** have been identified. The **Core** protein which forms the viral nucleocapsid (Yasui K, 1998) and shows a number of regulatory functions (Ray *et al.*, 2001; Yao *et al.*, 2001a) and the

envelope proteins **E1** and **E2**, which form noncovalent E1E2 heterodimers present at the surface of the HCV particles (fig.4.3), likely to mediate virus entry (Voisset *et al*., 2004). E1 and E2 are both highly glycosylated and supposed to be retained into host cell in the endoplasmic reticulum (Duvet S. *et al.*, 1998; Cocquette L. *et al.*, 1999). Structural proteins are processed by a still unknown cellular protease. Further proteolytic processing, by host peptidases, of the region between E2 and the non-structural proteins, yields a short hydrophobic peptide, **p7**. Its viral function is unknown but in host cell seems to be located on the Endoplasmic Reticulum (ER) and to function as a membrane channel (Carrère-Kremer, 2002; Pavlovic, 2003). The C terminal region of the polyprotein encodes for the ***non-structural (NS) proteins*** NS2, NS3, NS4A, NS4B, NS5A, and NS5B (fig.4.2).

NS2 and the amino-terminal domain of NS3 form the viral protease responsible for the autocatalytic cleavage at the NS2-NS3 junction (Reed *et al.*, 1995). Although the catalytic mechanism remains elusive, several studies have been reported on the **NS2/3** protease suggesting it is zinc-dependent with putative cysteine and histidine catalytic residues (Reed *et al.*,1995; Pieroni *et al.*, 1997)**.** Following proteolytic cleavage events, involved in the maturation of the NS proteins, are carried out by the major viral serine protease, **NS3**, in association with its cofactor, **NS4A** (Bartenschlager *et al*., 1994 and1995). In addition to its function as a protease, NS3 also contains helicase and nucleoside triphosphatase activities within its C-terminal domain (Kim *et al.*, 1995). Specific replicative functions have not been identified for **NS4B** and **NS5A**, but both are likely to contribute to the viral replicase complex. NS3/4A and NS5A appear to play important roles in modulating antiviral responses within infected cells and in promoting long-term persistence of the virus (Foy *et al.*, 2003; Lan *et al.*, 2002; Gale *et al.*, 1998; Pawlotsky *et al.*, 1999). NS5B constitutes the HCV RNA-dependent RNA polymerase and is thus the catalytic core of the replicase (Lohmann *et al*., 1997). It belongs to a class of integral membrane proteins termed tail-anchored proteins and its membrane association is essential for hepatitis C virus RNA replication (Moradpour *et al*., 2004).

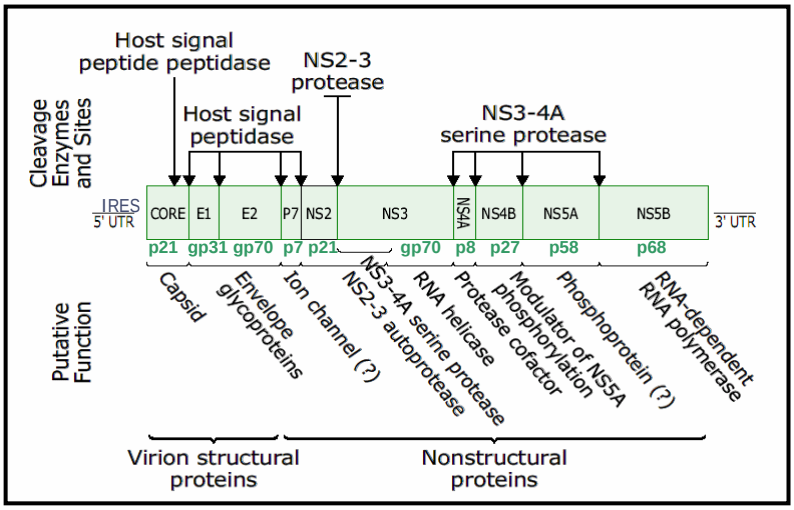

Fig.4.2 HCV genome processing and cleavage products of the polyprotein

HCV 9.6-kb positive single-stranded RNA genome comprising a 5' untranslated region (UTR), a large ORF of encoding all viral proteins, and a 3' UTR. 5' UTR contains the IRES which mediates cap-independent translation initiation and is necessary for efficient HCV replication. The functions of the gene products produced after co- and posttranslational polyprotein processing by host signal peptidases and HCV-encoded proteases are indicated in the Figure. The 3' UTR contains a poly (U/UC) tract immediately following the ORF stop codon and conserved RNA elements essential for HCV replication.

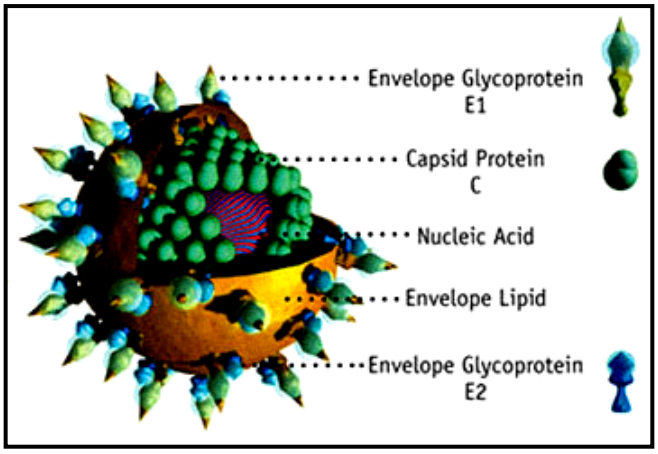

Fig. 4.3 HCV virion structure

4.4 HCV Life Cycle

HCV normally replicates into hepatocytes cytoplasm, but low efficiency viral replication into Peripheral Blood Mononuclear Cells (PBMC) has also been observed (Cribier *et al*., 1995; Fournier *et al*., 1998).
The lack of efficient cell culture system and a convenient animal model has been majors roadblocks for unrevealing the details of HCV replication. Based largely on analogies to the other members of the *Flaviviridae* family, the life cycle of HCV (Bartenschlager, 2000) can be summarized as follows (Fig.4.4): (1) penetration of the host cell and liberation of the genomic RNA from the virus particle into the cytoplasm; (2) RNA translation, processing of the polyprotein and formation of a replicase complex associated with intracellular membranes; (3) utilization of the input plus-strand for synthesis of a minus-strand RNA intermediate; (4) production of new plus-strand RNA molecules which in turn can be used to synthesize new minus strands, for polyprotein expression or packaging into progeny virions; (5) release of virus from the infected cell.

Virus entry. Several candidate receptors for HCV entry have been reported over the past years. Based on the observation that HCV RNA-containing particles are often associated with low-density or very-low-density lipoproteins and that these low-density fractions are infectious for chimpanzees, the low density lipoprotein receptor (LDLr) has been proposed LDLr to mediate uptake of HCV particles (Agnello *et al*., 1999). CD81, a cell surface tetraspanin capable of selective binding E2 glycoprotein, was identified (Pileri *et al*., 1998) and later the scavenger receptor B1 (Scarselli *et al*., 2002).
Recently, infectious HCV pseudotype particles (HCVpp) that are assembled by displaying unmodified HCV envelope glycoproteins on retroviral core particles have been successfully generated (Bartosch, 2003). They mimic the function of native HCV particles, thus representing a model to study the early steps of its life cycle. The noncovalent E1E2 heterodimers present at the surface of the HCVpp, which contain complex-type glycans indicating modification by Golgi enzymes, are likely to mediate virus entry and the CD81 with SR-BI are required for HCVpp entry (Voisset, 2004).
However, these two proteins are not sufficient to provide entry functions in non permissive cells and their widespread distribution does not explain the hepatocyte tropism of HCV, suggesting that additional unidentified cellular factor(s) are necessary for HCVpp entry.

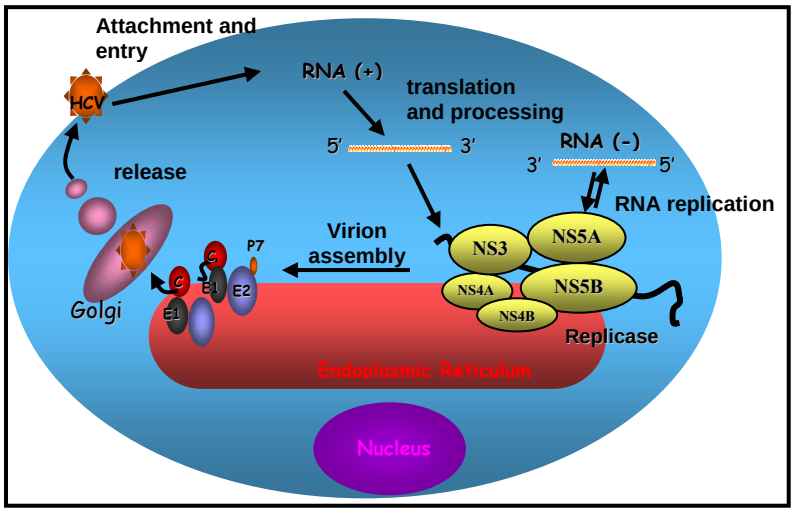

Fig.4.4 Hypothetical model of the HCV replication cycle. Upon infection of the host cell the (+)-strand RNA genome is liberated into the cytoplasm and translated. The polyprotein is processed and viral proteins remain tightly associated with membranes of the ER. (-)-strand RNA is synthesized by the replicase NS3–5B complex and serves as template for production of excess amounts of plus strand. Via interaction with the structural proteins (+)-strand RNA is encapsidated. Particles are enveloped by budding into the lumen of the ER and virus particles are exported via transit through the Golgi complex.

Translation of the incoming genome RNA is mediated by a highly conserved RNA element that functions as an internal ribosome entry site (IRES) capable of directly binding to initiation factor eIF3 and the 40S ribosomal subunit (Ji *et al*., 2004; Otto *et al*., 2004). Directed by the IRES, the polyprotein is translated at the rough endoplasmic reticulum (ER) and cleaved co- and post-translationally, into 10 mature proteins by the action of host cell and viral proteinases. The order and nomenclature of the HCV proteins is: NH2-C-E1-E2-p7-NS2-NS3-NS4A-NS4B-NS5A-NS5B-COOH Processing of the polyprotein is essential to form an active HCV RNA replicase. The HCV **RNA replication** machinery, or "replicase," is cytoplasmic and membrane-associated (Dubuisson *et al*., 2002; El-Hage&

Luo, 2003) consisting of at least NS3-NS5B, together with additional, as yet undefined, host components. The major enzymatic components of the HCV replicase are the NTPase/helicase activity of NS3 and the NS5B RNA-dependent RNA polymerase (RdRP). The first step in the RNA replication process involves the synthesis of a complementary negative-strand copy of the incoming genome RNA (Fig.4.5).

Although confusion exists in the literature, it is generally believed that the minus-strand synthesis occurs by a primer-independent de novo initiation mechanism (Luo *et al*., 2000; Zhong *et al*., 2000). The negative-strand template is then used for synthesis of additional genome-length RNAs that can in turn be used for translation, replication, or packaging into progeny virus.

Assembly and release. In the absence of systems allowing the production virus particles, the assembly assembly and release of HCV cannot be studied in detail. Based on results with other members of the *Flaviviridae*, it seems likely that HCV buds into intracellular vesicles and is transported out of the cell by the host secretory pathway and released into the extracellular space.

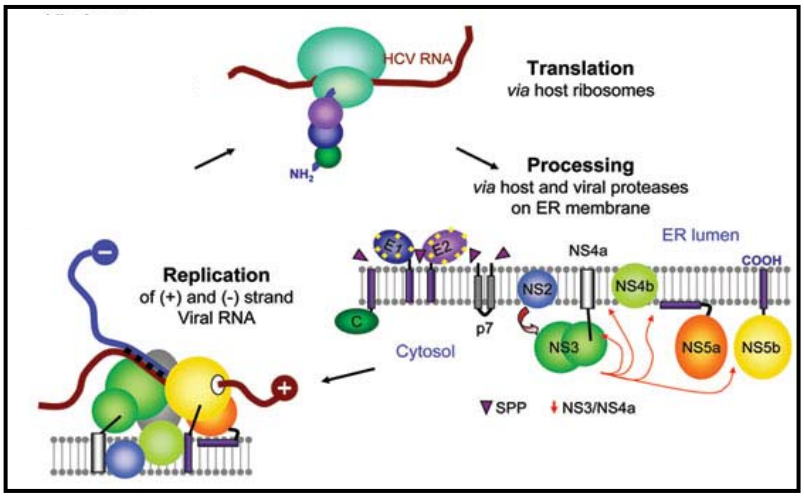

Fig.4.5 HCV Replication Complex. Non-structural HCV proteins in Huh7 cells were colocalized to the perinuclear ER membranes carrying a replicating HCV RNA (Gosert *et al*., 2003).

4.5 Cell-based model systems for HCV replication investigation

Investigation of HCV replication mechanisms and the cellular consequences of HCV infection have been significantly limited by the absence of an efficient in vitro infection-replication system, as well as the lack of a suitable small animal model. However, a major breakthrough came in 1999 when Lohmann and colleagues (Lohmann *et al.*, 1999) described engineered subgenomic HCV RNAs, or "replicons," that were capable of limited replication in a human hepatoma Huh-7 cell line (Fig 4.6). RNA replicons are defined as HCV RNA molecules that are capable of autonomous replication in an appropriate cell type. Based on the assumption that high expression levels of the structural proteins might be cytotoxic (Moradpour *et al*., 1998) and the observation that for flavi- and pestiviruses the structural proteins are not required for RNA replication (Behrens *et al*., 1998; Khromykh &Westaway, 1997), the sequences of the structural proteins were deleted. To allow selection for only those cells in which HCV efficiently replicates, the gene encoding the neomycin phosphotransferase, conferring resistance to the antibiotic G418, was introduced downstream of the HCV IRES (Fig.4.7). A second IRES element, derived from the picornavirus encephalomyocarditis virus, was included to allow translation of the HCV NS proteins.

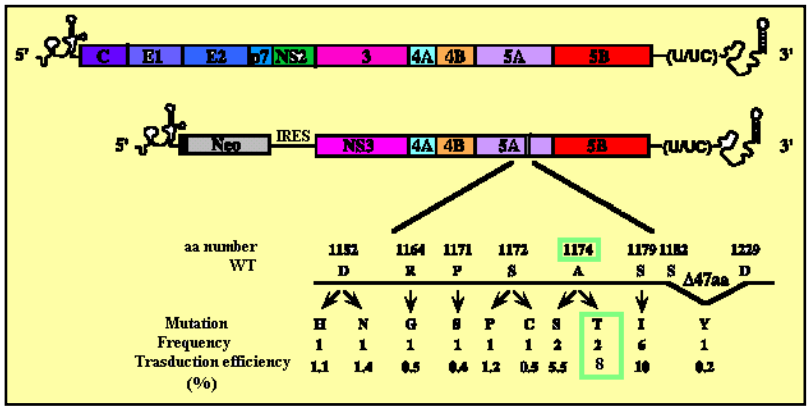

Fig.4.6 HCV replicons (Lohmnann *et al.*, 1999)

These autonomously replicating RNAs expressing only NS proteins could initiate and maintain replication in the human Huh-7 hepatoma cell line but just at low frequency. Diverse spectrum of mutations (mostly in NS5A region but also in NS3, NS4B, and NS5B) was later identified to enhance the ability of HCV (genotype 1b) to replicate in Huh-7 cells, as well as genome-length, selectable HCV RNAs that express all of the viral proteins (Lohmann *et al.,* 2003, Lohmann *et al.,* 2001, Krieger *et al.,* 2001, Blight *et al.,* 2000, Ikeda *et al.,* 2002, Pietschmann *et al.,* 2002).

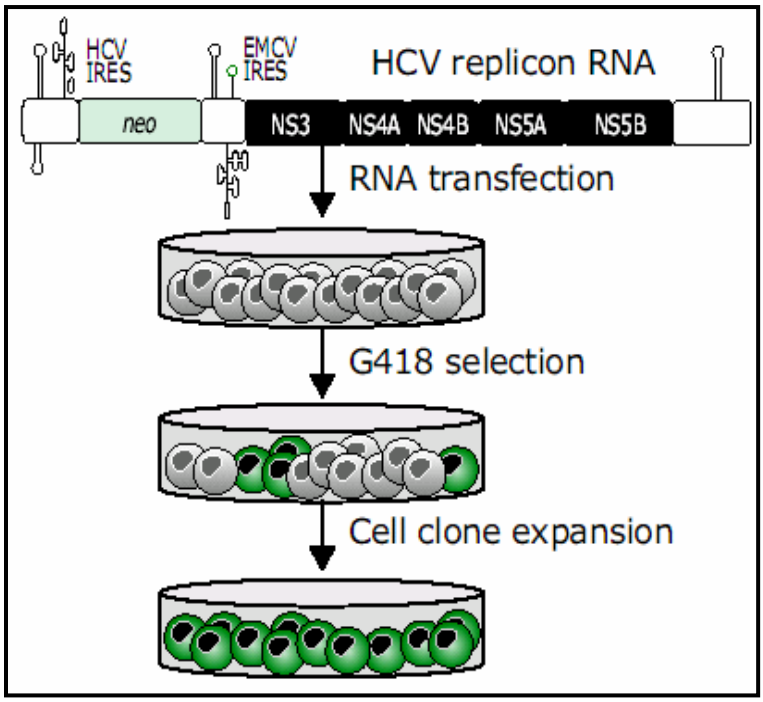

Fig.4.7 HCV-replicon-containing cell lines. RNA constructs containing the gene encoding neomycin phosphotransferase (neo) upstream of the HCV genes are transfected into Huh7 cells. The IRES of HCV drives translation of neo, and the encephalomyocarditis virus (EMCV) IRES directs HCV polyprotein translation. Transfected cells (grey) are selected by exposure to neomycin sulfate (G418) so that only those expressing neomycin phosphotransferase (green), and thus replicating HCV, survive.

These RNAs replicate efficiently and stably under selective pressure in Huh7 cells, however, their replication is strongly influenced by the proliferation status of the host cells, with the abundance of viral RNA rapidly declining when cells reach high density (Pietschmann *et al.,* 2001). The mechanism that underlies this requirement for host cell proliferation has not been identified yet, but it is possible that HCV RNA replication is more permissive in certain phases of the cell cycle than in others. It is likely that in well-established cell clones supporting HCV RNA replication, a balance is reached between HCV RNA degradation and S-phase-stimulated new synthesis, resulting in stable, homeostatic HCV RNA expression throughout the cell cycle (Scholle *et al*., 2004) .

Although little is known about the mechanism underlying cell culture adaptation and the role of host cells factors required for HCV replication (Huh-7 hepatoma cells still are the only cell line supporting efficient replication of HCV RNAs) replicon-containing cells have provided a source of active replicase for biochemical studies and a significant advance in the study of HCV biology.

5. HCV and CRYOGLOBULNS

Long-term HCV infection is often associated with B-cell immune-mediated pathologies, such as Mixed Cryoglobulinemia (MC), production of autoantibodies, the appearance of rheumatoid factors (RF) and eventually development of B-cell non-Hodgikin's lymphomas (B-NHL).
The term cryoglobulinaemia refers to the presence in the serum of one (monoclonal cryoimmunoglobulinaemia) or more (mixed cryoglobulinaemia) immunoglobulins, which precipitate at temperatures below 37°C and redissolve on rewarming. This is an *in vitro* phenomenon; the real mechanism(s) of cryoprecipitation remains obscure. It could be secondary to the intrinsic characteristics of both monoclonal and polyclonal immunoglobulin (Ig) components and can also be caused by interaction among single components of the cryoprecipitate. Different hypotheses have been suggested to explain this phenomenon, including structural modification of the variable portions of Ig heavy (H) and light (L) chains (Middaugh *et al*., 1987); non-specific Fc–Fc interactions to explain the self aggregation of some Igs, in addition to specific interactions involving the IgM cryoprecipitable rheumatoid factor (RF) and the Fc portion of IgG, the corresponding autoantigen (Gyotoku *et al.*, 1987).
Light scattering analysis of the dynamics of cryoaggregation suggests a slow, termodynamically disadvantageous initiation process maybe related to the formation of aggregates of small size (i.e. immuno complexes, IC) as nucleation event (Di Stasio *et al*., 2003). Di Stasio and coworkers also propose that the formation of insoluble cryoglobulin cluster occurs in four distinct step, that for MC can be describe in the following way:

1) $IgM + nIgG \leftrightarrow IgM(IgG)_n = IC$
2) nICs + other factors? → Cluster
3) Increased cluster concentration
4) cluster precipitation

They found that increasing the concentration of cryoglobulins, the system is driven to increase the number of clusters but not their size. This suggest that the temperature is the factor regulating the size of clusters while the protein concentration regulates their number.
Cryoglobulinaemia is usually classified into three subgroups, according to Brouet and colleagues (Brouet *et al*., 1974): type I, composed of a single

monoclonal immunoglobulin; types II and III, characterised by polyclonal IgG and monoclonal or polyclonal IgM RF, respectively. The main biological and clinico-pathological characteristics of these subgroups are reported in Table 1. Cryoglobulinaemia type I is found mainly in patients with overt lymphoid tumours; MC types II and III can be associated with different infectious, immunological, or neoplastic diseases.

Classification of cryoglobulins

	Type I cryoglobulinaemia	Type II mixed cryoglobulinaemia	Type III mixed cryoglobulinaemia
Composition	Single monoclonal Ig mainly IgG, IgM, or IgA, or monoclonal free light chains	Presence of monoclonal component: usually IgM, IgG, or IgA and polyclonal Ig (mainly IgG)	Polyclonal mixed Ig (all isotypes)
Biological characteristics	Self aggregation through Fc fragment of Ig	RF activity of monoclonal component against Fc portion of polyclonal Ig predominant, cross idiotype Wa mRF	RF activity of one polyclonal component (usually IgM)
Pathological characteristics	Tissue histological alterations of underlying disorder	Leucocytoclastic vasculitis, B cell expansion, and tissue B cell infiltrates	Leucocytoclastic vasculitis, B cell expansion, and tissue B cell infiltrates
Clinical associations	Lymphoproliferative disorders: multiple myeloma, Waldenstrom's macroglobulinaemia, chronic lymphocytic leukaemia, B cell NHL	Viral, bacterial, parasitic infections (mainly HCV, less HBV, others), autoimmune diseases, lymphoproliferative disorders rare in essential form	Viral, bacterial, parasitic infections (mainly HCV, less HBV, others), autoimmune diseases, lymphoproliferative disorders rare in essential form

HBV, hepatitis B virus; HCV, hepatitis C virus; Ig, immunoglobulin; m, monoclonal; NHL, non-Hodgkin's lymphoma; RF, rheumatoid factor.

Tab.5.1 Classification of cryoglobulins (Ferri et al., 2002).

The "essential" MC was first described by Meltzer et coworkers in 1966. Originally, this term was referred to as autonomous disease, when other known systemic, infectious or neoplastic disorders had been ruled out. Essential MC syndrome is clinically characterized by the so called Meltzer triad (purpurea, weakness and anthralgias) and by a series of pathological conditions, including chronic hepatitis, diffuse vasculitis, membrano-proliferative glomerulonephritis (MPGN), peripherl neuropathy, porphirya cutanea and less frequently by lymphatic and hepatic malignancies (Meltzer *et al*., 1966; Gorevic *et al*., 1980).
Since chronic hepatitis is frequently observed during the clinical course of MC, after the discovery of hepatitis C virus (HCV) as the major aetiological agent of non-A/non-B chronic hepatitis, an increasing number of epidemiological studies suggested an important role for HCV (70-90%) in the pathogenesis of MC (Ferri *et al*., 1991; Agnello *et al*., 1992). Therefore the term "essential" no longer seemed to be appropriate for most patients with MC (Trendelenburg *et al.*, 1998).

HCV has been recognised to be both a hepatotropic and lymphotropic virus, as suggested by the presence of active or latent viral replication in the peripheral lymphocytes of patients with type C hepatitis or MC (Zignego *et al*., 1992; Ferri *et al*., 1993). The infection of lymphoid tissues could represent an HCV reservoir that contributes greatly to viral persistence; moreover, the quasispecies nature of HCV permits it to escape immune surveillance and favours the persistence of infection in the host. These biological characteristics may explain the appearance of a constellation of both autoimmune and lymphoproliferative disorders in HCV infected individuals (Gumber *et al*., 1995). However, the lymphomagenic role of HCV is still a matter of debate. The HCV related lymphoproliferation, varying from the benign ployoligoclonal B-cell expansion frequently observed in MC patients to overt lymphoma, seems like a multifactorial and multistep process for which multiple genetic aberrations are probably necessary (Ferri *et al*., 2002)

There is remarkable geographical and racial heterogeneity in the prevalence of MC as well as other HCV-related immuno-lymphoproliferative disorders (Lenzi *et al*., 1991; 1998). This variability suggests that HCV per se may be insufficient to drive malignant lymphoma. Unknown genetic and/or environmental cofactors are possibly required for the full expression of malignancy. Moreover, HCV viral genome is not integrated into the host genome, therefore it has been proposed that HCV infection exerts a chronic stimulus on the immune system, which facilitates the development and selection of abnormal clones (Ferri & Zignego, 2000). The most plausible pathogenic hypothesis supposes that specific B-cell clones proliferate, mainly in the bone marrow and liver tissue, as a consequence of a chronic antigenic stimulation exerted by HCV associated antigens (De Vita *et al.*, 2000).

The continuous expansion of such chronically stimulated B-cells may represent a risk for malignant transformation.

De Re et coworkers supports such a pathogenic hypothesis, suggesting that premalignant and malignant lymphoproliferations in an HCV- MC patients were sequential phases of an antigen (HCV E2 protein)-driven pathologic process (De Re *et al*., 2000b). The binding of HCV-E2 on CD81 could finally results in an increase of V-D-J Ig gene rearrangements in antigen reactive B cells (Fig.5.1). One possible consequence could be the bcl2 gene recombination seen in an appreciable number of HCV infected individuals, and particularly in patients with MC. The bcl2 aberration may explain, at

least in part, the B cell expansion and the wide autoantibody production seen in HCV infected individuals (Zignego *et al*., 2002).
Other support to the antigen-driven pathogenesis hypothesis derives by the observation that HCV infection of B cells likely stimulates the production of oligoclonal-, monoclonal- IgM with rheumatoid factor activity (IgM RF).

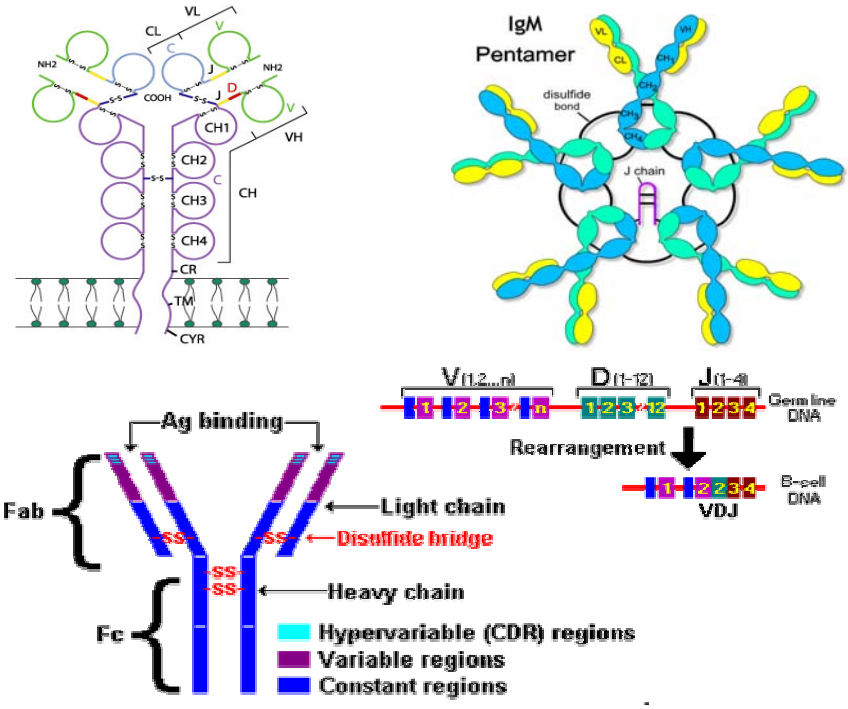

Fig.5.1 Schematic representation of IgM structure. Upon stimulation by antigen, the B-cell will differentiate into a plasma cell expressing large amounts of secreted IgM. IgM is a cyclic pentamer which is multivalent, and has 5 J-chains to hold it together. it contains TEN antigen binding sites (Fab) During differentiation of the B-cells rearrangement, recombination and mutation of the immunoglobulin V, D, and J regions occurs to produce functional VJ (light chain) and VDJ (heavy chain) genes. At this point, the antigen specificity of the mature B-cell has been determined. *Idiotypes,* determined by the amino acid sequence and corresponding three-dimensional structure of the variable region, reflect the antigen binding specificity of any particular antibody molecule. When Ig binds bound to pathogens, the Fc (crystallisable) portion can activate the complement system (classical pathway activation) and *Opsonization* (Ig Fc region can bind to receptors on macrophages and aid phagocytosis).

Like natural autoantibodies, monoclonal RFs share a common complementary determining region (CDR) idiotype. Clonal analysis of intrahepatic B cells from HCV patient with and without MC reveals the production of a cross idiotype WA CDR, expressing specific VH and VK germinal genes (Fig.5.1) proteins (human Kv 325), in most Type II MC patients (Sansonno *et al.*, 1998). Cross idiotype WA monoclonal RF has also been demonstrated in other B cell lymphoproliferative disorders, probably an expression of antigen indipendent clonal B cell lymphoproliferation. For almost all NHLs, both heavy and light chain CDR3 regions[2] show the highest similarity to antibodies with RF activity that have been found in MC syndrome. This suggests that the same antigen might be the triggering factor of both primary and lymphoma associated type II MC. Because type II and type III MC occur in a variety of infectious diseases, we could speculate that they are the result of chronic stimulation of the immune system by complexes composed of autologous IgG and antigen(s) of the involved infectious agent. When complexed, the IgG becomes autoantigenic and it can elicit the Wa or other RFs (Iavanovski *et al.*, 1998; Dammacco *et al.*, 1998).

The close association between IgM RF-WA and VDJ rearrangements suggests the accumulation of somatic mutations in Ig V genes forms the molecular basis for the production of Abs with high affinity. The preferential expansion of one clone would in turn lead to a monoclonal pattern. It should be emphasized that this pattern (IgM RF-WA) was observed only in HCV patients with cryoglobulinemia (De Re *et al.*, 2000). In particular, sequence analysis of the immunoglobulin antigen receptor of HCV-associated NHL suggests that the malignant cells are derived from the RF-producing cells that occur mainly in Type II CM. IgM RF-WA, in fact, are the same proteins that characterize the 2D-PAGE pattern of HCV Type II MC (Tissot *et al.*, 1999; Damoc *et al.*, 2003).

Patients with type II MC can develop a B cell lymphoma, usually after long term follow up (Pozzato *et al.*, 1994). However, unlike frank malignant lymphomas, they tend to remain unmodified for years or even decades, and are followed by overt lymphoid tumours in about 10% of cases only (Monteverde *et al.*, 1997).

Different HCV related diseases show a clinico-serological overlap with MC, suggesting that MC may represent a "crossroad" between a classic

[2] Antibody specificity is primarily dependent on CDR3 region, the most variable part of V region.

autoimmune disorder (such as autoimmune hepatitis, sicca syndrome, glomerulonephritis, thyroiditis, etc) and malignancy (such as B cell lymphoma, hepatocellular carcinoma) (Fig 5.2).
Thus, proteomic analysis of MC can provide further elucidation on the complex pathway involving the immune response to HCV infection and the consequential autoimmnune and lymphoproleferative disorders.

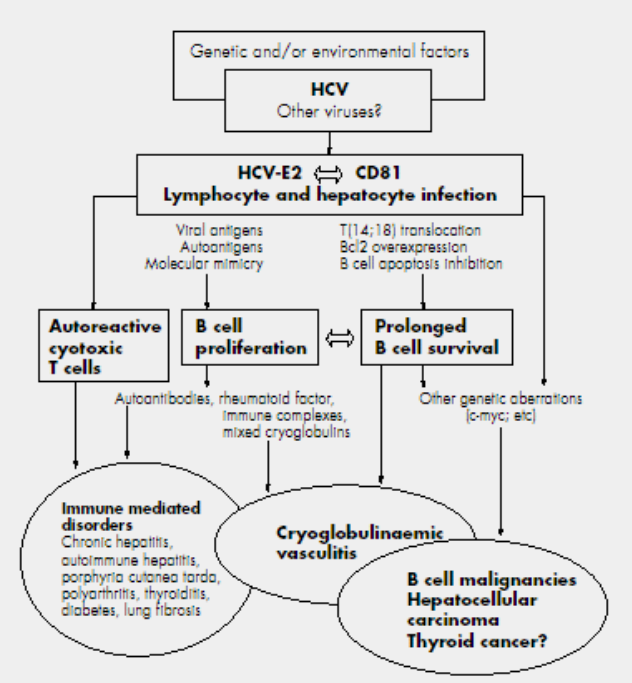

Fig. 5.1 Possible aetiopathogenesis of MC and other HCV related disorders. HCV infection exerts a chronic stimulus on the immune system. The interaction between HCV envelope protein E2 and CD81 on both hepatocytes and lymphocytes may be an important step in the cascade of events. T(14;18) translocation is commonly found in HCV infected individuals, particularly in patients with MC. The activation of the Bcl2 may lead to prolonged B cell survival. B cell expansion is responsible for the production of various autoantibodies, including RF and cryoprecipitable immune complexes. Consequently, various autoimmune disorders and cryoglobulinaemic vasculitis may develop. In a minority of cases, indolent B cell proliferation may be complicated by frank malignant lymphoma. HCV is the major causative factor of hepatocellular carcinoma. MC seems to represent a crossroad between these autoimmune and neoplastic disorders (Ferri & Zignego, 2000).

6. SEVERE ACUTE RESPIRATORY SYNDROME - CORONAVIRUS (SARS-CoV)

6.1 Epidemiology and History

Severe Acute Respiratory Syndrome (SARS), was firstly recognized following outbreaks of cases of severe atypical pneumonia among healthcare workers in hospitals in Hanoi and Hong Kong, which led WHO to issue a global alert on 12 March 2003 followed by a heightened global health alert on 15 March after cases were also identified in Singapore and Canada. It was later recognized that the starting point of the epidemic could be traced back to the Guangdong province of Southern China where initial cases occurred in November 2002 and from which it was carried out in February to Hong Kong and subsequently to some 30 countries around the world. According to the records of the World Health Organization, the epidemic had resulted in 8439 probable cases of SARS of which 812 were fatal, by 3 July 2003. More recently several cases were confirmed in 2004 in China and cases of laboratory contamination were recorded in Taiwan, Singapore and China.

Following unprecedented collaboration between laboratories and scientist worldwide, the etiologic agent of SARS was identified in late March 2003, as being a novel virus from the family Coronaviridae, termed SARS coronavirus (SARS-CoV) (Peiris *et al.*, 2003; Drosten *et al.*, 2003; Ksiazek *et al.*, 2003). It was then demonstrated that it met all four of Koch's postulates[3], that are required to prove this novel virus to be the causative agent of SARS (Fouchier *et al.*, 2003).

Helped by previous investigations on coronaviruses, the SARS epidemic has been the first infectious outbreaks to fully benefit from the revolutionary technologies of post-genomic era. Less then one month after the initial identification of the virus as the infectious agent of SARS, two independent genome sequences of the virus had been obtained (Rota *et al.*, 2003; Marra *et al.*, 2003).

Within three months, the genome sequences of 20 independent clinical isolates were made available in the GeneBank database. Comparative

[3] The pathogen must be found in all cases of the disease; it must be isolated from the host and grown in pure culture; it must reproduce the original disease when introduced into a susceptible host; it must be found in the experimental host so infected.

analysis of these isolates revealed more then 99% sequence conservation. The few differences, however, have allowed the organization of all viral isolates into two genetic lineage: one which is linked to infection acquired in Hong Kong and the other which corresponds to Chinese isolates (Ruan *et al*., 2003). These two lineages are characterized by mutations in the orf1a(nsp1), orf1ab(nsp11), the S1 portion of the spike protein and the non-coding region upstream of the N gene (see later the genome organization). Some additional polymorphism could be recognized including deletions but overall the virus seemed to be maintaining its consensus genotype upon inter-human transmission and thus seemed to be rather well-adapted to the human host.

Determination of the genome sequence of the SARS CoV revealed that it is neither a mutant of a known coronavirus nor a recombinant between known coronaviruses and, even if closely related with groups II coronavirus (which includes human coronavirus OC43, bovine coronavirus BCoV and mouse hepatitis virus MHV), SARS-CoV does not belong to any of the known groups of coronaviruses. It was thus proposed that this new virus defines a fourth lineage of coronavirus.

Interesting, the early cases of SARS in Guangdong, China, occurred in restaurant workers handling wild mammals. SARS-CoV-like strains isolated from Himalayan palm civets, found in a live-animal market in Guangdong, retain a 29-nucleotide sequence that is not found in most human isolates (Guan *et al.*, 2003). This observation raises the hypothesis that the 29-nucleotide deletion could have increase the fitness of the virus in human hosts and allowed the spread to the human population. Rapid adaptation of SARS-CoV has been reported even in cell culture system (Thiel *et al.*, 2003). To date, with the exception of IFNs, which has been reported to interfere with SARS-CoV replication in vitro (Tan *et al*., 2004), no licensed drug or vaccine is available.

6.2 Natural history of SARS

SARS is a type of viral pneumonia, with symptoms including fever (> 38°C), general influenza-like symptoms, chills, malaise, loss of appetite, and myalgia. The mean incubation period is 5 days with the range of 2-10 days although there are isolated reports of longer incubation periods. Transmission occurs mainly during the second week of illness. There have been no reports of transmission occurring before the onset of symptoms.

The typical clinical course of SARS involves an appearance of symptoms during the first week of infection, followed by a worsening during the second week. Has been suggested that this worsening may be related to host immune responses rather than uncontrolled viral replication (Ng *et al*., 2004). Dry cough, dyspnoea, hypoxemia and diarrhoea are more commonly reported in the second week of illness. Severe cases develop rapidly progressing respiratory distress and oxygen desaturation with about 20% requiring ventilatory support around day 12. Death may result from progressive respiratory failure due to alveolar damage (WHO reports). Hematological changes in patients with SARS are common and include lymphopenia, thrombocytopenia and occasionally leukopenia. A significant decrease was also observed in peripheral CD4+ and CD8+ T lymphocyte subsets and it was related to onset of SARS (Yang M. *et al*., 2004). Abnormal liver functions were common in patients with SARS. Abnormal activity of hepatic enzyme such as alanine aminotransferase (ALT), aspartate aminotransferase (AST) and lactic dehydrogenase (LDH) has been associated with virus replication in the liver and induced liver damage in the course of infection (Cui *et al*., 2004). Based on an analysis of data from Canada, China, Hong Kong SAR, Singapore, Viet Nam and the United States the case fatality ratio (CFR) of SARS is estimated to range from 0% to more than 50% depending on the age group affected, with an overall CFR estimate of approximately 11% (WHO reports). Higher mortality has also been associated with male sex and presence of co-morbidity in various studies.

6.3 SARS-CoV genome and expression

Coronaviruses are recognized at the electron microscopy by their characteristic corona solis - like envelope. The spherical capsid contains a single-stranded plus-sense RNA genome about 30 kb in length that has a 5-cap structure and 3- polyadenylation tract. Sequence analysis of the SARS-CoV genome (Marra *et al*., 2003; Rota *et al*., 2003) revealed the presence of the characteristic features of coronaviruses (Fig.6.1). Nucleotides 1-72 contain a predicted RNA leader sequence preceding an untraslated region (UNT) of 192 nucleotides (nt). Then, the viral replicase gene, which comprises the two overlapping open reading frames ORF1a and ORF1b, spans the following two-thirds of the genome (265-21485 nt). ORF1a encodes for the polyprotein 1a (pp1a) of 486kDa. A translational read-

through by a -1 ribosomal frameshift mechanism just upstream the ORF1a termination codon, allows the expression of the ORF1b-encoded region of the polyprotein 1ab (pp1ab) of 790 kDa. The remaining 3'-terminal region of the genome encodes for structural proteins that are arranged in the same order in all coronaviruses: spike glycoprotein, S; envelope, E; membrane glycoprotein, M and nucleocapsid, N. Furthermore, the structural region of the genome contains several 'accessory genes' coding for additional non-structural proteins. These genes differ significantly among coronaviruses groups and are also referred to as group-specific genes. The SARS-CoV has eight predicted ORFs of still unknown function. Finally, at the 3'-terminal of the genome, a second UTR is followed by a poly (A) tract.

Upon infection of an appropriate host cell, SARS-CoV genome expression starts with the translation of ORFs 1a and 1b into the two large poliproteins pp1a and its C-terminally extended version pp1ab. The polyproteins are rapidly, maybe co-translationally, autoprocessed by the two viral proteinases, the papain-like cystein proteinase PLpro and the 3C-like cystein proteinase 3CLpro (Thiel *et al.*, 2003). Exception from the Infectious Bronchitis Virus (IBV), all prevously characterized coronaviruses encode two papain-like proteinases. Conservation of only one PLpro in SARS-CoV is linked to an increase in narrow substrate specifity (Fig.6.3) (Thiel *et al.*, 2003). The autoprocessing of pp1a and pp1ab results into the release of several nonstructural proteins, including, an RNA-dependent RNA polymerase (RdRp), an adenosine triphosphatase helicase (Hel) and, of course, the proteases. These proteins, in turn, are responsible for replicating the viral genome as well as generating nested transcripts that are used in the synthesis of the viral proteins.

Coronaviruses use a unique strategy to synthesize a set of subgenomic RNAs with common 5'and 3' sequences (Fig.6.4) Each mRNA contains a short 5'-terminal ‘leader’ sequence. The fusion of the non-contiguous sequences is currently believed to be achieved by a discontinuous step during minus-strand synthesis and involves transcription regulatory sequences (TRSs). In addition to the TRS at the3'-terminal of the leader sequence (leader TRS), TRSs are located upstream of the genes in the 3'-proximal part of the genome (body TRSs).

Thiel and coworkers (Thiel *et al.*, 2003) have found that a minimal consensus sequence, 5'-ACGAAC-3', is sufficient to direct the synthesis of SARS-CoV subgenomic mRNAs, most probably by base-pairing of its negative-stranded counterpart to the leader TRS during minus-strand synthesis. This discontinuously synthesized minus strand then act as template for the synthesis of positive-sense mRNA product.

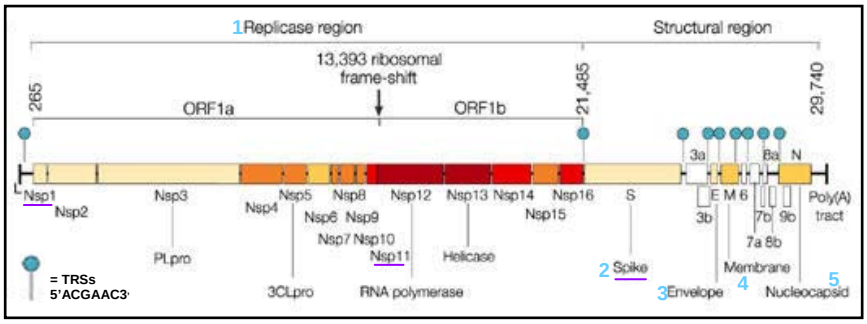

Fig.6.1 Genome structure of SARS - CoV. The 5 major ORFs are indicated. L at the 5'-terminal stands for Leading sequence. The region of main polymorphisms between the two lineages isolated respectively in Hong Kong and China (Nsp1, Nsp11, Spike) are underlined (Ruan *et al.*, 2003).

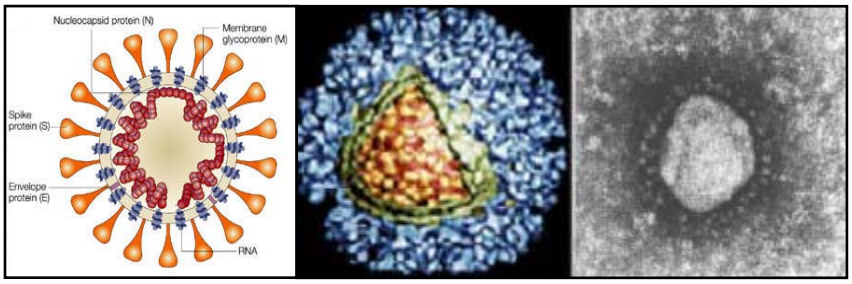

Fig.6.2 Schematic representations and of Electron microscopy image of SARS-CoV

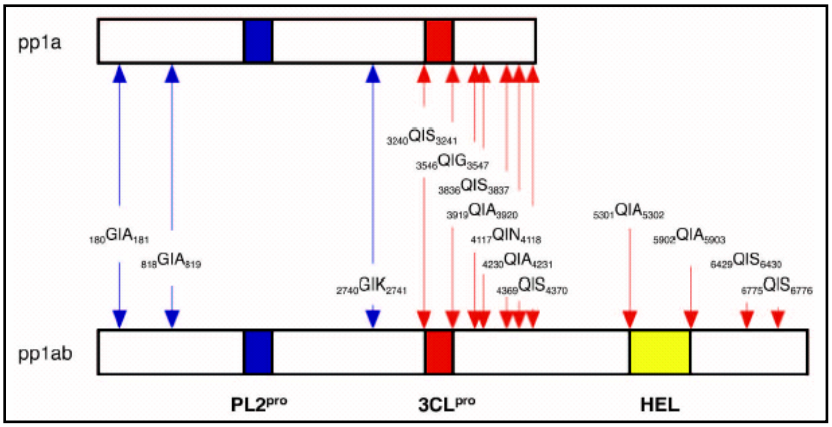

Fig.6.3. SARS-CoV proteases activity. The positions of cleavage sites predicted to be processed by PL2pro (blue) and 3CLpro (red) are indicated (Thiel *et al.*, 2003)

6.4 SARS-CoV Life Cycle

The message-sense RNA genome and the viral nucleocapsid phosphoprotein form a helical nucleocapsid (Fig.6.2) The eponymous crown of large, distinctive spikes in the envelope makes possible the identification of coronaviruses by electron microscopy. The life cycle of coronaviruses starts when the spikes, oligomers of the spike (S) glycoprotein, interacts with a receptors through its S1 domain. Electron microscopy analysis of Vero E6 cells inoculated with the virus revealed that the entry, which is probably mediated by S2 domain, occurs three hours post infection, by membrane fusion of the viral envelope with host cell membranes. Endocytosis was not observed (Qinfen *et al.*, 2004).

Coronaviruses have a strong tissue tropism. SARS-CoV is neither a mutant nor a recombinant of any known coronavirus. It is a previously unknown virus, probably from an animal natural host, that somehow acquired the ability to infect humans. During replication process, the error-prone RdRp of coronaviruses generates points mutations and large deletions or insertion of foreign RNA into the viral genome. The host range, tissue tropism, the acquired ability of coronaviruses to infect new species host-cells and virulence of animal coronaviruses highly depend from mutations in the sequence of the S gene.

The nucleocapsid enter the cell and the RNA genome is then released into the cytoplasm, where the replication takes place. SARS-CoV genome expression starts with the translation of the viral replicase gene that comprises ORFs 1a and 1b (Fig.6.1). The pp1a and pp1ab polyproteins are then processed by the viral protease to yield the functional components of the replicase complex, which synthesizes full length negative-strand RNA and discontinuous subgenomic RNAs (Fig.6.4).

The N protein has RNA-binding site and ribosome- binding site, causing the virus genome to bind ribosomes and begin translation. As for the three main

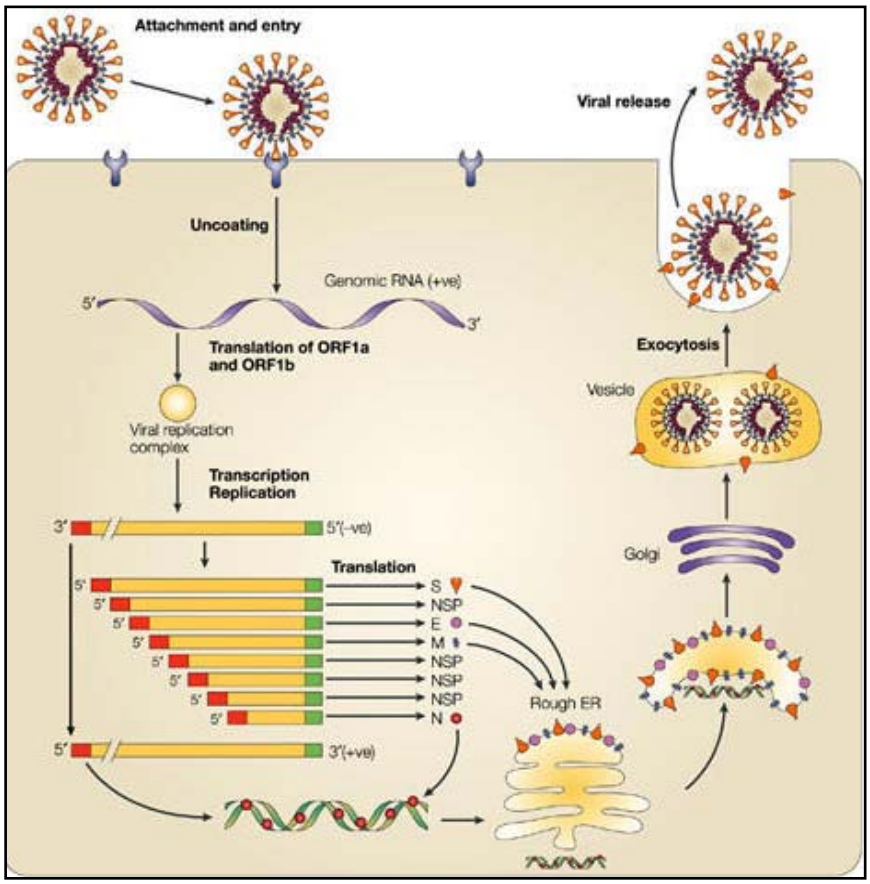

Fig.6.4 Coronaviruses Life Cycle. Spike protein (S) binds to specific receptors on target host cells, and membranes fusion results in the release of the nucleocapsid and ultimately the genome into the cytoplasm. The binding of nucleocapsid to host ribosomes produces the replicase complex, which then produces a full-length negative-strand copy of the genome and by multiple steps, a series of subgenomic m-RNAs (see in the text). The membrane proteins Spike (S), Envelope (E) and Membrane (M) go through the ER to the Golgi, where become glycosilated (S and M) and form the budding site. The nucleocapsid assembles in the cytoplasm, from the nucleocapsid protein (N) and progeny genomes, and then bud into the budding compartment, resulting in virion formation. All S proteins that are not incorporated into virions are trasported to the cell surface. Viruses are then transported via smooth vesicles out of the cell.

structural proteins of SARS virus (M,E,S), the N proteins are synthesized in the cytoplasm by free ribosomes and combining the new-synthesized genomic (+)-RNA forms the helical nucleocapsid (NC). According to previous studies on coronaviruses (Nguyen & Hogue, 1997), the S, M, E proteins congregate on Rough ER (RER) and then transported into Golgi apparatus. Seven hours post infection nucleocapsids first appear in the swollen RER (Qinfen *et al.*, 2004). As the nucleocapsids increased in their number, the ribosomes attached to the surface of the RER became fewer, and finally, disappear completely. This type of structure and changes is consistent with the virus morphogenesis matrix vesicae (VMMV) (Zhang *et al.*, 2003). At the same time, the Golgi apparatus is swollen as well, forming smooth vesicles. The S and M glycosylated proteins become inserted in the vesicle membrane and serve as sites for association with nucleocapsid. This vesicles increase in size and number resulting in a severe vacuolization of the cell. The nucleocapsid binds the M protein in the RER or Golgi apparatus, where M binds also S and E proteins. The structural proteins can form an assembly-competent complex, which provide a site for budding. The virus matures by budding from the VMMV into the smooth vesicles. Virions are released by exocytosis when the virion-filled vesicles fuse with the plasma membrane.

6.5 What is known about SARS-CoV?

To date, the details of the host response to SARS-CoV infection is still largely unknown and consequently the most appropriate treatment regime remains to be established.
Gene expression analysis of SARS-CoV infected PBMC, revealed a primary pro-inflammatory cytokine profile within the first 12 hours post infection (h.p.i.) and a secondary, longer period cascade of responses (Ng *et al*., 2004). Data suggest an early activation of the innate immunity pathway, consisting in monocyte-macrophage activation as well the complement pathway activation. This response results accompanied by un unusual cytokine transcription profile, which suggest an alteration of the IFNs response. Moreover, several chemokines and their receptor upregulation was seen, indicating a rapid mobilization and increased trafficking likely to be lung directed, in particular of the monocyte-macrophage lineage. Specific trafficking of these cells to the lung may account for the localized nature of the response.

Coagulation pathway upregulation was also reported, consistent with the observations, at the lungs autopsy of SARS patients, of unusually disseminated small vessel thromboses.
Featuring aspects of SARS-CoV infection belong from Electron Microscopy analysis. SARS-CoV grows faster then other known human coronaviruses and induce dramatic ultrastructural changed in the preferred host cell system, i.e. Vero cells. The formation of a continuous membrane system from the rough endoplasmic reticulum to the Golgi complex, which defines the "budding compartment" (Goldsmith *et al*., 2004). As already described, RER gradually turns into virus VMMV and Golgi forms increasing smooth vesicle, resulting in expanded vacuolization of the infected cell. The extension of the nuclear external membrane and the formation of multi-lamellar structures was also described (Qinfen *et al.*, 2004). Yan and collaborators (Yan *et al.*, 2004) have shown that CPE (cytopathic effects) induced by SARS-CoV in Vero E6 cells may be dependent on the activation of the apoptotic pathway.
In our laboratories, it has been investigated the molecular mechanism of apoptosis induced by SARS-CoV in Vero E6 cells and whether preventing cell death could result in modification of virus replication (Castilletti *et al.*, submitted).
The results indicate that replication of SARS-CoV *in vitro* causes extensive CPE and destruction of the cell monolayer. An increasing number of apoptotic cells was observed along CPE development, thus confirming that induction of apoptosis is a major event for the cytopathogenity of SARS-CoV as suggest by Yan *et al.* In addition apoptosis appears as a late event in SARS-CoV infected Vero cells if compared to the completion of virus replication cycle. The apoptotic cell death induced by SARS-CoV seems to involve the mitochondria pathway and the activation of effector caspases, being prevented by Bcl-2 over-expression. However, prevention of apoptosis does not seem to influence the kinetics and efficacy of virus replication (Fig.6.5). Whether SARS-CoV induced apoptosis is a direct consequence of virus replication or is mediated by host defence response has not been established, yet.

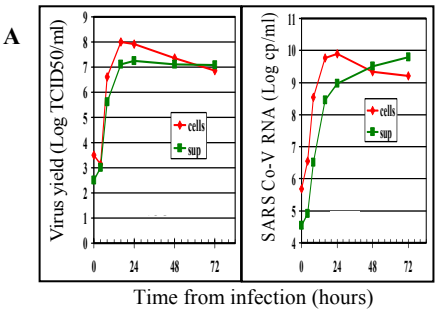

Fig. 6.5 **A**. Time course of either released or cell - associated virus yield. The virus progeny was evaluated in terms of both infectivity (left panel) and viral RNA (right panel). **B**. Quantification of cells displaying DNA fragmentation 48 h.p.i. by cytofluorimetric analysis (FACScan) of TUNEL positive cells, compared with negative control. **C**. Apoptosis was determined in SARS-CoV infected and mock cells at various time points measuring hypodiploid cells, which starts to increase at 48 h.p.pi.

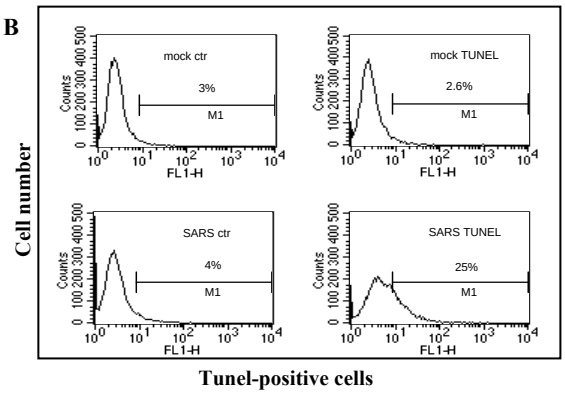

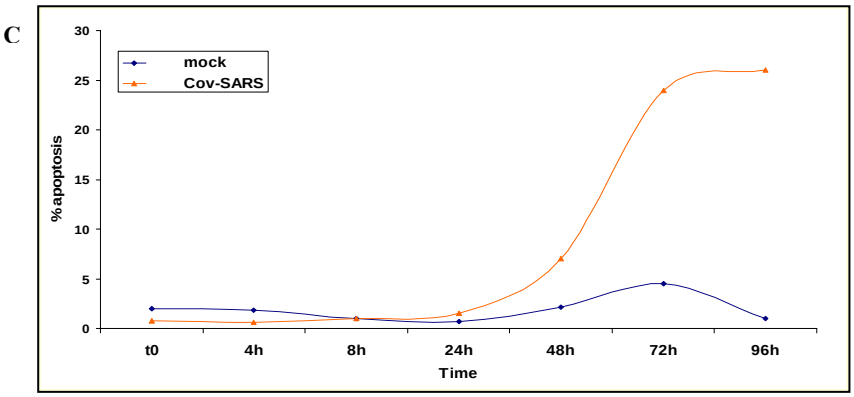

7. AIMS OF WORK

Proteins are involved in almost all biological processes. Besides their key roles in intracellular metabolism, proteins function, in intracellular and intercellular signalling, play a significant role in the immune system response and interactions between pathogen and host.
The work I will present in this thesis had the aim to investigate the mechanisms of HCV replication and the impact of infection into the host cell in such a way to get the most representative system of in vivo infection. We used the 'replicon system' and a proteomic approach looking for differences in the proteome expressed by Huh7 cells in the presence or absence of HCV replicon.
Looking to virus-host interaction, namely the host immune reaction to the presence of a virus, I have also apply the proteomic analysis to investigate Mixed Crioglobulinemia, one of the most common extracellular manifestation of HCV infection. Moreover, to better test this kind of technical approach in the investigation of virus-host interaction, I applied the same analysis to SARS-CoV infected cells. The molecular basis of SARS-CoV induced pathology is still largely unknown. Anyway, SARS infection course has a completely different characteristics in respect to HCV, included the ability to infect and replicate in different tissues and cell lines, a latent period of only 5 hours post infection (h.p.i.) and, mainly, a high replication rate that induce dramatic cytopathic effects within the first 24 h.p.i. and apoptosis within 48 h.p.i.
The basic experimental strategy adopted was to compare the proteomes of normal (control) and treated cells (transfected with HCV replicon or infected with SARS-CoV). Qualitative and quantitative differences was scored and the proteins of interest further processed for identification. In the case of cryoglobulins analysis all spot were analysed. Peptide mass mapping is currently the technique of choice for protein identification in proteomics. The proteins of interest resolved by 2D-PAGE were digested using trypsin. The masses of the tryptic peptides generated were then accurately determined by MALDI-TOF MS to produce a peptide mass fingerprint (PMF). This experimental profile was compared to the predicted tryptic PMF for all proteins derived from every sequenced open reading frame, including those that encode hypothetical proteins, by protein databases search engines. High scoring comparisons indicate potential identifications for the protein under investigation.

8. MATERIALS AND METHODS

8.1 Samples preparation

HUH7 and Rep60 cells. HuH7 cells were purchased from the American Type Culture Collection and grown in Dulbecco's Modified Eagle Medium (DMEM, Sigma Aldrich) supplemented with 10% v/v fetal bovine serum (Sigma Aldrich), 100 U of penicillin/ml, 100 µg of strepmycin/ml and 2mM L-Glutamine. Rep60 is a HuH7 cell line harbouring an HCV replicon I377neo/NS3-3'/wt (Lohmann *et al.*, 1999)obtained by the transfection of HuH7 and selection by 0,5 mg of G418/ml (Invitrogen).

Total lysate protein extraction. Cells were always lysated when sub-confluent (10^6 cells). Cells were washed twice with 1xPBS, detached by scraping and collected by centrifugation. The cell pellet was resuspended in Lysis buffer: 7M urea, 2M thiourea, 4%CHAPS, 0,5 % carrier ampholytes (CA).

Subcellular fraction. We start from 4-8 Ø15cm dishes for HuH7 and Rep60, respectively. Cells were washed twice with 1xPBS, detached by scraping and collected by centrifugation. The cell pellet The cell pellet was resuspended in hypotonic buffer: 20 mM HEPES, pH7.4, 10 mM KCl, 1.5 mM $MgCl_2$, 1mM DTT, 1:500 PIC (Protease Inhibitor Cocktail - Sigma Aldrich), and kept on ice for 30 min. The volume was then increased till 3ml with 5x OmS (0.32M Sucrose, 3mM $MgCl_2$, Tris-HCl 20mM pH8, PIC 1:500) . Cells were homogenized by pottering in ice and then centrifuge for 20 min at 600 x g at 4°C. The pellet consisting in the *nuclei* fraction was resuspended in 200 µl of Sample Buffer (SB): 2M thiourea, 7 M urea, 2% CHAPS, 1% SB3-12, 1% ASB14, 0,5% CA. The surnatant was centrifuged for 20 min at 15000 x g at 4°C. The pellet consisting of the *mitochondria* fraction was resuspended in 200 µl of SB.
To the surnatant was added OmS buffer to reach the volume of 5ml and the was centrifuge 1h 40 min at 80000 x g at 4°C in ultracentrifuge. The pellet consisting of the *microsomes* fraction was resuspended in 200 µl of SB.

Sample preparation for IEF. All samples where kept at least one hour at 37 °C and then centrifuge in bench top centrifuge at maximum speed (13000 rpm) for 15 min at r.t. Quantification was done by running SDS-PAGE mini-

gel applying a quantified standard. The samples were always preciptated using Plus-One 2D Clean-Up Kit (Amersham Biosciences), following manufacturing instructions, and then resuspended to ca. 10 µg/µl.

Sequential extraction. Cells were washed twice with 1xPBS, detached by scraping on ice with 1ml for Ø15cm dishes of White Buffer (40mM Tris, 0,5% Tween 20, 10 mM NaCl, PIC 1:500) and homogenized by 40 strokes in 2 ml Potter tube on ice. The homogenate was then centrifuged for 15 min at 18000 RPM at 4° C. Supernatant was precipitated with Magic Solution (5 volume of 50% ethanol, 25 % methanol, 25% acetone, at least 3h at -20°C). The pellet was resuspended with 0,5 ml of Blue Buffer (40 mM Tris, 0,5% Triton X-100, 10 mM NaCl, PIC 1:500), kept one hour in cold room with gently agitation and centrifuged for 15 min at 18000 RPM at 4° C. Supernatant was precipitated with Magic Solution. The pellet was resuspended in 0,2 ml of Green Buffer (Urea 8M, CHAPS 4%, 50 mM DTT, 40 mM Tris, 0,5% CA), kept one hour at 37°C and centrifuged 15 min at 13000 RPM r.t. Supernatant was precipitated with Magic Solution and pellet resuspended in 0,2 ml of Orange Buffer (Urea 7M, Thiourea 2M, 2% CHAPS, 1% ASB14, 1% SB3-12, 50 mM DTT, 40mM Tris, 0,5 % CA).
Quantification was performed by SDS-PAGE mini gel applying a quantified standard.

Vero E6 and SARS-CoV-Vero E6 cells. Vero E6 cells were maintained in DMEM supplemented with 5% Fetal calf Serum (FCS) at 37° C in a humidified atmosphere. The SARS-CoV (Tor 2 isolate) was kindky provided by H. Feldmann (Dept. of Medical Microbiology of Manitoba, Canada). Sub-confluent cell monolayers were exposed to SARS-Cov at MOI 10 $TCID_{50}$/cell (single replication cycle) for 30 min at 37 °C. Then, the cells were extensively washed and fresh medium, supplemented with 2% FCS, was added. This time was taken as time 0 (T0). At 24h and 48h, detached and adherent cells were collected and worked separately.
1 ml of Blue Buffer was add to each aliquot and cells where lysated by pipetting up and down 20 times on ice. After 15 min, they were centrifuged 12000 RPM for 10 min at 4°C. The supernatants were precipitated with Magic Solution. Pellets were resuspended by adding 0,2 -0,5 ml of Orange Buffer, vortexing and incubate at 37°C for 1h. After centrifugation (5 min 13000 RPM) they were precipitated with Magic Solution. Quantification was performed by SDS-PAGE mini gel applying a quantified standard.

HCV cryoglobulins. Samples were kindly provided by Dr. LP Pucillo (Laboratory of Chemical-Clinical Analysis and Microbiology , IRCCS "L. Spallanzani"). Cryo-precipitates were obtain from serum of three HCV patients. After 96h at 4°C the resulting precipitates were washed 3-5 times with PBS buffer at 4°C. Proteins were quantified by Bradford assay (Biorad).
IgG depletion. Cryoglobulins were dissolved at 37°C. 50 µl of Protein A-Sepharose beads (Pharmacia) and 50 µl of Protein B Sepharose beads (Pharmacia) were washed twice in PBS and twice in PBS - 0,1% CHAPS and then added to an aliquot of cryoglobulins (about 500 µg) containing 0,1% CHAPS. The mixture was left over night in gently agitation and the centrifuge for 5 min at 2500 RPM. The surnatant was precpitated with Magic Solution. Beads were washed with PBS-CHAPS 0,1 % and then add to a volume equal to the removed supernatant of 0,1M Glycine pH 2,4. After a while the mixture was centrifuged for 5 min at 2500 RPM. To the supernatant was added Tris-HCl pH 7,5 till 50 mM and then it was precipitated with Magic Solution.

8.2 2D-PAGE

In-gel Rehydratation. 18 cm IPG strips (Pharmacia) were rehydrated at 20°C, over night with 0,2 -1 mg of proteins diluted to a final volume of 350 µl with Rehydratation Buffer: 6M urea, 2M thiourea, 4% CHAPS, 15 mM DTT; 0,5 % of IPG buffer (Pharmacia) of corresponding IEF-run pH range. Passive rehydratation (0V) for 6-10 hrs and active rehydratation (30V) for 6-10 hrs was normally performed. Strips were covered with a protective layer of DryStrip Cover fluid (Pharmacia).

IEF run. IEF was performed on Ettan IPGphor Isoelectric Focus System with 18 cm Ettan IPGphor Strip Holders (Amersham Biosciences) at 20°C, 50µA/strip. Running conditions described by Gorg *et al.* (Gorg *et al.*, 2000) with slightly modification were applied. Entry steps time and IEF to steady-state were increased proportionally to sample's protein amount.

IPG 3-10 NL / L (0,2 -1 mg)

Step 100V 1-2 h	Step 1000 V 1h
Step 200V 1-2 h	Grad 8000 V 1-2 h
Step 500V 1h	Step 8000 V 3-5 h
Grad 1000V 10-30 min	Total Volts/Hour: 30-50 KV/h

IPG 4-7 (200µg)

Step 100V 1 h	Step 1000 V 1h
Step 200V 1 h	Grad 8000 V 1 h
Step 500V 1h	Step 8000 V 4 h
Grad 1000V 10 min	Total Volts/Hour: ~ 40 KV/h

IPG 5,5-6,7 (4,5-5,6) (1mg)

Step 100V 2 h	Step 1000 V 1h
Step 200V 2 h	Grad 8000 V 2 h
Step 500V 1h	Step 8000 V 12 h
Grad 1000V 30 min	Total Volts/Hour: ~ 100 KV/h

Filter paper electrode pads moisten with deionised water were applied after rehydratation step and changed every 2 hours during IEF course. IPG strips not used immediately were store in plastic sheets at -80°C.

Equilibration Step. Equilibration of IPG strips in SDS buffer was perfermed in two steps each time for 15 min in 2x10 ml of Equilibration Buffer: 50mM Tris-HCl pH 8,8; 6M urea, 30% v/v glycerol, 2% w/v SDS, BPB trace. The first step, reducing conditions, was performed in the presence of 1% w/v DTT while the second step, alkilating conditions, was performed in the presence of 4% w/v Iodoacetamide (the excess is necessary to remove the excess of DTT).

Second dimension: SDS-PAGE. Second dimension was run on Protean II Xi Cell (Bio-Rad). Equilibrated strips were washed into the Tris-Glycine-SDS (TGS) Running Buffer (25 mM Tris, 192 mM glycine, 0,1% SDS), placed on top of vertical 12%, 1mm thickness, SDS gels and embedded in agarose (0,5% w/v in TGS). Runs were performed at 20mA/gel for the first 40 min and 40mA/gel until the tracking dye reached the anodic end of the gels.

Visualisation. Fluorescent dye Sypro-Ruby (Bio-Rad) staining was performed according to manufacturing instructions. Fixing for 40 min in 10% v/v Methanol, 7% v/v Glacial Acetic Acid. Staining with 150ml/gel Sypro-Ruby was performed for 3hrs or over night. Destaining by several washes in 10% v/v Methanol, 7% v/v Glacial Acetic Acid. To visualize gels Typhoon 9400 (Amersham Biosciences) setting was:

Green laser 532 nm; 610BP30 emission filter; PMT(photomultiplier tube) voltage – 800V; focal plane setting +3 mm; Pixel size – 100 μm; Sensitivity – Normal.

8.3 Image Analysis.

We used Phoretix 2D Investigator (Nonlinear Dynamics). Spots detection was performed using the set-up wizard and manual processing (spot volume filtering, spot splitting, spot erasing etc). Background subtraction was performed by mode of "Non Spot" and "Total Spot Volume" Normalization method was used. Matching was dome automatically and then eventually correct with the option of user-defined seeds. The software allows to build up virtual averaged gels obtained by summarise different run gels. Treated virtual gel is then compared to virtual control gel. The software performed automatically a "difference" map based on user-defined parameters. We set parameters to get differences of 2 fold based on the normalized volume and standard error of the mean.
At the end of the analysis it has been possible to generate a spot picking list to be exported to Investigator-ProPic robot (size picking tips:1.2 mm).

8.4 In gel-digestion.

Gel spots were washed once in mQ water and twice with 200 μL of wash solution, 100 mM NH_4HCO_3, 50 % AcCN: firstly just with NH_4HCO_3 and incubate at room temperature for 5 min after vortexing and then adding AcCN to get a 1:1 wash solution. Then the gel was dehydrate in 50 μL 100% acetonitrile and completely air-dry. Rehydratation with a minimal volume of 4ng/μL modified sequencing grade Trypsin (Promega, Madison, WI) in 50mM NH_4HCO_3 was performed on ice for 1 hour. Trypsin solution was then replaced with 10-20μL of 50 mM NH_4HCO_3 and digestion performed over night at 37°C. The digestion solution was than concentrated with ZipTip (Millipore) and peptides eluted with 1μL of diluted 1:2 of matrix solution: saturated solution of α-cyano-4-hydroxycinnamic acid (CHCA) in 50% AcCN, 0,1% TFA.

8.5 Peptide-Mass-Fingerprint

Mass spectrometric analysis was performed with Voyager DE-PRO (Applyed Biosystem) in reflectron mode and protein identification performed both on MASCOT (http://www.mascot.com) and Profound (http://129.85.19.192/profound_bin/WebProFound.exe?FORM=1) peptide mass fingerprint search engines. Mass determination accuracy was always <100ppm (typically 50 ppm).

9. RESULTS and DISCUSSION

9.1 HuH7 proteome alteration induced by the presence of HCV-replicon

We looked for differences in the proteome of HuH7 cells (control) and Rep60 cells. We initially analysed total cell lysates in wide pH range, applying the sample by in-gel rehydratation on pH 3-10 NL (data not shown) and pH 4-7 IPG strips.
The image analysis of 3 pairs series of gels does not reveal any relevant difference into the protein expression pattern of Rep60 cells *vs* HuH7 cells.
To reduce the complexity of the sample and to look deeper inside protein expression of less abundant protein, we repeated the analyses on enriched subcellular fraction obtain by differential centrifugations.
We have called *nuclei*, the fraction containing nuclei but also heavy mitochondria, cytoskeletal networks and plasma membrane; the fraction *mitochondria* was actually composed of light mitochondria lysosomes and peroxisomes as the *microsomes* was in fact composed by Golgi apparatus, endosomes and microsomes, and endoplasmic reticulum (ER).
Again, the image analysis does not reveal differences(Fig. 9.1).
We go further then with zoom gel analysis, narrow pH range analysis, applying *mitochondria* and *microsomes* on pH 4,5-5,6 (data not shown) and pH 5,5-6,7 IPG strips. The resulting maps till show high complex protein expression patterns and little differences induced by the replication of HCV replicon into HuH7 cells in respect to control (Fig.9.2).
These differences were not always exactly reproducible, mostly due to the complexity of proteins pattern in which they were localised. Moreover, the amount of peptides recovered after in gel-digestion of these little, not intense Sypro-Ruby spots, were not sufficient to perform a successful MALDI-TOF mass spectrometry analysis.
We also fractionate the entire proteome by sequential protein extraction recovering four different fraction from high soluble proteins (hydrofilic, cytosolic protein) to high insoluble protein (hydrophobic, membrane protein). Despite the nice patterns we get, the reproducibility of the experimental procedures was not sufficient to get standard inter- and intra-fractions between controls and treated samples. Anyway, the maps we get does not show significant differences (Fig.9.3).
We have tried several approaches to investigate the impact of replication of HCV RNA (Rep60) on the HuH7 proteome, besides the ones I have just

described, also the over-expression of single HCV proteins (NS5A, NS3, Core) or treatments with IFN-α (data not shown).

The inability to identify differences in the proteomes of Rep60 *vs* HuH7 cells can be addressed to different reasons: first of all the limits of 2D-PAGE technique concerning low abundant proteins, but also the characteristics of the system we investigated. HCV is a very low rate replicating virus which can remain asymptomatic for decades and we were even not transfecting with the complete viral RNA genome.

Moreover, the factors that render HuH7 cells uniquely permissive for HCV replication remain uncertain and it could be possible that this permissiveness and the failure of HCV to relevantly alter HuH7 cells proteome are functionally related.

Our results are supported by a recent work of Scholle and coworkers (Scholle *et al.*, 2004). They report a detailed mycroarrays investigation of the impact on HuH7 cells of the full-length HCV RNA genome replication and expression of the complete polyprotein. They show minimal effects on the homeostasis of the host cell, including the cellular mRNA transcription profile and regulation of the cell cycle.

The nature of the transcriptional pathways that are influenced by HCV polyprotein expression and RNA replication still remain to be fully elucidated.

Fig. 9.1 **Huh7** **Rep60** **pH 4-7**

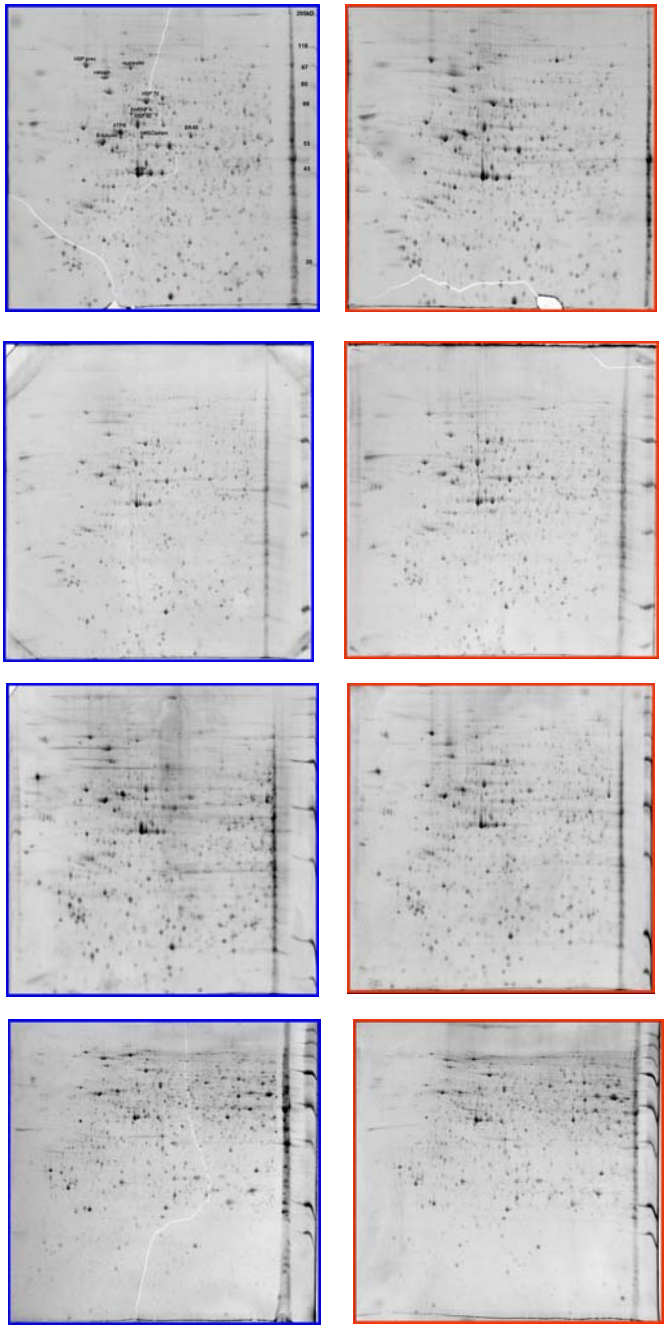

Total Lysate

Nuclei 20’; 600g

Mitochondria 20’; 15k x g

Microsomes 1h40’; 80k x g

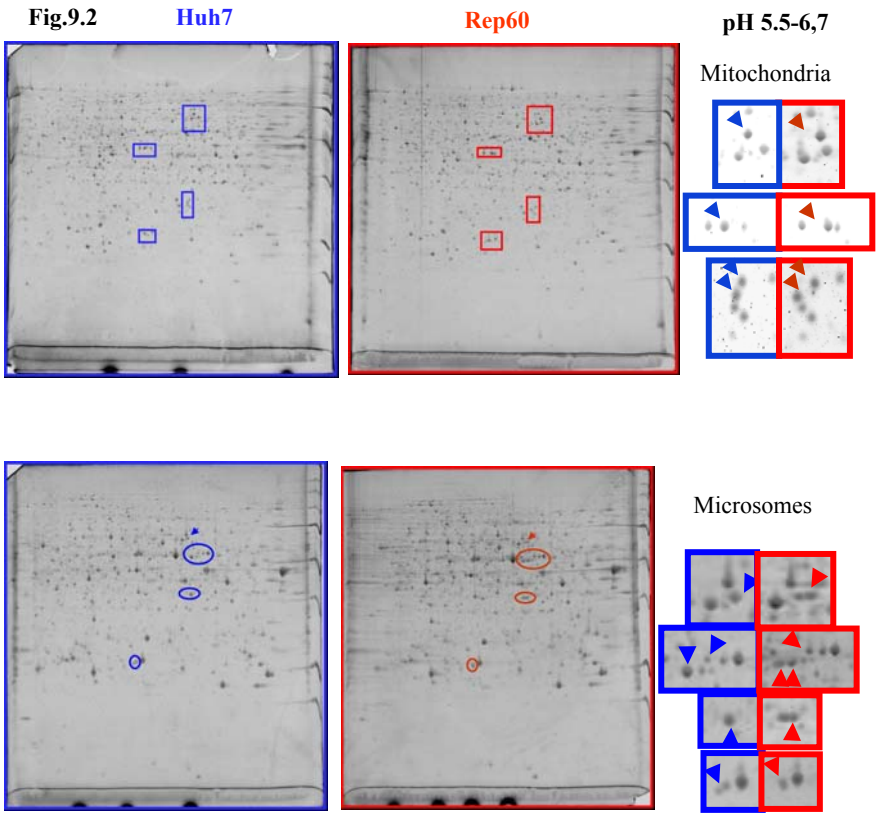

Fig.9.1 On left side HuH7 (control) and on right side Rep60 2-DE pH 4-7 maps are reported. From top to bottom: Total extract, Nuclei, Mitochondria, Microsomes.

Fig. 9.2 On left side HuH7 (control) and on right side Rep60 2-DE pH 5,5-6,7 maps. On top Mitocondria, bottom Microsomes. Slightly differences are shown in zooming boxes on left side of maps.

Fig. 9.3 Sequential extraction of proteins from HuH7 cells (left) and Rep60 cells (right). From top to bottom: White Buffer, Blue Buffer, Green Buffer, Orange Buffer (see Materials and Methods).

Fig.9.3 Huh7 Rep60 **Sequential Extraction pH3-10**

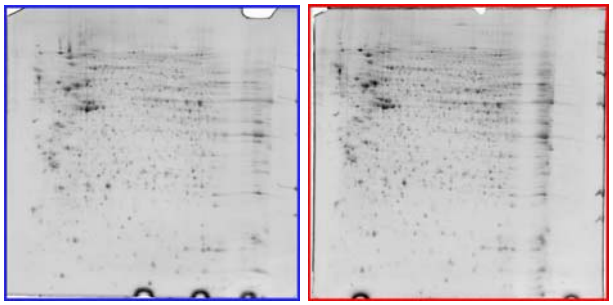

Tris 40mM,
0,5% Tween 20

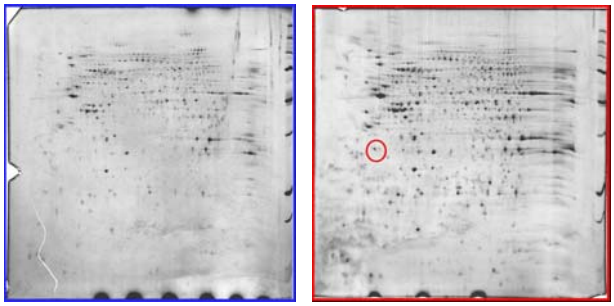

Tris 40mM,
0,5% Triton

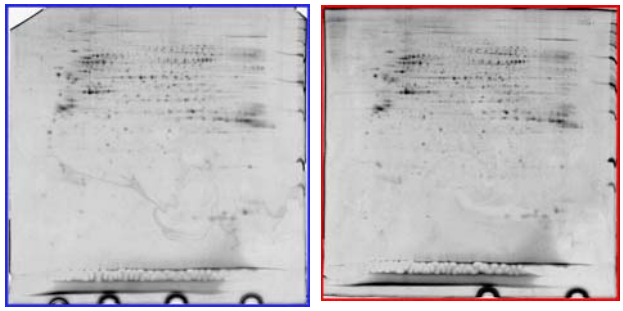

Urea 8M,
4% CHAPS

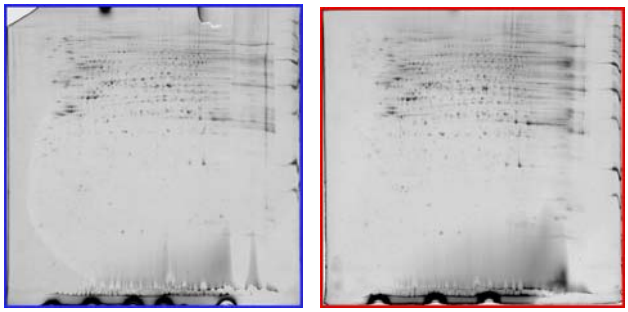

Urea 5M,
Thiourea 2M,
2%, CHAPS
1% SB3-12,
1%ASB14

9.2 HCV and Cryoglobulins

2D-PAGE analysis combined with MALDI-TOF mass spectrometry of cryoglobulins from HCV infected patients resulted in the identification of 20 proteins (Tab 9.1). Mass determination accuracy was always <100ppm (typically 50 ppm) and protein identification performed both on Profound and MASCOT peptide mass fingerprint search engines.

As already known, the cryoprecipitates of HCV patients consist mainly of Type II MC. The principal components, polyclonal IgG and monoclonal IgM, were identified, by MALDI-TOF MS after separation on 2D-PAGE, as μ- and γ-heavy chains (H), κ- and λ-light (L) chains and J-chain. Fig. 4a and 4b show the IgG-depleted and IgG-enriched fraction, respectively. Monoclonal IgM μ-chains appear as trains of well-resolved abundant spots displaying charge micro-heterogeneity in an area of the gel corresponding to mass 70-80 kDa and pI 5,2-6,5 (entire chain: VH, CH1, CH2,CH3,CH4) (Fig.9.4a, Spot n.6) and also at lower molecular weight, 45-50 kDa, as fragments (CH2,CH3,CH4) (Fig.9.4a, Spot n.10). Polyclonal IgG γ-chains localise at the basic side of the gels (pI 7-10) at 50-55 kDa and appear as fuzzy, cloudy zones of unresolved spots, likely corresponding to IgG1 and IgG3 (Fig.9.4b, Spot n.17). The analysis of light chains revealed a complex mixture of κ and λ-chains resulting from monoclonal IgM (κ-chains) and polyclonal IgG (κ- and λ-chains). Anyway, MALDI-TOF resolution has permitted the identification of monoclonal RF, already reported for Type II MC (Damoc *et al*., 2003). Three different spots (Fig.4a, spots n.9, 9a. 9b) have been identified as VK chains belongs to the Hum/Kv325/kIIIb sub-subgroup, that is preferentially selected in human IgM autoimmune response. The sequences of cross idiotype WA CDR (CDR1 and CDR2) have been directly identified by MALDI-TOF spectrometry as reported in Fig.9.5 and their were identical in spots n.9, 9a and 9b (Box 9.1).The presence of the IgM associated protein Spα and Apopoliprotein A-1 has been confirmed as well.

We have also identified the components C1q and C3β (Fig.9.6) of the complement. Complement proteins are involved in early innate immune responses against pathogens and play an important role in the clearance of circulating viral antigens. The presence of C1q in the cryoprecipitate confirms the hypothesis that HCV induced an inflammatory response with activation of the classical complement pathway. C1q, in fact, is the first component in the classical pathway of complement activation. A role for

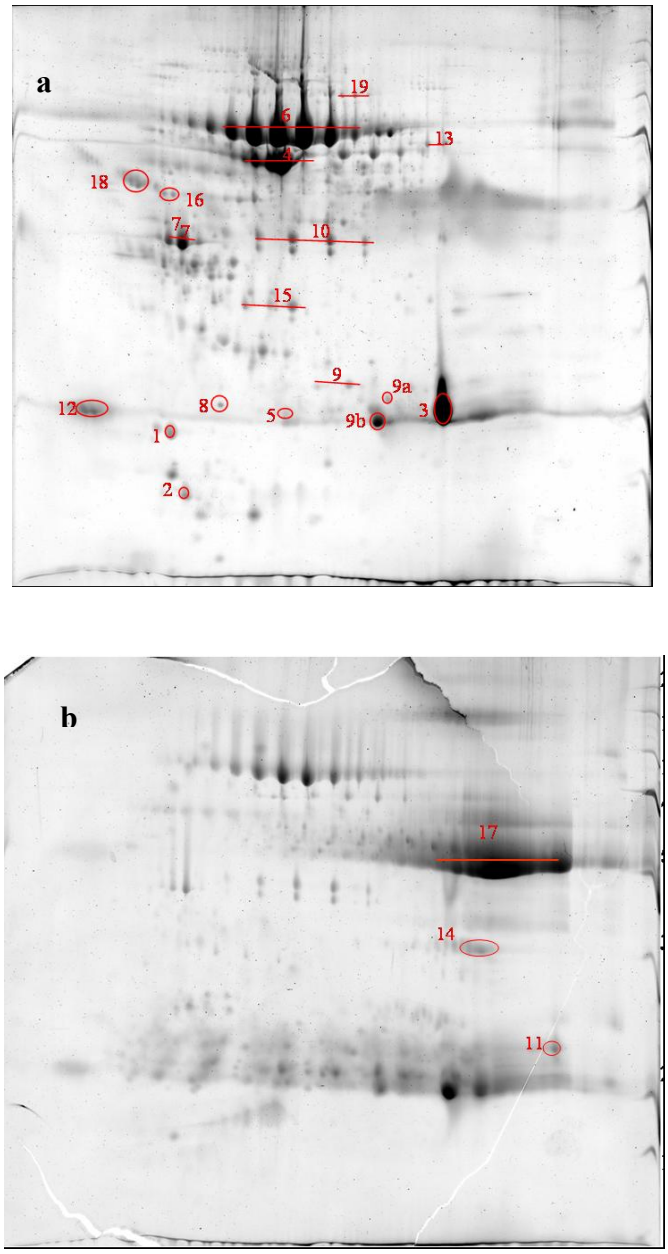

Fig.9.4 2-DE, pH 3-10, of a serum cryoprecipitate of a patient with HCV and presenting Type II MC. Numbers corresponds to identified proteins reported in Table 1. a) IgG depleted fraction (1b) IgG enriched fraction.

Table 9.1. Identified proteins from serum cryoprecipitate of two HCV patients; Est'd Z refers to Profound probability score.

N	Est'd Z	Protein Information	Seq %	pI	kDa
1	2.05	gi|4557321|ref|NP_000030.1| apolipoprotein A-I precursor [Homo sapiens]	39	5.6	30.76
2	1.94	gi|20141667|sp|P02753|RETB_HUMAN Plasma retinol-binding protein precursor (PRBP) (RBP) (PRO2222)	25	5.8	23.37
3	2.43	gi|8918520|dbj|BAA97671.1| (AB030640) immunoglobulin kappa light chain [Homo sapiens]	24	7.9	23.54
4	2.29	gi|28592|emb|CAA23754.1| (V00495) serum albumin [Homo sapiens]	28	6.1	71.34
5	1.73	gi|4502133|ref|NP_001630.1| serum amyloid P component precursor; pentaxin-related; 9.5S alpha-1-glycoprotein [Homo sapiens]	27	6.1	25.48
6	2.36	gi|14602658|gb|AAH09851.1| IGHM protein [Homo sapiens]	21	6.0	68.65
7	2.37	gi|5174411|ref|NP_005885.1| (NM_005894) Sp alpha, CD5 antigen-like (scavenger receptor cysteine rich family); [Homo sapiens]	46	5.3	39.61
8	2.43	gi|7438711|pir||JE0242 Ig kappa chain NIG26 precursor - human	25	5.5	23.79
9	2.43	gi|21669451|dbj|BAC01750.1| immunoglobulin kappa light chain VLJ region (Kv325)[Homo sapiens]	30	6.8	29.58
9a	2.43	gi|21669427|dbj|BAC01738.1| immunoglobulin kappa light chain VLJ region (KIIIb SON) [Homo sapiens]	30	6.2	29.80
9b	2.43	gi|10835792|pdb|1QLR|A Chain A, Crystal Structure Of The Fab Fragment Of A Human Monoclonal Igm Cold Agglutinin (Hum/Kv325/kIIIb sub-subgroup)	24	5.8	23.55

N	Est'd Z	Protein Information	Seq %	pI	kDa
10	2.43	gi|127514|sp|P01871|MUC_HUMAN Ig mu chain C region	28	6.4	50.22
11	1.09	gi|11038662|ref|NP_000482.2| complement component C1q, B chain [Homo sapiens]	17	9.2	26.9
12	2.32	gi|400044|sp|P01591| IGJ_HUMAN IMMUNOGLOBULIN J CHAIN	24	4.6	16.03
13*	2.39	gi|4557385|ref|NP_000055.1| complement component 3 [Homo sapiens]	27	6	188.6
14	1.8	gi|184747|gb|AAC82527.1| immunoglobulin gamma-1 heavy chain constant region [Homo sapiens]	35	8.8	36.53
15	1.04	gi|7770217|gb|AAF69644.1| PRO2675 [Homo sapiens]	24	6.1	33.47
16	1.96	gi|139641|sp|P02774|VTDB_HUMAN Vitamin D-binding protein precursor (DBP) (Group-specific component) (Gc-globulin) (VDB)	14	5.4	54.54
17	2.43	gi|13623575|gb|AAH06402.1|AAH06402 (BC006402) Similar to immunoglobulin heavy constant gamma 3 (G3m marker) [Homo sapiens] gi|230581|pdb|2IG2|H Chain H, Immunoglobulin G1	29 26	8.6 8.9	53.01 50.46
18	2.38	gi|15990507|gb|AAH15642.1| Serine (or cysteine) proteinase inhibitor, clade A (alpha-1 antiproteinase, antitrypsin), member 1 [Homo sapiens]	25	5.4	46.86
19	Mascot Score: 104	gi|190026 plasminogen	30	7.0	93.23

* As shown in Fig.9.6 100% of peptide masses submitted match with the sequence of C3-beta chain (residues 23 - 667; pI: 6.82; 71.3 kDa)

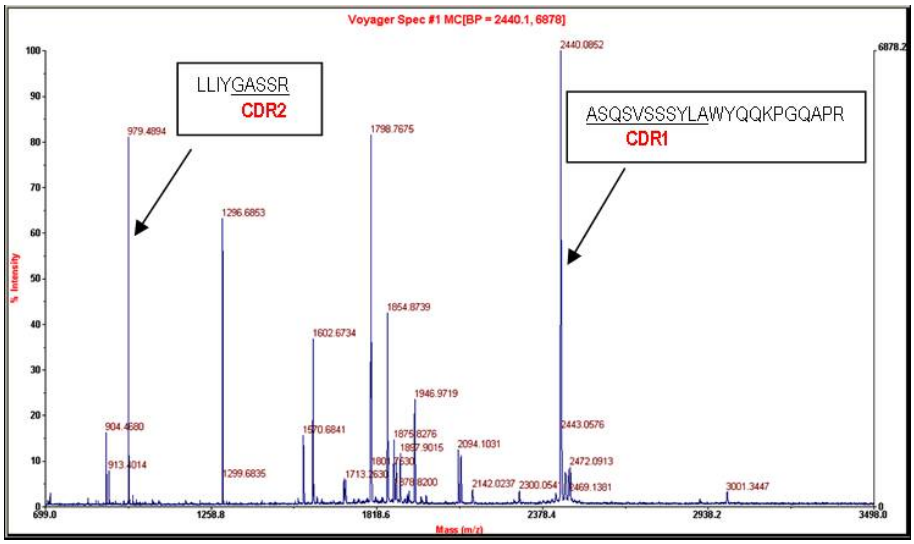

Fig. 9.5. Identification of VLJ IIIb SON - spot 9a. MALDI-TOF direct identification of peptides sequences containing WA cross idiotype CDR 1 (MH+ 2439.105) and CDR 2 (MH+ 979.482) is indicated. Mass error range 50 ppm.

Box 9.1. IgK VLJ sequences identified belongs to WA cross idiotype.

WA CDR cross idiotype: **CDR1** RASQSVSSSYLA; **CDR2** GASSRAT; **CDR3** QQYGSSP.

Spot n 9a.
gi|21669427|dbj|BAC01738.1| immunoglobulin kappa light chain VLJ region
MKYLLPTAAAGLLLLAAQPAMAEIVLTQSPGTLSLSPGERATLSCRASQSVSSSYLAWYQQKPGQAPRL
LIYGASSRATGIPDRFSGSGSGTDFTLTISRLEPEDFAVYYCQQYGSSPPYTFGQGTKLEIKRTVAAPSV
FIFPPSDEQLKSGTASVVCLLNNFYPREAKVQWKVDNALQSGNSQESVTEQDSKDSTYSLSSTLTLSKA
DY

gi|224377|prf||1102971D **Ig M kappa IIIb SON**
EIVLTQSPGTLSLSPGERATLSCRASQSVSSSYLAWYQQKPGQAPRLLIYGASSRATGIPNRFSGSGSG
TDFTLTISRLEPEDFAVYYCQQYGSSPPYTFGGGTKVEIKRTVAAPSVFIFPPSDEQLK

Spot n 9.
gi|21669451|dbj|BAC01750.1| immunoglobulin kappa light chain VLJ region
MKYLLPTAAAGLLLLAAQPAMAETTLTQSPGTLSLSPGERATLSCRASQSVSSSYLAWYQQKPGQAPR
LLIYGASSRATGIPDRFSGSGSGTDFTLTISRLEPEDFVVYYCQQYGSSPPGTFGQGTKLEIKRTVAAPS
VFIFPPSDEQLKSGTASVVCLLNNFYPREAKVQWKVDNALQSGNSQESVTEQDSKDSTYSLSSTLTLSK
ADYEKHKVYACEVTHQGLSSPVTKSFNRGECSARQSTPFVCEYQGQSSDLPQPPVNAG

gi|106602|pir||A30601 **IG KAPPA CHAIN V-III REGION (KV325)**
EIVLTQSPGTLSLSPGERATLSCRASQSVSSSYLAWYQQKPGQAPRLLIYGASSRATGIPDRFSGSGSG
TDFTLTISRLEPEDFAVYYCQQYGSSP

ProFound - Search Result Details

Details for rank 1 candidate in search B6F93654-0708-61CE0516

gi|4557385|ref|NP_000055.1| complement component 3 precursor; acylation-stimulating protein cleavage product [Homo sapiens]

gi|116594|sp|P01024|CO3_HUMAN Complement C3 precursor [Contains: C3a anaphylatoxin]

```
Sample ID :   [Pass:0]
Measured peptides     : 18
Matched peptides      : 18
Min. sequence coverage: 27%
```

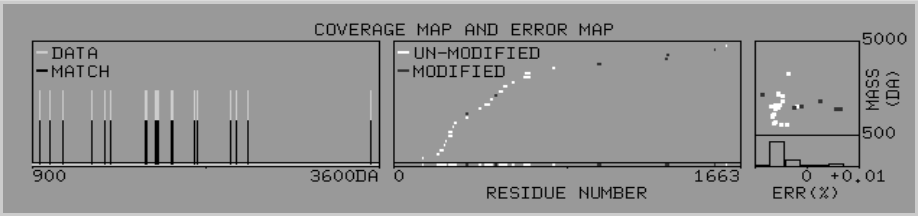

Measured Mass(M)	Avg/ Mono	Computed Mass	Error (%)	Residues Start	Residues To	Missed Cut	Peptide sequence
958.496	M	958.544	-0.005	250	258	0	GLEVTITAR
1041.550	M	1041.618	-0.007	282	290	1	ISLPESLKR
1138.461	M	1138.533	-0.006	242	249	0	FYYIYNEK
1369.631	M	1369.724	-0.007	137	148	0	TIYTPGSTVLYR
1469.673	M	1469.772	-0.007	291	304	0	IPIEDGSGEVVLSR
1510.717	M	1510.814	-0.006	531	544	0	LVAYYTLIGASGQR
1786.847	M	1786.961	-0.006	344	359	0	SGIPIVTSPYQIHFTK
1864.824	M	1864.931	-0.006	265	281	0	VEGTAFVIFGIQDGEQR
1870.910	M	1871.026	-0.006	463	478	0	TELRPGETLNVNFLLR
1877.849	M	1877.965	-0.006	226	241	0	EYVLPSFEVIVEPTEK
1889.933	M	1890.068	-0.007	409	425	0	LSINTHPSQKPLSITVR
1984.856	M	1984.962	-0.005	567	584	1	SGQSEDRQPVPGQQMTLK
1992.899	M	1993.026	-0.006	264	281	1	KVEGTAFVIFGIQDGEQR
2164.892	M	2164.994	-0.005	208	225	0	AYYENSPQQVFSTEFEVK
2443.180	M	2443.299	-0.005	509	530	0	EPGQDLVVLPLSITTDFIPSFR
2493.000	M	2493.140	-0.006	634	657	0	DYAGVFSDAGLTFTSSSGQQTAQR
2577.153	M	2577.300	-0.006	440	462	0	TMQALPYSTVGNSNNYLHLSVLR
3536.479	M	3536.610	-0.004	623	657	1	ADIGCTPGSGKDYAGVFSDAGLTFTSSSGQQTAQR

Fig. 9.6 Identification of C3β. 100% of peptides match to complement component C3- beta chain (residues 23 - 667; pI: 6.82; 71.3 kDa)

C1q in modulation of the humoral immune response, and also in protection against development of autoimmunity has been reported (Botto, 2001).
C1q can control the inflammatory and adaptive immune response through binding to its receptors expressed in most cell types, including T cells and macrophages. Engagement of C1q with the globular domain of C1q receptor (gC1qR) complex delivers an antiproliferative signal to T lymphocytes (Chen *et al.*, 1994; Ghebrehiwet *et al.*, 1990). However, the molecular mechanism for inhibition of T lymphocite responses mediated by C1q/gC1qR has yet to be identified. Interestingly, HCV core protein binds gC1qR with an affinity similar to that of C1q but delivers a stronger inhibitory signal of T cells activation and proliferation (Yao *et al*., 2004; Kittlesen *et al*., 2000; Yao *et al*., 2001b). It will be now interesting to assess whether Core-C1qR interaction would have a role in cryoprecipitates formation by interfering with an efficient clearing of immunocomplexes mediated by C1q.
Serum Amyloid P component (SAP) is a plasma protein termed acute-phase reactants, like C-reactive protein (CRP) and serum amyloid A protein (Steel D.M. and Whitehead A.S., 1994). These proteins are expressed as part of the systemic reaction to inflammation, the acute-phase response. Despite SAP is universally associated with amyloid deposists, details of interactions between SAP and the complement system have been elucidated. SAP can bind to C1q and activate the early complement cascade of the classical pathway (Ying *et al*.,1993; Hicks *et al*.,1992). SAP solubilizes chromatin of apoptotic cells and associated C1q and C4b moieties mediate the tolerance or the clearance of these macromolecular complexes from the circulation, thereby minimizing the opportunity for a vigorous autoimmune response (Bickerstaff *et al.*, 1999). The finding of SAP into cryoglobulins still confirm the active state of the classical immune response to the presence of HCV.
Human Spα is a soluble protein expressed by macrophages present in lymphoid tissues (spleen, lymph node, thymus, and bone marrow), for which little functional and structural information is available. It belongs to the group B of the scavenger receptor cysteine-rich superfamily (SRCR-SF) that includes the lymphocyte surface receptors CD5, CD6, WC1 and M130 (Gebe *et al*., 1997). Spα expression seems to be tightly regulated and preliminary studies revealed that this protein is able to bind to resting myeloid cells, monocytes and lymphocytes. The findings that this protein is expressed in lymphoid organs and can bint to different cells of the immune system suggest that it may play an important role in regulating the immune

system (Sarrias 2004). Analysis of hundreds of serum immunoglobulins samples of different isotype, revealed that monoclonal and polyclonal IgM are always associated with Spα. IgM association suggest that this protein may have a role in the control/regulation of the B-cell's synthesis and homeostasis of IgM (Tissot *et al*., 2002). However the functionality of this interaction is not yet elucidated. Interestingly, CD5+ B cells (or B1a) seem to constitute a separate lineage of B-cells that expresses a limited set of VK genes with few mutations, mostly the Hum/Kv325; produces IgM with RF activity and has the capacity of self-renewal (Weber *et al.*, 1993). HCV chronic infection patients with MC present lymphoproliferation of CD5+ B-cells overexpressing CD81, suggesting an antigen-driven clonal proliferation maybe related to CD81 signalling and bcl-2 rearrangement (Curry *et al*., 2003).

In both MC and chronic hepatitis patients, liver biopsy investigations showed portal infiltrates consisting of T-cells, associated with a significant B-cell component; the latter particularly abundant in MC, where it was frequently arranged in pseudo-follicles. The B-cell component expressed the bcl-2 oncogene product and CD5 antigen. It is worth noting that only in MC patients these CD5+/bcl-2+ B-cells frequently also exhibited a monotypic restriction bearing IgM kv325 (Monteverde *et al.*, 1995). The absence of higher-affinity RFs in normal individual suggests that there are very efficient peripheral mechanisms for the silencing of higher affinity, potentially pathologic, RF-expressing B cells. A failure of this mechanism combined with the antigen-driven bcl-2 dependent lymphoproliferation could be reasonable explanations of the occurrence of RF production in MC patients.

Spα is a secreted protein that has the same domain organization of the extracellular region of CD5 and 100% homology to AIM, apoptosis inhibitor expressed by macrophages. AIM expression appears to be increased in activated macrophages at inflammatory sites. As the apoptosis of both effector hematopoietic cells and target cells is involved in the progression of inflammation and infectious disease, AIM might regulate the progression of disease balancing the apoptosis of those cells by its inhibitory effect (Miyazaki *et al.*, 1999).

It is reasonable to wonder if Spα/AIM may have a role in the impairment of depletion mechanism of RF-expressing cells.

The correspondence between CD5+ B cells proliferation, MC and IgM-kv325 and the characteristic presence of Spα in MC associated with IgM-RF activity let hypotheses that beside the structural analogy between CD5 and Spα (CD5 antigen like) there could be a functional link. Further

characterization on Spα-IgM association, their receptor and signalling has to be carry out to validate this hypothesis.
Besides the identification of proteins known to be correlated with the formation of immune-complexes and cryoglobulins, we have identified several other proteins, which mainly fall into the category of serum transporters:
- Plasma retinol-binding protein. This protein belongs to the lipocalin family and is the specific carrier for retinol (vitamin A alcohol) in the blood. It delivers retinol from the liver stores to the peripheral tissues. In plasma, the RBP-retinol complex interacts with transthyretin which prevents its loss by filtration through the kidney glomeruli. A deficiency of vitamin A blocks secretion of the binding protein posttranslationally and results in defective delivery and supply to the epidermal cells.
-Vitamin D-binding protein: This protein belongs to the albumin family. It is a multifunctional protein found in plasma, ascitic fluid, cerebrospinal fluid and on the surface of many cell types. It binds to vitamin D and its plasma metabolites and transports them to target tissues.
-Albumin: is a soluble, monomeric protein which comprises about one-half of the blood serum protein. Albumin functions primarily as a carrier protein for steroids, fatty acids, and thyroid hormones and plays a role in stabilizing extracellular fluid volume.
The relevance of these proteins in the cryoprecipitate formation need to be further investigated.

9.3 Vero E6 cells proteome alteration induced by the presence of SARS-CoV

The investigation on proteome alteration induced by SARS-CoV on Vero cells is still in course. Here I report just a very preliminary analysis of control *vs* infected cells 48 hrs after infection. At this time, it is possible to observe a high percentage of detached cells (60- 70%) and abut 20% of apoptotic cells (Castilletti *et al.*, submitted). We have worked separately on detached and adherent cells in order to avoid a mixed population which eventually could result in compensation, decrease and suppression of differences in 2D-PAGE maps. Moreover, we have sub-fractionated each population by sequential protein's extraction. We got all cytoplasmatic and membrane-bound proteins (0,5% Triton-soluble proteins) in the first extraction and "insoluble" integral membrane proteins in the second

extraction. 2D-PAGE maps (Fig. 9.7; 9.8) show an huge amount of differences in protein expression as also, probably, the presence of viral proteins. However, as in the case of sequential-protein-extraction proteome analysis of HCV-Rep60 vs HuH7 cells, differences in proteins expression due to irreproducibility of experimental procedures cannot be excluded and several experiments need to be run to build up virtual gels (by Image Analyser) in which these artefacts are suppressed.
We have pick-up and digested more then 100 spots, but the spectrometry analysis by MALDI-TOF-TOF has provided, till now, few identifications.
The biggest problem is the high content of post-translational-modification presented by viral proteins which requires MS/MS analysis and expertises in both the use of the very powerful instrument that is a MALDI-TOF-TOF and the read out of data.
By now, an interesting identification we have done is Prohibitin. We found an over-expression of this protein in the "soluble" fraction of infected cells, and the identification by MALDI-TOF-TOF provides the identification of the proteins in a phosphorilated state.
Although originally identified as putative negative regulator of the cell cycle, Prohibitin (Phb) has been shown to localize to the mitochondrial inner membrane and also into the nucleus (Nijtmans *et al.*, 2000; Steglich *et al.*, 2000, Fusaro *et al.*, 2003). It has been shown that Phb, forming large multimeric complexes bound to the mitochondrial inner membrane, functions as a membrane-bound chaperone for the stabilization of mitochondrial proteins and maintaining of mitochondrial morphology. In the nucleus, instead, it has been found able to bind to retinoblastoma family members and repress all transcriptionally active members of the E2F (transcription factors) family, acting as a tumor suppressor protein (Wang *et al.*, 1999). The same authors propose Phb as a unique regulator of both E2F1 and p53. They suggest that Phb, repressing the E2F1 transcriptional activity while activating p53 transcriptional activity, might be able to affect the balance between proliferation and apoptosis. It has also been observed that upon receiving apoptotic or stress signals, Phb translocates from the nucleus to cytoplasm and mitochondria, where it can regulate cell death through the mitochondrial function (Fusaro *et al.*, 2003).
Cytofluorimetric analysis of TUNEL positive SARS-CoV infected cells has shown about 20% of apoptotic cells (Castilletti *et al.*, submitted).

The finding of Phb in the first extraction of detached infected cells could represent an indication of the apoptotic state of infected cells.
The finding of Phb in a phosphorilated state could be the sign of a negative balance in cells fate. It has been suggested, in fact, that phosphorylation may disturb the correct assembling of Phb complexes on the mitochondria membrane, leading to programmed cell death through the mitochondrial permeability transition (Takahashi *et al.*, 2003).

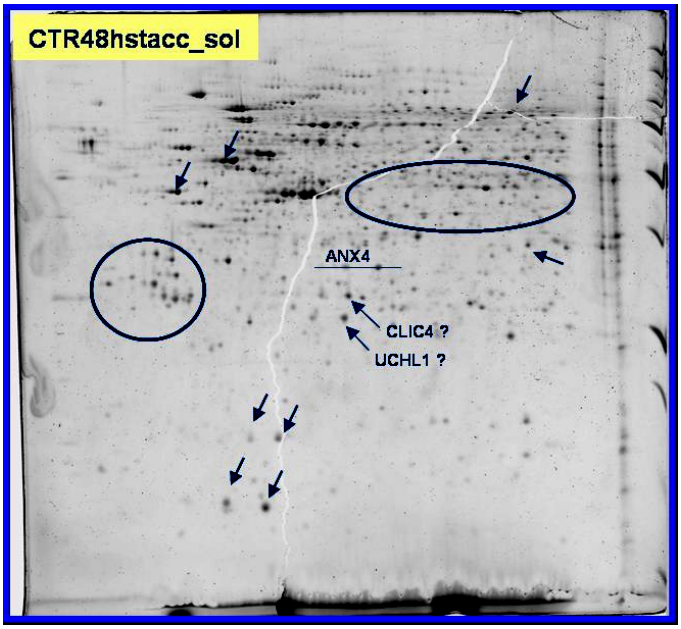

40 mM Tris,
0,5%Triton
10mM NaCl,
PIC 1:500

Fig. 9.7 2D maps of detached-cells "soluble" fractions, 48h.p.i. The buffer used is reported in the box and differences indicated.

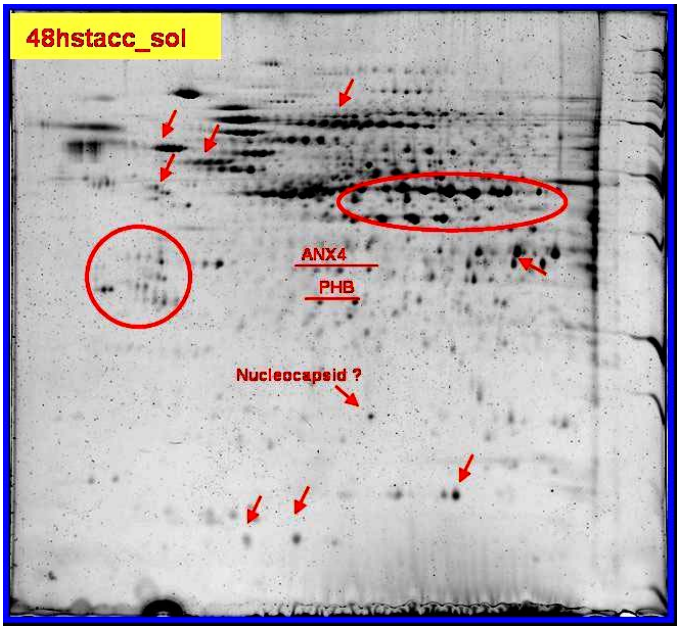

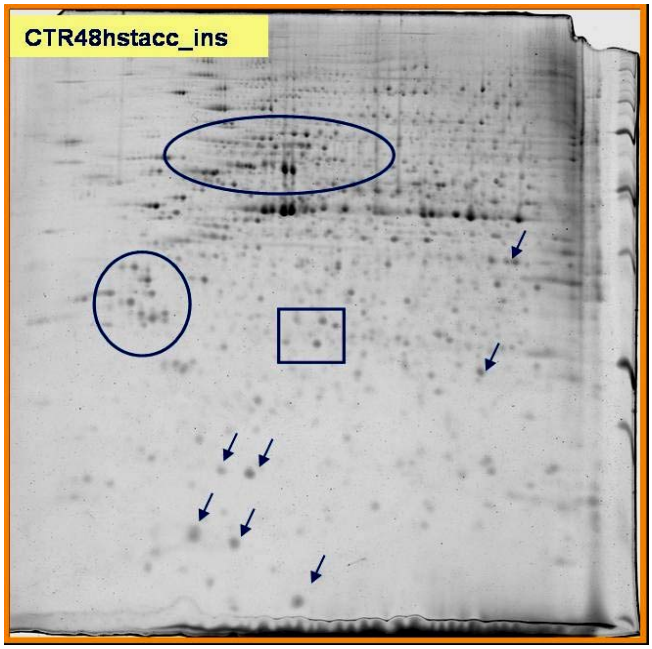

7M Urea,
2M Thiourea,
40 mM Tris,
2%CHAPS,
1%SB3-12,
1% ASBB14,
0,5% CA

Fig. 9.8 2D maps of detached-cells "insoluble" fractions, 48h.p.i. The buffer used is reported in the box and differences indicated

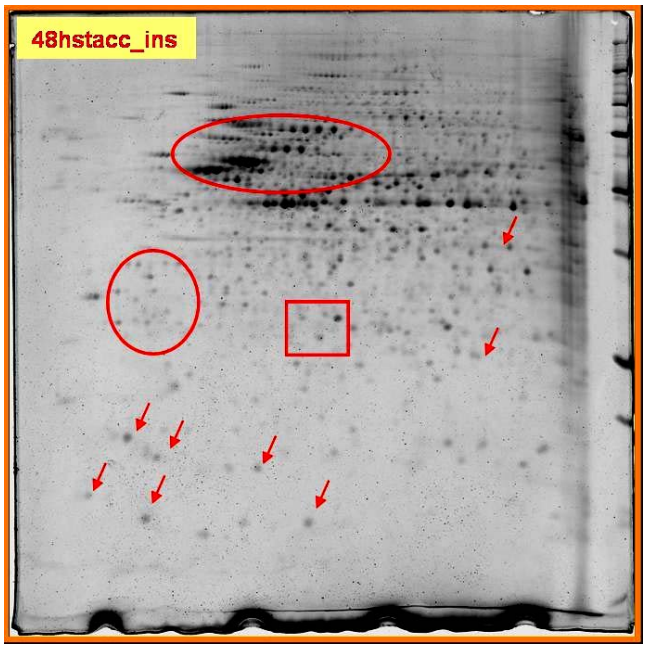

10. CONCLUSIONS

The application of the proteomic approach MALDI-TOF / 2D-PAGE to investigate host-virus interactions seems to be not always successful or, at least, it needs to be improved. Many factors have to be taken into account and to optimize, starting from the preparation of the sample till the complete assignation of spectra.
On the other hand, it has to be chosen in opportune way the system to investigate. HCV is a very low rate replicating virus which can remain asymptomatic for decades. The viral proteins which seem to cause cytopathic effects, mostly related to aberration in the immune system response, result to be the structural proteins, mainly E2. Recent works claim the inefficacy of HCV protein expression on cell cycle regulation, nor on induction of any type I IFNs, and only minimal effects on the cellular transcriptome (Scholle *et al.*, 2004; Mihim *et al.*, 2004; Abe *et al.*, 2005).
HCV seems to be a virus able to induce a persistent chronic infection without disturbing the normal function of the host cells. Rather then a direct involvement of viral proteins, it can be reasonable to address the origin of HCV-induced diseases to its chronic stimulation of the immune system, which in its turn often causes aberration in the immune response.
The application of the same approach on SARS-CoV infected cells will surely provide the possibility to express all the potentiality of MALDI-TOF mass spectrometry in identifying viral and host proteins involved in the host-cell proteome alteration, particularly in the identification of post translational modification.
Concerning the investigation on cryoglobulins, this approach has been the most appropriate for the identification of protein content of the cryoprecipitates. It has provided interesting information useful for further analytical investigation towards the comprehension of mechanism involved in the immune system response and their failures as possible causes of malignancies.

The fascination of virus-host interactions research, besides the necessity to overcome diseases, mainly consists in the host-virus interactions research, I mean, in the possibility to increase our knowledge about the immune system.

REFERENCES

Abe K, Ikeda M, Dansako H, Naka K, Shimotohno K, Kato N. (2005) *Virus Res*. **107** :73-81.

Agnello V, Chung RT, Kaplan LM. (1992) *N Engl J Med*: **327**:1490–5.

Agnello V, Abel G, Elfahal M, Knight GB, Zhang Q-X. (1999) *Proc Natl Acad Sci U S A.*;**96**:12766-12771.

Alter H.J., Purcell R.H., Holland P.V. and Popper H., (1978) *Lancet* **1**:459-463.

Barber M., Bordoli R. S.,. Sedgwick R. D, Tyler A. N. (1981) *Nature* **293**, 270–275.

Bartenschlager R. and Lohmann V. (2000). *J. Gen. Virol.* **81**:1631.1648.

Bartenschlager, R., L. Ahlborn-Laake, J. Mous, and H. Jacobsen. (1994) *J. Virol.* **68**:5045–5055.

Bartenschlager, R., V. Lohmann, T. Wilkinson, and J. O. Koch. (1995) *J. Virol*.**69**:7519–7528.

Bartosch, B., J. Dubuisson, and F. L. Cosset. (2003) *J.Exp. Med.* **197:**633–642.

Beavis RC, Chait BT. (1991), *Chem Phys Lett* **5**:479-484.

Behrens, S. E., Grassmann, C. W., Thiel, H. J., Meyers, G. & Tautz, N. (1998) *J. Virol.* **72**, 2364±2372.

Bickerstaff, M.C.M. et al. (1999) *Nature Med*. **5**, 694–697.

Bjellqvist B, Ek K, Righetti PG, Gianazza E, Görg A, Westermeier R, Postel, W (1982) *J Biochem Biophys Methods* **6**: 317-339

Blight, K. J., A. A. Kolykhalov, and C. M. Rice. (2000) *Science* **290:**1972–1974.

Borowski P, J. S. zur Wiesch, Resh K., Feucht H., Laufs R. And Shmitz H. (1999) *J. Biol. Chem.* **274**:30722-28.

Botto M (2001) *Arthritis Res,* **3:**207-210.

Brouet JC, Clouvel JP, Danon F, et al. *Am J Med* (1974) **57**:775–88.

Brown RS, Lennon JJ.(1995). *Anal Chem* **67** 1998-2003.

Carrère-Kremer S., Montpellier-Pala C., Cocquerel L., Wychowski C., Penin F. and Dubuisson J. (2002). *J. Virol.* **76**:3720-3730.

Castilletti C., Falasca L., Ciccosanti F., Bordi L., Rozera G., Di Caro A., Zaniratti S., Rinaldi A., Ippolito G., Piacentini M., Capobianchi MR., *Archives of Virology* submitted.

Chau TN, Lee KC, Yao H, Tsang TY, Chow TC, Yeung YC, Choi KW, Tso YK, Lau T, Lai ST, Lai CL. (2004) *Hepatology*. **39**:302-10

Chen, A., S. Gaddipati, Y. Hong, D. J. Volkman, E. I. Peerschke, and B. Ghebrehiwet. (1994) *J. Immunol*. **153**:1430.

Choo Q.L., Kuo G., Weiner A.J., Overby L.R., Bradley D.W. and Houghton M. (1989), *Science* **244**:359-362.

Cocquerel L., Duvet S., Meunier J.C., Pillez A., Cacan R., Wychowski C. and Dubuisson J. (1999) *J. Virol.* **73**:2641-2649.

Cribier B., Schmitt C., Bingen A., Kirn A. and Keller F. (1995). *J. Gen. Virol.* **76**:2485-2491.

Cui HJ, Tong XL, Li P, Hao YX, Chen XG, Li AG, Zhang ZY, Duan J, Zhen M, Zhang B, Hua CJ, Gong YW. (2004) *World J Gastroenterol* **10**: 1652-1655

Curry MP, Golden-Mason L, Doherty DG, Deignan T, Norris S, Duffy M, Nolan N, Hall W, Hegarty JE, O'Farrelly C. (2003)
J Hepatol.**38**:642-50.

Dammacco F, Gatti P, Sansonno D. (1998) *Leuk Lymphoma*.;**31**:463-476.

Damoc E., Youhnovski N., Crettaz D., Tissot JD., Przybylski M (2003) *Proteomics*, **3**:1425-1433

Delhem N, Sabile A, Gajardo R, Podevin P, Abadie A, Blaton M A, Kremsdorf D, Beretta L and Brechot C (2001) *Oncogene* **20** 5836–5845

Deutzmann R. *Methods Mol Med.* 2004;94:269-97.

De Re V, De Vita S, Marzotto A, Rupolo M, Gloghini A, Pivetta B, Gasparotto D, Carbone A, Boiocchi M. (2000) Blood. **96**:3578-84

De Re V, De Vita S, Marzotto A, et al.. (2000b) *Int J Cancer*. **87**:211-216.

De Vita S, De Re V, Gasparotto D, et al. (2000) *Arthritis Rheum*.;**43**:94-102.

Dreger M. (2003) *Mass Spec Rev* **22**:27-56

Drosten, C., Gunther, S., Preiser, W. & 23 other authors (2003).
N Engl J Med **348**, 1967–1976.

Dubuisson J, Penin F, Moradpour D. (2002) *Trends Cell Biol.*;**12**:517-523.

Duvet S., Cocquerel L., Pillez A., Cacan R., Verbert A., Moradpour D., Wychowski C. and Dubuisson J. (1998). *J. Biological Chemistry* **273**:32088-32095.

El-Hage N and Luo G (2003), *J. Gen. Virol*. **84**, 2761–2769

Enomoto, N., I. Sakuma, Y. Asahina, M. Kurosaki, T. Murakami, C.Yamamoto, Y. Ogura, N. Izumi, F. Maruno, and C. Sato. (1996) *N. Engl. J. Med*. **334**:77–81.

Fenn J. B., Mann, M. Meng C. K.,. Wong S. F,. Whitehouse C. M (1989) *Science* **246**, 64–71.

Fenn, J. B., M. Mann, C. K. Meng & S. K. Wong. (1990) *Mass spectrometry Rev*, **9**, 37-70

Fenn, J.B., **(**1993) *J Am Soc Mass Spectrom*, **4**, 524-535

Ferri C, Greco F, Longombardo G, et al. (1991) *Clin Exp Rheumatol* **9**:621–4.

Ferri C, Zignego AL. (2000) *Curr Opin Rheumatol*: **12**:53–60.

Ferri C, Monti M, La Civita L, et al. (1993) Blood **82**:3701–4.

Ferri A, Zignego AL, Pileri SA 2002 *J Clin Path* **55**:4-13

Fields S (2001), *Science.* **291**(5507):1221-4.

Fimia G.M., C. Evangelisti, T. Alonzi, F. Fratini, M. Romani, G. Paonessa, G. Ippolito, M. Tripodi and M. Piacentini. (2004) *J Virol.* **78**:12809-16.

Forns X, Bukh J. 1999 *Clin Liver Dis.* Nov;3(4):693-716

Fournier C., Sureau C., Coste J., Ducos J., Pageaux G., Larrey D., Domergue J. and Maurel P. (1998). *J. Gen. Virol.***79**:2367-2374.

Foy, E., K. Li, C. Wang, R. Sumpter, Jr., M. Ikeda, S. M. Lemon, and M.Gale, Jr. 2003. *Science* **300:**1145–1148.

Francki, R. I. B., D. L. Knudson, and F. Brown. 1991. *Arch. Virol*. **2:**223.

Fouchier, R. A., Kuiken, T., Schutten, M. & 7 other authors (2003) *Nature* **423**, 240.

Fusaro G, Dasgupta P, Rastogi S, Joshi B, Chellappan S. (2003) *J Biol Chem.* **278**:47853-61.

Gale, M., Jr., C. M. Blakely, B. Kwieciszewski, S. L. Tan, M. Dossett, N. M.Tang, M. J. Korth, S. J. Polyak, D. R. Gretch, and M. G. Katze. (1998). *Mol. Cell. Biol.* **18:**5208–5218.

Gale, M., Jr., M. J. Korth, N. M. Tang, S.-L. Tan, D. A. Hopkins, T. E. Dever, S. J. Polyak, D. R. Gretch, and M. G. Katze. (1997) *Virology* **230**:217–227.

Gale, M., Jr., B. Kwieciszewski, M. Dossett, H. Nakao, and M. G. Katze. (1999) *J. Virol.* **73**:6506–6516.

Gale, M., Jr., S. L. Tan, and M. G. Katze. (2000) *Microbiol. Mol. Biol.Rev.* **64**: 239-280

Gebe JA, Kiener PA, Ring HZ, Li X, Francke U, Aruffo A. (1997) *J Biol Chem.* **272:**6151-8

Geiss GK, Carter VS, He Y, Kwieciszewski BK, Holzman T, Korth MJ, Lazaro CA, Fausto N, Bumgarner RE, Katze MG. (2003) *J Virol*.**77**:6367-75

Ghebrehiwet, B., G. S. Habicht, and G. Beck. (1990). *Clin. Immunol. Immunopathol.* **54**:148.

Gorevic PD, Kassab HJ, Levo Y, et al. (1980). *Am J Med:* **69**:287–308.

Gorg A., Weiss W., and Dunn MJ (2004) *Proteomics* **4**: 3665-3885

Goldsmith CS, Tatti KM, Ksiazek TG, Rollin PE, Comer JA, Lee WW, Rota PA, Bankamp B, Bellini WJ, Zaki SR. (2004)
*Emerg Infect Dis.***10:**320-6.

Gosert, R., Egger, D., Lohmann, V., Bartenschlager, R., Blum, H. E., Bienz, K. & Moradpour, D. (2003) *J Virol* **77**, 5487–5492.

Goodbourn S., Didcock L., and Randall RE (2000) *J Gen Virol.* **81**:2341-64. Review.

Guan Y, Zheng BJ, He YQ, Liu XL, Zhuang ZX, Cheung CL, Luo SW, Li PH, Zhang LJ, Guan YJ, Butt KM, Wong KL, Chan KW, Lim W, Shortridge KF, Yuen KY, Peiris JS, Poon LL. (2003) Science. **302**:276-8.

Gumber S, Chopra S. (1995) *Ann Intern Med*;123:615–20.

Gyotoku Y, Abdelmoula M, Spertini F, et al. (1987) *J Immunol*;**138**:3785–92.

Hager JW, Yves Le Blanc JC. (2003) *Rapid Commun Mass Spectrom.* **17**: 1056-64.

Hasnain SE, Begum R, Ramaiah KVA, Sahdev S, Shajil EM, Taneja TK, Mohan M, Athar M, Sah NK and Krishnaveni M (2003) *J. Biosci*. **28** 349–358

Hay S, Kannourakis G. (2002) *J Gen Virol.* **83**:1547-64. Review.

Hicks, P.S., Saunero-Nava, L., Du Clos, T.W. & Mold, C. *J. Immunol.* **149**, 3689–3694 (1992).

Higuchi M, Tanaka E, Kiyosawa K. (2002) *Jpn J Infect Dis.* **55**:69-77. Review.

Hopfgartner G, Varesio E, Tschappat V, Grivet C, Bourgogne E, Leuthold LA (2004) *J Mass Spectrom.***39**:845-55. Review.

Hunt DF, Yates JR 3rd, Shabanowitz J, Winston S, Hauer CR. (1986) *Proc Natl Acad Sci U S A.* **83**:6233-7.

Ikeda, M., M. Yi, K. Li, and S. M. Lemon. 2002. *J. Virol.* **76:**2997–3006.

Ivanovski M, Silvestri F, Pozzato G, et al.. (1998) *Blood.*;**91**: 2433-2442.

Ji H, Fraser CS, Yu Y, Leary J, Doudna (2004) *JA.PNAS* **101**:16990-16995

Karas M., Glueckmann M. and Shaefer J. (2000) *J. Mass Spectrom.* **35**, 1-12.

Karas M., Hillenkamp F. (1988), *Anal. Chem.* **60**, 2299–2301.

Katze MG, He Y, Gale M Jr. (2002) *Nat Rev Immunol.* **2**: 675-87. Review.

Khromykh, A. A. & Westaway, E. G. (1997) *J. Virol.* **71**, 1497-1505.

Kim D.W., Gwack Y., Han J.H. and Choe J. (1995), *Biochem. Biophys. Res. Commun.* **215**:160-166.

Kittlesen DJ, Chianese-Bullock KA, Yao ZQ, Braciale TJ, Hahn YS. (2000) *J Clin Invest*. **106:**1239-49

Kountouras J., Zavos C., Chatzopoulos D., (2003) *J Viral Hepat* **10**: 335-342

Krieger N, Lohmann V, Bartenschlager R.. (2001) *J. Virol.* **75**: 4614-4624.

Krutchinsky, A. N., Kalkum, M. & Chait, B. T. (2001) *Anal. Chem*. **73**, 5066–5077.

Krylov SN & Dovichi NJ (2000), *Anal. Chem.* **72,** 111-128

Ksiazek, T. G., Erdman, D., Goldsmith, C. S. & 23 other authors (2003). *N Engl J Med* **348**, 1953–1966.

Kussmann M., Nordhoff E., Rahbek-Nielsen H., haebel S., Larsen M., Jakobsen L., Gobom J., Mirgorodskaya E., kristensen A., Palm L., Roepstorff P. (1997) *J. Mass Spectrom.* **32**, 593-601

Lan, K. H., M. L. Sheu, S. J. Hwang, S. H. Yen, S. Y. Chen, J. C. Wu, Y. J.Wang, N. Kato, M. Omata, F. Y. Chang, and S. D. Lee. 2002. *Oncogen*e **21:**4801–4811.

Lenzi M, Johnson PJ, McFarlane IG, et al. 1991 *Lancet*;**338**:277–80.

Lenzi M, Frisoni M, Mantovani V, et al. 1998 *Blood*;**91**:2062–6.

Lilley KS, Razzaq A, Dupree P. 2002 *Curr Opin Chem Biol* **6.**:46-50.Review.

Loboda, A. V., Krutchinsky, A. N., Bromirski, M., Ens, W. & Standing, K. G. (2000) *Rapid Commun. Mass Spectrom*. **14**, 1047–1057.

Lohmann V, Koch JO, Bartenschlager R. (1996), *J Hepatol*. **24**: 11-9. Review.

Lohmann V, Korner F, Herian U, Bartenschlager R. *J Virol*. (1997) **71**(11):8416-28.

Lohmann V., Körner F., Koch J.O., Herian U., Theilmann L. and Bartenschlager R. (1999). *Science* **285**:110-113.

Lohmann V, Korner F, Dobierzewska A, Bartenschlager R. (2001) *J Virol*. **75**:1437-1449.

Lohmann V, Hoffmann S, Herian U, Penin F, Bartenschlager R. (2003) *J Virol*. **77**:3007-3019.

Luo, G., Hamatake, R. K., Mathis, D. M., Racela, J., Rigat, K. L., Lemm, J. & Colonno, R. J. (2000) *J. Virol.* **74**, 851±863.

Mamyrin BA, Karatajev VJ, Shmikk DV, Zagulin VA. (1973) *Soviet Phys JETP* **37**:45-48.

Mann M and Jensen O.N. (2003) *Nat Biotechnol.* **21**:255-261

Mann M. (1990) *Organic Mass Spectrometry* **25**: 575-587

Mann M. (1995) *Trends Biochem Sci.,* **20** (6):219-24

Mann, M., Meng, C.K., Fenn, J.B. (1989), *Anal. Chem*. **61**, 1702-1708.

Marra, M. A., Jones, S. J., Astell, C. R. & 56 other authors (2003). *Science* **300**, 1399–1404.

Medzihradszky KF, Campbell JM, Baldwin MA, Falick AM, Juhasz P, Vestal ML, Burlingame AL. (2000) *Anal. Chem.* **72,** 552–558.

Meltzer M, Franklin EC, Elias K, et al. (1966) *Am J,Med*;**40**:837–56.

Middaugh CR, Litman GW. (1987). *J Biol Chem* **262**:3671–3.

Mihm S, Frese M, Meier V, Wietzke-Braun P, Scharf JG, Bartenschlager R, Ramadori G. (2004) *Lab Invest*. **84**:1148-59

Miyazaki T, Hirokami Y, Matsuhashi N, Takatsuka H, Naito M. (1999) *J Exp Med.* **189**:413-22.

Molloy MP, Brzezinski EE, Hang J, McDowell MT, VanBogelen RA. (2003) *Proteomics*. **3** :1912-9.

Monteverde A, Ballare M, Pileri S. (1997) *Springer Semin Imunopathol*;19:99–110.

Monteverde A, Ballare M, Bertoncelli MC, Zigrossi P, Sabattini E, Poggi S, Pileri S. (1995) *Clin Exp Rheumatol*. **13** Suppl 13:S141-7.

Moradpour, D., Wakita, T., Wands, J. R. & Blum, H. E. (1998). *Biochem. Biophys. Res. Commun.* **246**, 920-924.

Moradpour D, Brass V, Bieck E, Friebe P, Gosert R, Blum HE, Bartenschlager R, Penin F, Lohmann V. (2004) *J Virol.* **78**:13278-84.

Nijtmans, L. G., de Jong, L., Artal Sanz, M., Coates, P. J., Berden, J. A., Back, J. W., Muijsers, A. O., van der Spek, H., and Grivell, L. A. (2000) *EMBO J*. **19**, 2444–2451

Ng LF, Hibberd ML, Ooi EE, Tang KF, Neo SY, Tan J, Murthy KR, Vega VB, Chia JM, Liu ET, Ren EC. (2004) *BMC Infect Dis.* **4**:34.

Nguyen VP, Hogue BG. (1997) *J Virol*. **71**:9278-84

Niessen W.M.A., Tinke A.P. (1995), *J. Chromatogr. A,* **703**, 37-57

Nobel Prize in Chemistry 2002 (accessed September 21, 2003) www.nobel.se/chemistry/laureates/2002/index.html.

O' Farrell PH (1975) *J Biol Chem* **250**: 4007-4021

Otto GA, Puglisi JD. (2004) *Cell.* **119**:369-80.

Pavio N, Taylor D R and Lai M M (2002) *J. Virol*. **76** 1265–1272

Pavlovic, D., D. C. Neville, O. Argaud, B. Blumberg, R. A. Dwek, W. B. Fischer and N. Zitzmann. **(**2003). *Proc. Natl. Acad. Sci. USA* **100:**6104–6108.

Pawlotsky JM, Germanidis G. (1999) *J Viral Hepat.* **6**:343-56.

Peiris, J. S., Lai, S. T., Poon, L. L. & 13 other authors (2003). *Lancet* **361**, 1319–1325.

Perkel J. (2001) *The Scientist* 15 | Issue 16 | 31 | Aug. 20, 2001

Pieroni L, Santolini E, Fipaldini C, Pacini L, Migliaccio G, La Monica N. (1997) *J Virol.* **71**:6373-80.

Pietschmann, T., V. Lohmann, A. Kaul, N. Krieger, G. Rinck, G. Rutter, D. Strand, and R. Bartenschlager. 2002. *J. Virol.* **76:**4008–4021.

Pietschmann, T., V. Lohmann, G. Rutter, K. Kurpanek, and R. Bartenschlager. (2001) *J. Virol.* **75:**1252–1264.

Pileri P, Uematsu Y, Campagnoli S, Galli G, Falugi F, Petracca R, Weiner AJ, Houghton M, Rosa D, Grandi G, Abrignani S (1998) *Science*.;282:938-941.

Pozzato G, Mazzaro C, Crovatto M, et al. (1994) *Blood*;84:3047–53.

Qinfen Z, Jinming C, Xiaojun H, Huanying Z, Jicheng H, Ling F, Kunpeng L, Jingqiang Z. 2004 *J Med Virol*. **73**:332-7

Raman C. (2002) *Immunol Res*.;**26**:255-63. Review.

Ray RB, Ray R. (2001) *FEMS Microbiol Lett*.;**202**(2):149-56. Review.

Reed K.E., Grakoui A. and Rice C.M. (1995). *J. Virol.* **69**:4127-4136.

Reed KE, Grakoui A, Rice CM. (1995) *J Virol,***69**:4127-36.

Reinhold BB & Reinhold VN (1992), *J Am Soc Mass Spectrom*, **3,** 207

Rota, P. A., Oberste, M. S., Monroe, S. S. & 32 other authors (2003). *Science* **300**, 1394–1399.

Ruan, Y. J., Wei, C. L., Ee, A. L. & 17 other authors (2003).*Lancet* **361**, 1779–1785.

Russel DH & Edmondson RD (1997), *J. Mass Spectrom.* **32**, 263-276

Sansonno, D., S. De Vita, AR Iacobelli, V. Cornacchiulo, , M. Boiocchi, and F. Dammacco. 1998. *J Immunol* **160**:3594-601

Samuel CE (2001) *Clin Microbiol Rev* **14**:778-809.

Sarrias MR, Padilla O, Monreal Y, Carrascal M, Abian J, Vives J, Yelamos J, Lozano F. (2004) *Tissue Antigens*. **63**:335-44.

Scarselli E, Ansuini H, Cerino R, Roccasecca RM, Acali S, Filocamo G, Traboni C, Nicosia A, Cortese R, Vitelli A. (2002) *EMBO J*.**21**:5017-5025.

Sen GC. (2001) *Annu Rev Microbiol*.;**55**:255-81. Review.

Schwartz JC, Jardine I. (1996) *Methods Enzymol*.;**270**:552-86.

Scholle F, Li K, Bodola F, Ikeda1 M, . Luxon B. A, and Stanley M. Lemoni (2004) J. Virol. **78:**1513–1524

Simmonds P, Holmes EC, Cha TA, Chan SW, McOmish F, Irvine B, Beall E, Yap PL, Kolberg J & Urdea MS (1993). *J. Gen.Virol.* **74**: 2391-2399.
Spengler B, Kirch D and Kaufmann R. (1991) *Rapid Cornmun Mass Spectrom* **5***:* 198-202.

Steel D.M., Whitehead A.S., (1994) *Immunol. Today*, **15**, 81-8.

Steglich, G., Neupert, W., and Langer, T. (1999) *Mol. Cell. Biol.* **19**, 3435–3442

Tabor E., Gerety R.J., Drucker J.A., Seeff L.B., Hoofnagle J.H., Jackson D.R., April M., Barker L.F. and Pineda-Tamondong G**.** (1978). *Lancet* **1**:463-466.

Tan EL, Ooi EE, Lin CY, Tan HC, Ling AE, Lim B, Stanton LW. (2004) *Emerg Infect Dis.* **10**:581-6.

Takahashi A, Kawasaki T, Wong HL, Suharsono U, Hirano H, Shimamoto K. (2003) *Plant Physiol*. **132**:1861-9.

Tan, S.-L., and M. G. Katze. (2001). *Virology* **284**:1–12.

Tanaka K., Waki H., Ido Y., Akita S., Yoshida Y., Yoshida T. (1988) *Rapid Commun. Mass Spectrom.* **2**, 151–153.

Thiel V, Ivanov KA, Putics A, Hertzig T, Schelle B, Bayer S, Weissbrich B, Snijder EJ, Rabenau H, Doerr HW, Gorbalenya AE, Ziebuhr J. (2003) *J Gen Virol.* **84**:2305-15.

Thogersen D.F., Skowronski R.P. and Macfalane R.D. (1974) *Biochem. Biophis. Res . Commun.* **60**, 616-621

Tissot JD, Sanchez JC, Vuadens F, Scherl A, Schifferli JA, Hochstrasser DF, Schneider P, Duchosal MA. . 2002 *Electrophoresis* **23**:1203-6.

Trendelenburg M, Schifferli JA. 1998 *AnnRheum Dis*;**57**:3–5.

Tseng C T and Klimpel G R (2002) *J. Exp. Med.* **195** 43–49

Vestal ML, Juhasz P, Martin SA. (1995) *Rapid Cornmun Mass Spectrom* **9***:* 1044-1050.

Vilcek J. & Sen G. (1996) In *Fields Virology*, 3rd edn, 375-399.

Voisset C and Dubuisson J 2004 *Biol Cell*. **96**:413-20.

Wack A, Soldaini E, Tseng C, Nuti S, Klimpel G and Abrignani S (2001) *Eur. J. Immunol*. **31** 166–175

Wang S, Nath N, Fusaro G, Chellappan S. (1999) *Mol Cell Biol*. **19**:7447-60.

Wasinger VC, Cordwell SJ, Cerpa-Poljak A, Yan JX, Gooley AA, Wilkins MR, Duncan MW, Harris R, Williams KL, Humphery-Smith I. *Electrophoresis* 1995, **16**(7):1090-4.

Weber JC, Blaison G, Martin T, Knapp AM, and Pasquali JL (1994) *J. Clin. Invest*.:**93**:2093-2105.

Wilm M, Mann M. (1996) *Anal Chem*. Jan 1;**68**(1):1-8.

Wong SC, Chew WK, Tan JE, Melendez AJ, Francis F, Lam KP. (2002) *J Biol Chem.* **277**:30707-15.

Wu C.C, and Yates JR, (2003) *Nat Biotechnol.* **21**:262-7. Review.

Yan H, Xiao G, Zhang J, Hu Y, Yuan F, Cole DK, Zheng C, Gao GF. (2004) *J Med Viro* **73**:323-31.

Yang L, Amad M, Winnik WM, Schoen AE, Schweingruber H, Mylchreest I, Rudewicz PJ. (2002) *Rapid Commun Mass Spectrom.***16**:2060-6

Yang M, Li CK, Li K, Hon KL, Ng MH, Chan PK, Fok TF. (2004) *Int J Mol Med*. **14**:311-5.

Yao ZQ, Eisen-Vandervelde A, Waggoner SN, Cale EM, Hahn YS. 2004 *J Virol* **78**:6409-19.

Yao ZQ, Ray S, Eisen-Vandervelde A, Waggoner S, Hahn YS. (2001a) *Viral Immunol* **l4**: 277-95.

Yao ZQ, Nguyen DT, Hiotellis AI, Hahn YS. (2001b) *J Immunol.*; **167**:5264-72.

Yasui K., Wakita T., Tsukiyama-Kohara K., Funahashi S.I., Ichikawa M., Kajita T., Moradpour D., Wands J.R. and Kohara M**.** (1998). *J. Virol.* **72**:6048-6055.

Ying, S.C., Gewurz, A.T., Jiang, H. & Gewurz, H. (1993) *J. Immunol*. **150**, 169–176.

Zhang LK, Rempel D, Pramanik BN, Gross ML, 2004.*Mass Spectrom Rev*., PMID: 15389857

Zhang QF, Cui JM, Huang XJ, Lin W, Tan DY, Xu JW, Yang YF, Zhang JQ, Zhang X, Li H, Zheng HY, Chen QX, Yan XG, Zheng K, Wan ZY, Huang JC. (2003) *Acta Biochimica et Biophysica Sinica* **35**:587-91

Zhong, W., Uss, A. S., Ferrari, E., Lau, J. Y. N. & Hong, Z. (2000**).** *J. Virol.* **74**, 2017±2022.

Zhou J, Ens W, Standing K. Verentchikov A. (1992) *Rapid Commun Mass Spertrom* **6**: 571-678.

Zhu N, Khoshnan A, Schneider R, Matsumoto M, Dennert G, Ware C and Lai M M (1998) *J. Virol.* **72** 3691–3697

Zhu N, Ware C F and Lai M M (2001) *Virology* **283** 178–187

Zignego AL, Macchia D, Monti M, et al. (1992) *J Hepatol*;**15**:382–6.

Zignego AL, Ferri C, Giannelli F, Giannini C, Caini P, Monti M, Marrocchi ME, Di Pietro E, La Villa G, Laffi G, Gentilini P. (2002) *Ann Intern Med*. **137** :571-80.